University of Rome "La Sapienza"

Doctorate School of
"Human Pathology and Drug Sciences"

PhD thesis in
"Pharmaceutical Sciences"

SONICATION BASED POLYSACCHARIDE HYDROGELS FOR MODIFIED DRUG DELIVERY SYSTEMS

Tutor: Prof. Tommasina Coviello *PhD student: Siddique Akber Ansari*

XXVI cycle
2010-2013

Dedicated To
Almighty God
&
My SON
DANISH

Index

Chapter 1 – General part

Chapter 1
General Part

1. Introduction

During the past decades, the pharmaceutical industry is grown up at a very fast rate. Along with the discoveries of new drugs for various preventive and therapeutic treatments, the need for novel materials, new methods and approaches for drug delivery represented new opportunities for material scientists. Drug delivery companies have thus redefined the picture of the pharmaceutical industry not only by providing tools for the delivery of new drugs but also by applying their technologies to bioactive substances already available on the market.

The administration of these systems for therapeutic treatments shows several advantages, if compared to the conventional formulations (tablets, liquids and injections) (Figure 1):

- Reproducible and prolonged constant delivery rate
- Need of fewer administrations
- Reduced side effects

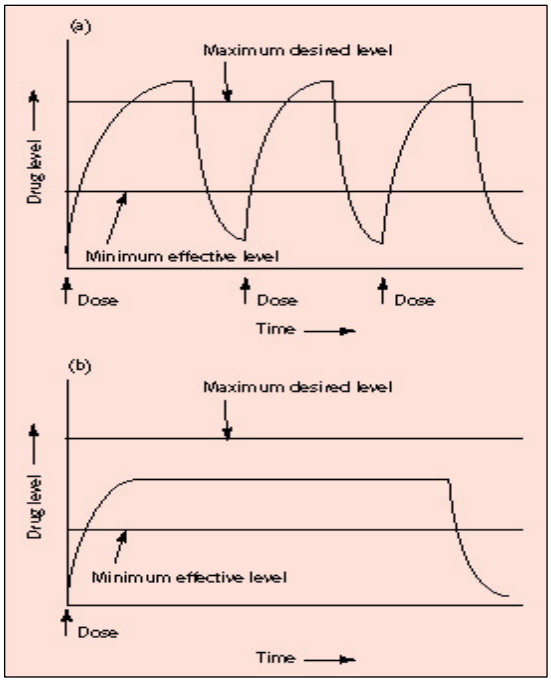

Figure 1. Drug levels in the blood with (a) conventional formulation and (b) modified delivery formulation.

The drug releases by non-conventional formulations can be controlled in terms of time or site-specific targeting, though the achievement of the therapy depends also on the physiological conditions of the patient [1-3].

2. Polysaccharides

Polymers are actually the most used materials as drug delivery carriers and as scaffolding material for tissue engineering applications. Their chemical and physical properties are influenced by several factors (including the composition of the backbone and side groups, the structure of the chains and the molecular weight distribution) and they can be chemically and biochemically easily modified according to the pharmaceutical needs [4].

Among polymers, natural polysaccharides, as well as their derivatives, are the more utilized materials in the pharmaceutical field [5-11] because they are natural, in most cases present in abundance, often inexpensive, available in a variety of structures with a variety of properties. Polysaccharides are polymeric carbohydrate structures, formed of repeating units linked together by glycosidic bonds. These polymers can be either linear or branched, and they can contain only one type of monosaccharide (homopolysaccharides), or various carbohydrate monomers (heteropolysaccharides). They are highly stable, safe, usually nontoxic, hydrophilic, biodegradable and gel forming. A large number of polysaccharides is actually used in numerous fields (food, cosmetic and pharmaceutical industry) and tested as drug carriers (Table 1) [12, 10] since in several cases their presence plays a fundamental role in determining the mechanism and rate of drug release from the dosage form.

Table 1. Main structural features of some polysaccharides.

Polysaccharide	Main chain	Side chain	Source	Applications	Ref.
Alginates	Copolymer of(1,4) linked β-D mannuronic acid and α-L-guluronic acid	-----	Marine brown algae and bacteria (*Azotobacter vinelandii* and *Pseudomonas*)	Used in pharmaceutical fields as immunostimulants, as gastroprotector and as gel-forming agents for immobilization of cells	[13,14]
Chitosan	Deacetylated P-1,4 N-acetyl -D-glucosamine	-----	Shell of marine invertebrates	Deacetylated chitin; used in medicine as tablet component and absorption enhancing agent	[15]
Dextran	α-1,6-D-glucose	α-1,3-D glucose	Bacteria (*Leuconostoc* and *Streptococcus*)	Used in medicine as plasma expander; iron dextran is used in veterinary medicine for the treatment of anemia; dextran sulphate has been used a substitute for heparin in anticoagulant therapy	[13]

Galactomannan	α-1,4-D-mannose	α-1,6-D galactose	Plant seed	Use in food industry as thickening agent, excipient in various cosmetic and pharmaceutical emulsions.	[16]
Glucomannan	Random copolymer of (1,4) linked β-D mannose and β-D glucose	-----	Amorphophallus konjac plant	Used as drug carrier, enzyme entrapment, reduces cholesterol level	[17]
Pectins	α-1,4-D galactopyranosyluronic acid	------	Structural elements in all higher plants	Used in food industry for jams, jellies, confectionary and fruit preparations, and tested as matrix for colon drug delivery	[14]
Scleroglucan	(1,3) linked β-D glucopyranosyl units	At every third unit it bears a single β-D glucopyranosyl unit linked (1,6)	fungi (*Sclerotium*)	Used widely in industry, used for laxative, antitumor, antimicrobial effects	[16,11]
Xanthan	β-1,4-D glucose	β-D-mannose-(1,4)-β-D glucuronic acid-	Bacteria (*Xanthomonas campestris*)	Used in food industry, in textile printing and in pharmaceutical field as	

2.1. Scleroglucan

The production of Scleroglucan (Sclg) was first reported by Halleck [18], who observed that this extracellular polysaccharide is secreted by *Sclerotium glucanicum*. Because of its physical properties, academia and industry soon realized that Sclg might have several potential applications. The ability of native Sclg to dissolve readily in water and act as a thickener or stabilizer. Or the gelling properties of modified Sclg, combined with biopolymer thermal stability, were its main advantages. Sclg was introduced to the market by the Pillsbury Co. (Minneapolis) with the tradename Polytran®, and in 1976 it was commercialized by CECA S.A. (France) under the name Biopolymer CS® (Sandford 1979). Subsequently, SATIA (a division of Mero Rousselot) produced Sclg under the name of Actigum CS6 and CS11 (Morris, 1987), but nowadays it is possible to buy Sclg from Cargill (Minneapolis), from CarboMer (San Diego, California) and Degussa (Hanau, Germany). The main use of Sclg was in chemically enhanced oil recovery, acting as a viscosifier in watered-out oil reservoirs, as well as in oil drilling, stabilizing oil mud and improving its mobility. Sclg can also be used in the food industry, where it functions as a bodying, gelling or stabilizing agent. The use of Sclg as an antitumor, antiviral, and antimicrobial compound has also been investigated [19-22]. Sclg has shown immune stimulatory effects [23], compared with other biopolymers, and its potential contribution to the

treatment of many diseases should be taken into account in therapeutic regimes [24]. Sclg, in particular, also seems to be potentially useful for the formulation of modified release dosage forms and numerous studies have been devoted to this specific topic [25-29].

Because of its peculiar rheological properties and its resistance to hydrolysis, temperature and electrolytes, Sclg has various industrial applications, especially in the oil industry for thickening, drilling muds and for enhanced oil recovery [30-31]. Other industrial uses include the preparation of adhesives, water colours, printing inks and liquid animal feed composition [32]. In the cosmetic industry, Sclg may be used in hair control compositions [33] and in various skin care preparations, creams and protective lotions [34-35]. In pharmaceutical products, Sclg may be used as a laxative [36] in tablet coatings [37] and in general to stabilize suspensions. In the food industry, numerous Japanese patents describe quality improvements of frozen foods [38], Japanese cakes [39], steamed foods [40], rice crackers [41] and bakery products [42]. Sclg is a branched homopolysaccharide that gives only D-glucose upon complete hydrolysis.

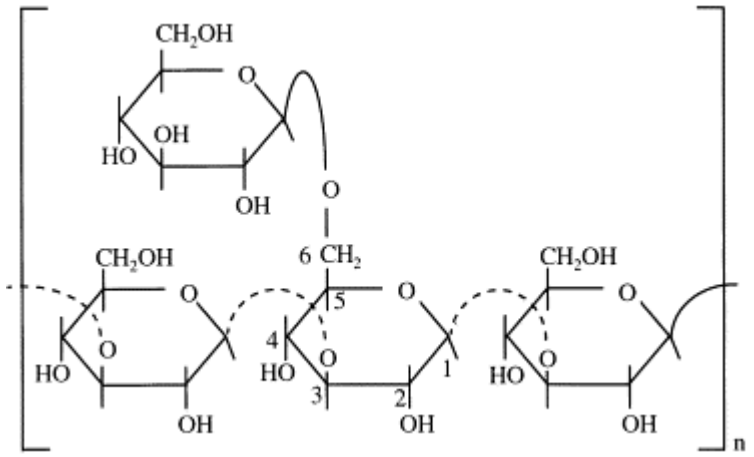

Figure 2. Scleroglucan repeating unit.

The polymer consists of a main chain of (1→3)-linked β -D-glucopyranosyl units; every third unit it bears a single β -D-glucopyranosyl unit linked (1→6) (Figure 2).

The length of the polymer chain and hence the molecular weight varies according to the microbial cultures used. Sclg is synthesized extracellularly by species of the genus *Sclerotium*, i.e., *S. glucanicum*, *S. rolfsii*, and *S. delphinii*. The first two species mainly used for the Sclg

production [43-44], *S. glucanicum* and *S. rolfsii* are heterotrophic, filamentous fungi which are characterized as plant pathogenes and parasites. They possess enzymes which enable them to attack plant cells [45]. The role of Sclg in the life of the organism is mainly to assist in the attachment to plant surfaces and the protection of sclerotia against unfavorable environmental conditions, e.g., desiccation [46]. Sclg may have a role as a energy reserve: the presence of hydrolytic enzymes in *Sclerotium* species which can degrade Sclg into glucose molecules, indicates that the biopolymer may be utilized by the microorganism when other carbon sources are depleted.

A very important attribute of Sclg is its function as a biological response modifier. Many β-glucans show antitumor and antimicrobial activity, but Sclg seems to have a greater effect than other polysaccharides [19, 21]. The mode of action against herpes virus [47] and rubella virus [48] has been investigated. The key reaction of the inhibitory effect seems to be the binding of Sclg with glycoproteins of the cell membrane, which impedes interactions between the virus and the host cell plasma, with a mechanism similar to that proposed for the inhibition of HIV virus replication reported for sulfated biopolymers [49]. As far as the antitumor activity of Sclg is concerned, it was suggested [21, 50] that it occurs through the increase in number and activity of macrophages in the presence of water-soluble β-D-glucans. The structural conformation plays also a vital role. In some cases, as in macrophage stimulation, the existence of a triple helix is important while in the case of lipopolysaccharide-triggered tumour necrosis factor synthesis, a single helix Sclg was more effective [51]. Studies concerning the immunological effects of neutral glucans, including Sclg, revealed [51-52] that Sclg has high affinity for human monocytes and possess two primary biological activities: the stimulation of phagocytic cells and monocyte, neutrophil and platelet hematopoietic activity.

The greatest potential market for Sclg is the oil industry. Recently, the attractive properties of the polymer in controlled drug release and especially in immunopharmaceutical applications have created a demand in the medical market, though in terms of quantity this market is comparatively limited. Sclg is also not used to any great extent in the food industry because of its high cost, despite its thickening and stabilizing abilities that might be exploited in several foodstuffs. Sclg could be especially useful in food manufacturing where a heating process is involved, because of the thermal stability that it exhibits.

Oriented fiber X-ray diffraction indicates that Sclg has a triple-helical backbone conformation and also that dissolved Sclg chains assume a rod-like triple helical structure, in which the D-glucosidic side groups are on the outside and prevent the helices from coming close to each other and aggregating. In dimethyl sulfoxide, or in solutions of pH=12.5 or higher, Sclg molecules are dispersed as single chains (Figure 3) [53-56]. Sclg, and its derivatives, have been extensively studied and seem to be good candidates for the preparation of matrices suitable for sustained drug release [57-60].

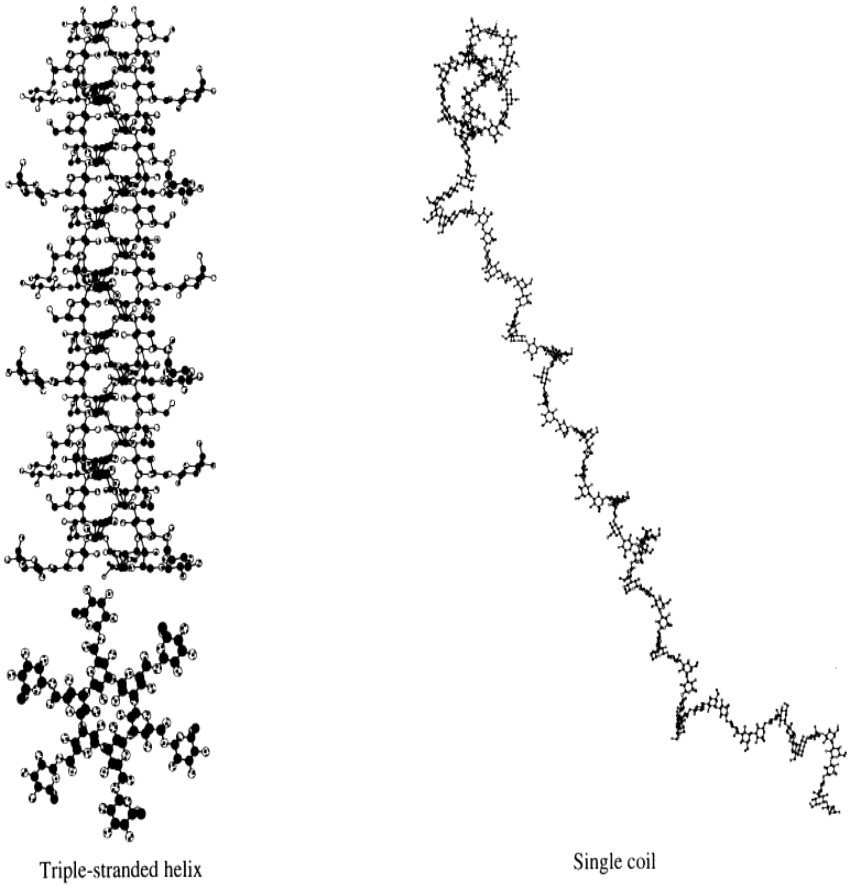

Figure 3. Molecular models for Scleroglucan triple helix and single coil [56].

It is well known that polysaccharides can form gels in the presence of borate ions [61-62] and also that Sclg is able to react with borax [63-64] to give a three-dimensional network. The gel, in this case, is very peculiar as it appears to be formed *via* both physical and chemical linkages [65].

The effect of borate ions is crucial is in organizing the triple helices of Sclg in a more compact arrangement, leading to a more rigid polymeric network. The flow properties of the polysaccharide (Figure 4) are those typical of a macromolecular system with a shear thinning behaviour and a Newtonian region at low shear stress values. The presence of borax does not modify qualitatively the dependence of η from τ, while it determines a noticeable increase of the Newtonian plateau and a shift towards higher values of the shear stress at which the system starts to flow; furthermore, such effect is strongly dependent on polymer concentration.

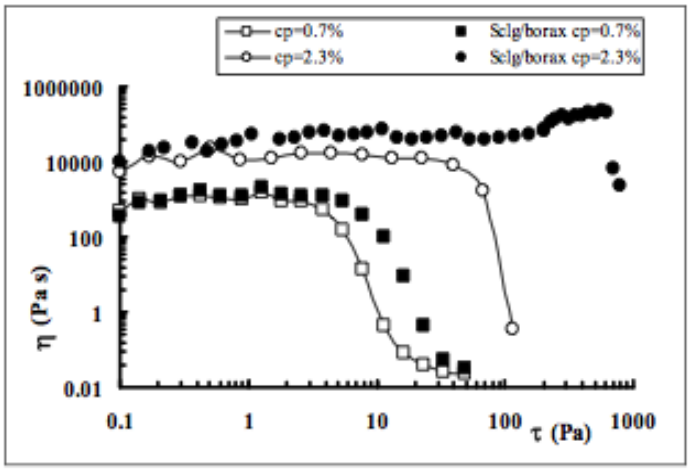

Figure 4. Flow curves at 25 °C for Sclg and Sclg/borax (cp = 0.7 and 2.3 %(w/v)) [29].

Similar effect was found in terms of hardness, adhesiveness, force of cohesion, and force of adhesion of Sclg alone and in presence of borax when a change of more than two orders of magnitude was recorded in the values of these parameters [29].

Model molecules of different size, Theophylline (TPH), Vitamin B12 (Vit. B12) and Myoglobin (MGB), were loaded inside the gel and release studies [11] were performed (Figure 5).

Figure 5. Release profiles of TPH, Vit. B12 and MGB from gel in Simulated Intestinal Fluid at 37 °C [11].

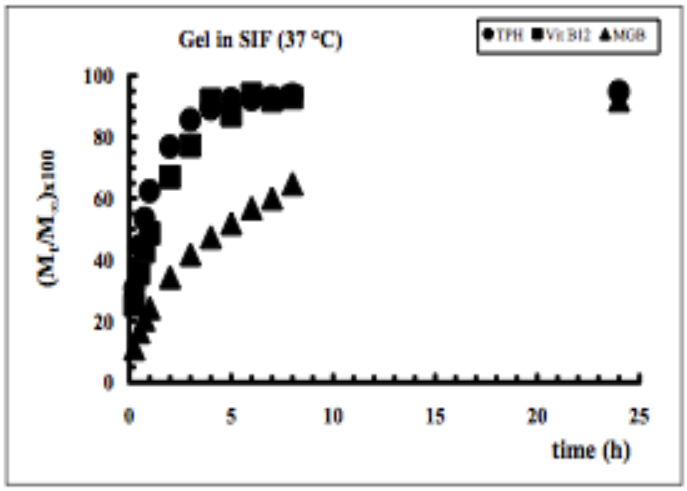

The gels were used also for the preparation of tablets and the delivery of the guest molecules was followed (Figure 6) [29].

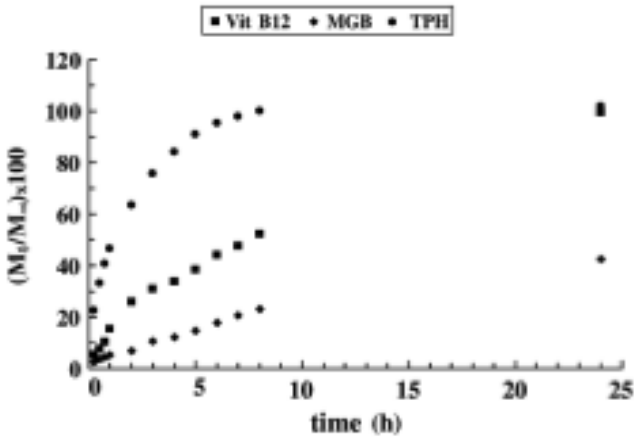

Figure 6. Release profiles of TPH, Vit. B12 and MGB from tablets in distilled water and 37°C [29].

It was clear that the gel modulates the release of the guest molecules as a function of their steric hindrance with relation to the mesh size of the network formed with borate ions.

By means of conformational analysis and molecular dynamics calculations a structure of the hydrogel was proposed [29] in which the diol groups of the side chains of Sclg react with borate ions, *via* chemical and physical interactions. A diligand complex is formed in which the borate ions act as "bridge-atoms" between the polysaccharide chains, leading to a three-dimensional network with some kind of channels along which small molecules can be allocated (Figure 7).

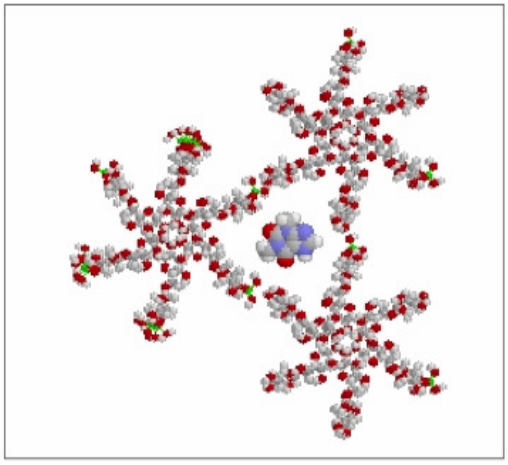

Figure 7. Proposed structure for Sclg/borax gel loaded with TPH, showing the channel obtained from the aggregation of three helices including a molecule of the model drug [29].

Tablets, prepared with Sclg/borax system, showed [28] a peculiar anisotropic swelling (Figure 8).

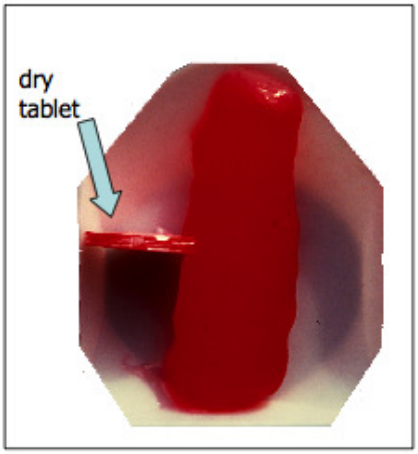

Figure 8. Picture of a tablet before (left) and after (right) swelling.

This unusual and unique swelling behaviour was related [65] to the microscopic structure: a series of triple helices (i.e., rod-like molecules), tied together by the "glue borax" along a preferential direction that corresponds, for energetic reasons, to the helix axis as supported by molecular dynamic simulations (Figure 9).

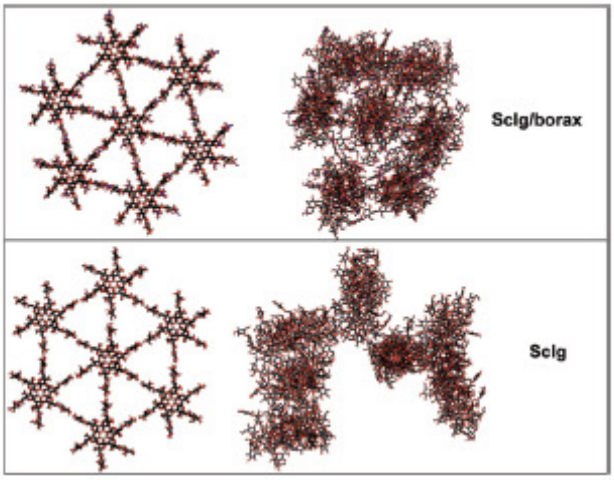

Figure 9. Top view of the starting (left) and final (right) structures in the simulation of seven triplexes with (top) and without (bottom) borax [65].

2.2. Galactomannans

Galactomannans are seed gums, widely diffused in nature. Found mainly in the endospermic parts of the seed, these gums serve as food reserves for seed germination (Figure 10).

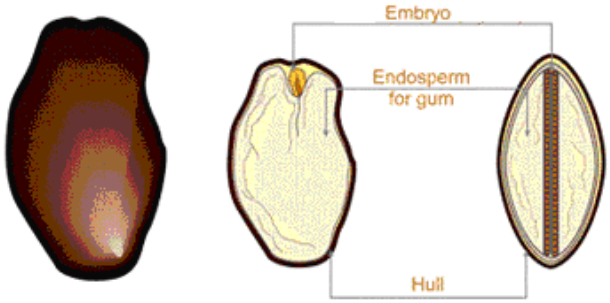

Figure 10. Endospermic section of the seed for gums extraction.

The viscosity and thickening properties of seed gums have found many applications in the food and nonfood industries, such as paints, cosmetics, paper products, and pharmaceuticals [66]. In particular Guar Gum (GG) and Locust Bean Gum (LBG) may be used in food in accordance with

the FDA Code of Federal Regulations Title 21, Section 184.1339 and 184.1343 respectively (see Table 2).

Table 2. Maximum usage level (%) of Guar and Carob bean gum permitted in accordance with the FDA code of Federal Regulation Title 21 [16].

Food (as served)	*Guar gum*		*Carob bean gum*	
	Level	*Function*	*Level*	*Function*
Baked goods and baking mixes	0.35	Emulsifier and emulsifier salts, formulation aid, stabilizer and thickener	0.15	Stabilizer and thickener
Beverages and beverage bases, nonalcoholic			0.25	Stabilizer and thickener
Breakfast cereals	1.20	Formulation aid, stabilizer and thickener		
Cheese	0.80	Formulation aid, stabilizer and thickener	0.80	Stabilizer and thickener
Dairy products analogs	1.00	Firming agent, formulation aid, stabilizer and thickener		
Fats and oils	2.00	Firming agent, formulation aid, stabilizer and thickener		
Gelatins, puddings, and fillings			0.75	Stabilizer and thickener
Gravies and sauces	1.20	Formulation aid, stabilizer and thickener		
Jams and jellies (commercial)	1.00	Formulation aid, stabilizer and thickener	0.75	Stabilizer and thickener
Milk products	0.60	Formulation aid, stabilizer and thickener		
Processed vegetables and vegetable juices	2.00	Formulation aid, stabilizer and thickener		
Soups and soup mixes	0.80	Formulation aid, stabilizer and thickener		
Sweet sauces, toppings and syrups	1.00	Formulation aid, stabilizer and thickener		
All other food categories	0.50	Formulation aid, stabilizer and thickener	0.50	Stabilizer and thickener

Guar Gum seeds yield a high level of galactomannan from the endosperm (42%), most of it (80%) being soluble, only slightly lower than in the case of Locust Bean Gum (48%).

Guar gum and Locust Bean Gum are extracted from the seeds of *Cyamopsis tetragonolobus* and from the seeds of *Ceratonia siliqua*, two evergreen and leguminous plants (Figure 11), respectively.

Figure 11. Extraction of Guar Gum and Locust Bean Gum from *Cyamopsis tetragonolobus* (left) and *Ceratonia siliqua* seeds (right) respectively.

The galactomannans consist of a linear backbone of β(1-4)-linked D-mannose units (M) and are solubilized by the presence of randomly attached α(1-6)-linked galactose units (G) as side chains [67]. The individual galactomannans differ from each other in their mannose/galactose ratio (Man/gal) and distribution pattern of the G residues along the mannan chain (Table 3).

Table 3. Mannose/galactose ratio and galactosyl distribution of selected galactomannans [16].

Galactomannan	Man/gal ratio	Distribution	Reference
Guar	1.40–1.83	Blockwise	1, 2
Tara	2.50–3.00	Random and blockwise	1, 2
Carob bean	3.20–5.73	Random, blockwise, and ordered	1, 2, 3
Cassia	3.00–8.40	Regular	1, 2, 3
Fenugreek	1.10–1.20	Highly substituted	1, 4
Mesquite	1.20–4.65	Blockwise	1, 2, 5, 6, 7

In particular Man/gal ranges from 1.4:1 to 1.8:1 for Guar Gum and is ca. 3.5 for Locust Bean Gum (Figure 12 a and b). These differences are apparently due to climate variations.

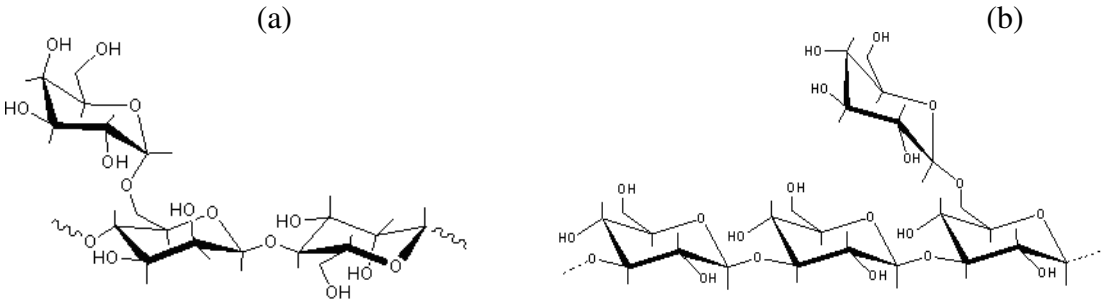

Figure 12. Repeating unit of Guar Gum (a) and Locust Ben Gum (b).

All commercially available Guar samples show a blockwise distribution of galactose while the greatest variations are found with Locust Bean Gum (carob bean) where random, blockwise, and ordered galactose distributions were observed (Figure 13).

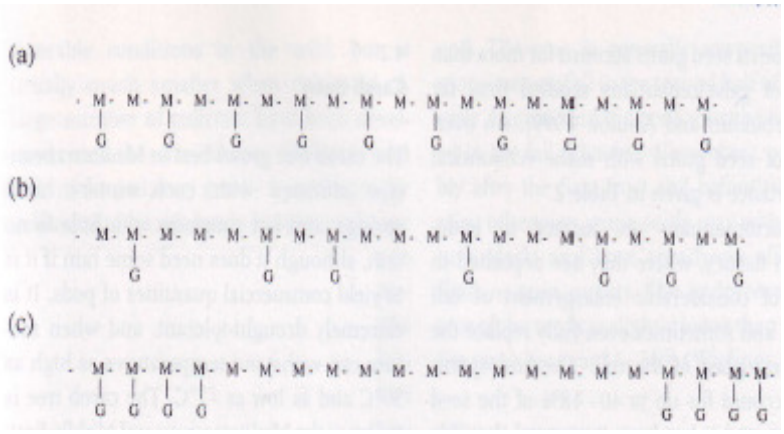

Figure 13.Arrangements of galactosyl side chain in galactomannans.(a) Regular; (b) random distribution; (c) blockwise distribution [16].

Usually, the β-1, 4-mannans, like galactomannans, adopts the conformation of rigid, ribbon-shaped chains. The chains can approach each other to form a supramolecular structure, which can only be solvated from the surface. Inner regions remain inaccessible to the solvent molecules, and the partial solvation is insufficient for solubilization of aggregated molecules. Side chains of the linear chain, like galactose in the galactomannans, prevent the macromolecules from approaching each other closely and thus restrict the possibility of the formation of dense aggregates [68].

The solubility of galactomannans in water depends on the galactose content. GG, with a high

galactose content, swells and dissolves in cold water (70-90%) while LBG is only 10% soluble in cold water and must be heated to temperatures above 80 °C.

The Guar plant is native of Northwest India and Pakistan, where it is of considerable importance. Guar means “cow food” in Hindi, and in the Asian region this is its historical use. Indeed, parts of the Guar plants are still used as cattle feed today. The plant is extremely drought-resistant, and grows in areas with small rainfalls where most other plants would perish. In India, the green pods are picked young and cooked: the Guar protein is not usable by humans unless toasted to destroy the trypsin inhibitor. It was introduced into the USA at the beginning of the twentieth century (1903), and became a commercial commodity in 1940. The technology of GG extraction was commercialized in 1953 in the USA, and about 10 years later in India. Unlike the Locust Bean tree, which grows to a height of about 15 m in favourable conditions, the Guar plant reaches a height of only 1-2 m at full growth, and is grown as an annual crop. The growing season is about 20-25 weeks. The seed pods grow in cluster on the vertical stalks, and are about 5-10 cm in length. Each pod holds six to nine grayish-white pea-shaped seeds, each of which is about 2-3 mm in diameter. The plant requires intermittent rainfall with an abundance of sunshine. Too much rain may lead to a more leafy plant but also to a reduction in the number of pods and the number of seeds per pod. The annual world market for GG has been estimated by P.L. Thomas & Co, Inc. (USA) to be around 150,000 tons of powder and/or splits, with India and Pakistan accounting for about 70% of this production. The unique, thickening properties of LBG and GG have found extensive applications in several industries, including food, mining, pharmaceuticals, explosives, and petroleum technology. The viscosity and thickening properties of the other galactomannans are quite similar to those of GG and LBG, although most of them are obtained in much lower yields. Therefore, only LBG and GG are used extensively [16].

GG has proven particularly useful for colon delivery as it can be degraded by the specific enzymes present in this tract of the intestine. Like other polymers used for colon targeting, GG can protect the drug in the stomach and the small intestine environment, while it delivers the drug to the colon where it undergoes assimilation by specific microorganisms or degradation by the enzymes, leading to the final delivery of the drug. Hence, it is used to form prodrugs, as a coating material or as a hydrogel entrapping drugs inside its network [12, 16]. GG, like Sclg can form gel in the presence of borate ions. Very peculiar was the behaviour observed for the tablets prepared with GG/borax system.

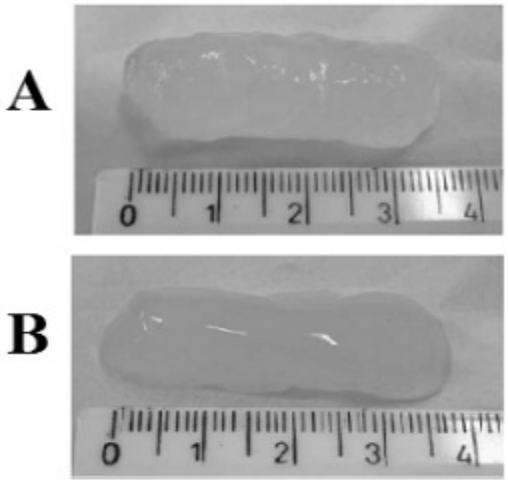

Figure 14. Tablets of Sclg/borax (A) and GG/borax (B) after swelling for 24 h in distilled water at 37 °C [71].

An interesting anisotropic swelling was observed (Figure 14); similar to that shown by the Sclg/borax tablets, although GG assumes a flexible random coil conformation in water and Sclg is one of the more rigid polymers in nature. Also the interaction with borax takes place in a different way. In the case of Sclg the borax promotes mixed (chemical and physical) interactions between triplexes; on the contrary, in the case of GG the borax forms chemical bridges between chains by means of reversible linkages, as evaluated by molecular dynamics simulation [69].

2.3. References

1. Marchessault R H, Ravenelle F, Zhu X X. Polysaccharides for Drug Deliv Pharm applications ed. ACS Symposium series 934, Oxford University Press, Washington (USA). 2006.

2. Dumitriu S. Polymeric biomaterials. Marcel Dekker Inc (USA).1994.

3. L. Brannon-Peppas. Polym Control Drug Deliv. Medical plastics and biomaterials. 1997.

4. Dee K C, Puleo D A, Bizios R. An introduction to Tissue-biomaterial interactions. J Wiley & Sons inc. Hoboken (New Jersey). 2002.

5. Hoffman A S. Adv Drug Deliv Rev. 2002;43:3.

6. Peppas N A,Bures P, Leobandung W,Ichikawa H. Eur J Pharm Biopharm. 2000;50:27.

7. Kikuchi A,Okano T. Adv Drug Deliv Rev. 2002;43:53.

8. Coviello T, Matricardi P, Alhaique F. Expert Opin Drug Deliv. 2006 ;3:395.

9. Matricardi P, Di Meo C, Coviello T, Alhaique F. Expert Opin Drug Deliv. 2008;5:417.

10. Coviello T, Matricardi P, Marianecci C, Alhaique F. J Control Release.2007;119:5.

11. Coviello T, Palleschi A, Grassi M, Matricardi P, Bocchinfuso G, Alhaique F. Molecules. 2005; 10:6.

12. Peppas N A, Bures P, Leobandung W, Ichikawa H. Eur J Pharm Biopharm. 2000;50:27.

13. Vandamme E J, Baets S D, Steinbüchel A. Biopolymers Biology, Chemistry, Biotechnology, Applications, Polysaccharides II.Wiley VCH Weinheim (Germany). 2002;5:135.

14. Whistler R L, Be Miller J N. Industrial gums polysaccharides and their derivates. (3rd edn) ed. Academic Press, New York (USA).1993.

15. Illum L. Pharm Res.1998; 15:1326.

16. Vandamme E J, Baets S D, Steinbüchel A. Biopolymers Biology, Chemistry, Biotechnology Applications, Polysaccharides II (polysaccharides from Eukarotes). Wiley VCH Weinheim (Germany). 2002;6:37.

17. Maeda M, Shimahara H, Sugiyama N. Agric Biol Chem.1980; 38:315.

18. Halleck F E. US Patent No. 3,301,848.1967. Chem Abstr. 1967; 66: 84772b.

19. Singh P, Wisler R, Tokuzen R, Nakahara W. Carbohyd Res. 1974;37:245.

20. Jong S, Donovick R. Adv Appl Microbiol.1989; 34:183.

21. Pretus H, Eusley H, McNamee R, Jones E, Browder I, Williams D. J. Pharmacol Exp Ther. 1991; 257:500.

22. Mastromarino P, Petruzziello R, Macchia S, Rieti S, Nicoletti R, Orsi N. J. Antimicrob Chemother.1997;39:339.

23. Patchen L, Bleicher P. US Patent No. 2000; 6,117,850.

24. Giavasis I, Harvey L M, McNeil B. Scleroglucan in Biopolymers Polysaccharides II. 2002; 6:37.

25. Coviello T, Grassi M, Rambone G, Santucci E, Carafa M, Murtas E, Riccieri F M, Alhaique, F. J Control Release. 1999;60:367.

26. Coviello T, Grassi M, Rambone G, Alhaique F. Biomaterials. 2001; 22:1998.

27. Coviello T, Dentini M, Rambone G, Desideri P, Carafa M, Murtas E, Riccieri F M, Alhaique F. J Control Release. 1998;55:57.

28. Coviello T,Grassi M, Lapasin R, Marino A, Alhaique F. Biomaterials. 2003;24:2789.

29. Coviello T, Coluzzi G, Palleschi A,Grassi M, Santucci E, Alhaique F. Intl J Biol Macromol. 2003;32:83.

30. Doster M S, Nute A J, Christopher C A.US Patent. 1984; 4,457,372. Chem Abstr.1984, 101, 113713g.

31. Pirri R, Gadioux J, Riveno R. Societé Nationale Elf Aquitaine (Courbevoie, France). 1996;5, 555,936.

32. Halleck F E. US Patent.1969; 3,447,940.Chem Abstr. 1969; 100, 51304a. Fed Reg. 1969; 34, 13162.

33. Halleck F E. US Patent .1970; 3,507,290. Chem Abstr. 1970; 73, 28775n.

34. Halleck F E. US Patent.1972; 3,659,025. Chem Abstr. 1972; 77, 52227p.

35. Dubief C. US Patent.1996; 5,536,493.

36. Duc A N C. Eur. Patent.1982;45:338. Chem Abstr .1982; 96,168769p.

37. Sheth P, Lachman L. Fr Patent .19671; 480,874. Chem Abstr. 1967; 67, 111442y.

38. San-Ei Chemical Industries.Japan Kokai Tokkyo Koho.1982; 57,163,451. Chem Abstr .1983; 98, 15728r.

39. San-Ei Chemical Industries. Japan Kokai Tokkyo Koho.1982;57,163,442. Chem Abstr.1983;98, 15729s.

40. San-Ei Chemical Industries. Japan Kokai Tokkyo Koho.1982;163,163,441. Chem Abstr. 1983;98, 15730k.

41. San-Ei Chemical Industries. Japan Kokai Tokkyo Koho.1982;57,163,440. Chem Abstr.1983;98, 15731m.

42. San-Ei Chemical Industries Japan Kokai Tokkyo Koho.1982;57,163,432. Chem Abstr. 1983;98, 15732n.

43. Wang Y, Mc N B. Enzyme Microb Tech.1995; 17:893.

44. Schilling B, Henning A, Rau U. Bioprocess Eng.2000; 22:51.

45. Wang Y, Mc N B. Rev Biotechnol.1996;63:215.

46. Backhouse D. Trans. Br. Mycol Soc. 1987; 89:561.

47. Marchetti M, Pisani S, Petropaolo V, Seganti L, Nicoletti R, Degener A, Orsi N. Planta Medica. 1996;62:303.

48. Mastromarino P, Petruzziello R, Macchia S, Rieti S, Nicoletti R, Orsi N. J. Antimicrob Chemother. 1997;39:339.

49. Jagodzinski Paul P, Wiaderkiewicz R, Kurzawski R, Kloczewiak M, Nakashima H, Hyjek E, Yamamoto N, Uryu T, Kaneko Y, Posner M R, Kozbor D. Virology.1994;202:735.

50. Ohno N, Miura N, Chiba N, Adachi Y, Yadomae T. Biol Pharm Bull.1995;18:1242.

51. Jamas S, Easson J, Davidson D. US Patent No. 1998; 5,817,643.

52. Jamas S, Easson J, Davidson D. US Patent No. 1998; 5,783,569.

53. Bluhm T L, Deslandes Y, Marchessault R H,Perez S, Rinaudo M. Carbohyd Res.1982;100: 117.

54. Bluhm T L, Deslandes Y, Marchessault R H,Perez S, Rinaudo M. Molecules 2005;10:30.

55. Yanaki T, Norisuye T. Polymer J. 1983;15:389.

56. Maeda H, Rambone G, Coviello T, Yuguchi Y, Urakawa H, Alhaique F, Kajiwara K. Int J Biol Macromoleules. 2001;28:351.

57. Touitou E, Alhaique F, Riccieri F M, Riccioni G, Santucci E. Drug Des Deliv.1989;5:141.

58. Rizk S, Duru C, Gaudy D, Jacob M, Ferrari F, Bretoni M, Caramella C. Int J Pharm. 1994;112:125.

59. Alhaique F, Feltrami E, Riccieri F M,Santucci E. Drug Des Deliv. 1990;5:249.

60. Alhaique F, Carafa M, Riccieri F M, Santucci E, Touitou E. Pharmazie .1993;48:432.

61. Deuel H, Neukom H,Weber F. Nature. 1948; 161:96.

62. Shibayama M, Yoshizawa H, Kurokawa H, Fujiwara H,Nomura S. Polymer. 1988;29:2066.

63. Sandford P. Adv Carbohydr Chem Biochem.1979;36:265.

64. Brigand G, Whistler R L, BeMiller J N. Eds Academic Press.1993; 17: 46.

65. Bocchinfuso G, Palleschi A, Mazzuca C, Coviello T, Alhaique F, Marletta G. J Phys Chem B. 2008;112:6473.

66. Soni S K, Bose S. J Sci Ind Res.1985; 44:544.

67. Scherbukhin V D, Anulov O V. Appl Biochem Microbiol.1999; 35:229.

68. Whistler R L. Adv Chem Ser. 1973;117:242.

69. Bocchinfuso G, Mazzuca C, Sandolo C, Margheritelli S, Alhaique F, Coviello T,. Palleschi A. J Phys Chem B. 2010; 114:13059.

3. Hydrogels

Hydrogels are three-dimensional, hydrophilic, polymeric networks capable of imbibing large amounts of water or biological fluids.

The networks are composed of homopolymers or copolymers, and are insoluble due to the presence of chemical crosslinks (tie-points, junctions), or physical crosslinks, such as entanglements or crystallites (Figure 1). The latter provide the network structure and physical integrity.

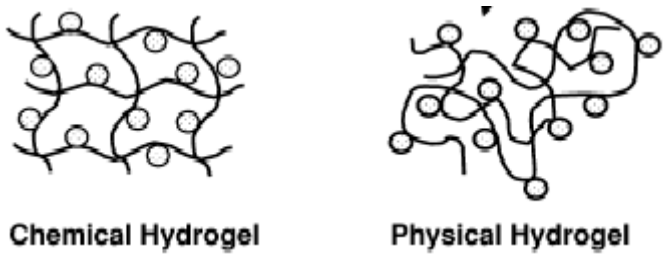

Figure 1. Schematic representation of hydrogels.

Hydrogels can be classified as neutral or ionic, based on the nature of the side groups. They can be homopolymer or copolymer networks, based on the method of preparation. Finally, they can be classified based on the physical structure of the networks as amorphous, semicrystalline, hydrogen-bonded structures, supramolecular structures and hydrocolloidal aggregates [1].

Hydrogels may show a swelling behavior dependent on the environment. Some polymers can form physiologically-responsive hydrogels, where polymer complexes can be broken or the network can be swollen as a result of environmental variations. Thus, these systems may show drastic variations in their swelling ratio. Some of the factors affecting the swelling of physiologically-responsive hydrogels are listed in Table 1 [2].

Table 1. Effects of various external stimuli on different stimuli-responsive hydrogels [2].

Stimulus	Hydrogel type	Release mechanism
pH	Acidic or basic	A change in pH causes swelling of the hydrogel.
Ionic strength	Ionic	Change in ionic strength causes a change in the concentration of ions inside the gel. This causes a change in swelling.
Chemical species	Electron-accepting groups	Electron-donating compounds cause charge transfer. This causes a change in swelling.
Enzyme substrate	Immobilized enzymes	When a substrate is present enzymatic conversion occurs. The product causes swelling.
Magnetic	Magnetic particles in microspheres	An applied magnetic field causes a change in pores in gel. This results in change in swelling.
Thermal	Thermo-responsive	Change in temperature causes a change in polymer–polymer and water–polymer interactions. This causes a change in swelling.
Electrical	Polyelectrolyte	Applied electric field causes membrane charging. Electrophoresis of charged drug changes swelling.
Ultrasound	Ethylene-vinyl alcohol	Ultrasound irradiation causes temperature increase.

Among the numerous macromolecules that can be used for hydrogel formation, polysaccharides are extremely advantageous, compared to synthetic polymers, being widely present in living organisms and often being produced by recombinant DNA techniques. Coming from renewable sources, polysaccharides have also frequently economical advantages over synthetic polymers.
There are numerous applications of these hydrogels, in particular for medical and pharmaceutical purposes, due to the fact that hydrogels resemble natural living tissue more than any other class of synthetic biomaterials. This is due to their high water contents and soft consistency which is similar to that of natural tissues. Furthermore, the high water content of the materials contributes to their biocompatibility. Thus, hydrogels can be used as contact lenses, membranes for biosensors, linings for artificial hearts, materials for artificial skin, and drug delivery devices [3, 1].

3.1. Nanoparticles-nanohydrogels

Definition of nanoparticles

Nanoparticles (NPs) are colloidal particles with a diameter between 10 and 1000 nm. The nanoparticles are ultrafine particles in the size of nanometer order. “Nano” is a prefix denoting the minus 9th power of ten, namely one billionth. Here it means nanometer (nm) applied for the length (Figure 2). One nm is extremely small length corresponding to one billionth of 1 m, one millionth of 1 mm, or one thousandth of 1μm. In the larger scope of nanotechnologies applied to

biomedical and pharmaceutical samples, nanoparticles offer new therapeutic opportunities. Different types of nanoparticles can be used as drug delivery systems and each of them can be made with different materials, with a particular structure which allows achieving the stated objectives in the treatment of a particular disease.

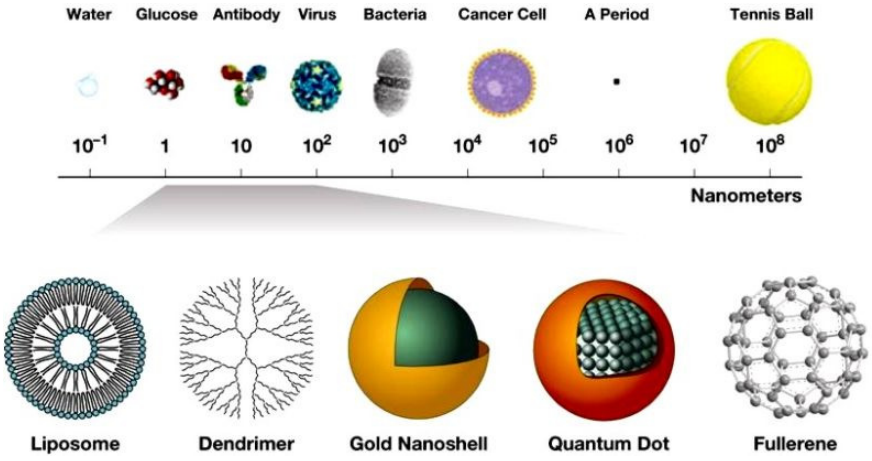

Figure 2. Scheme of the nanoparticle sizes.

The active ingredient can be encapsulated or entrapped in the nanoparticle or it can simply be attached. The NPs, thanks to the small size, are able to easily overcome the barriers of the organism through the capillaries to reach the individual cells. All this guarantees an efficient accumulation of the drug at the target and a series of advantages that include:

- Increase in water solubility of the drug
- Protection of the drug from degradation
- Controlled release of the drug
- Increased bioavailability of the drug
- Reduction of toxicity and side effects of the drug

The possible applications are numerous, but the stability of such systems always deserves attention for this reason, surfactants or surface modifiers are adsorbed or grafted on the surface of the nanoparticles so as to generate repulsive forces which prevent their inactivation. The most used method for imparting stability to the NPs consists in "PEGylation ": this is the "decoration" of the surface of the same with chains of polyethylene glycol (PEG) through adsorption,

entrapping, grafting or copolymerization method. The latter has the advantage of slowing down desorption of the PEG molecules and to improve the stability of the system even if it does not allow to control and optimize the amount of surface coverage and conformation. Several theories have been proposed to explain the improved stability imparted by PEG to NPs. According to the most accepted theory, the flexibility of the surface of PEG chains, allows them to assume an extended conformation in solution: in this way when the opsonins present in the circulation are attracted to the surface of the NPs by Van deer Waals forces meet the PEG chains and compress. This compression results in a conformational change in the PEG molecules to a state with the highest energy which in turn determines the appearance of repulsive forces. This latest, if sufficiently intense, may counteract or even exceed the attractive forces between the NPs but also between the same NPs and opsonins, preventing the interaction and increasing in this way the residence time in the circulation [4]. Opsonins, in fact, are proteins that bind to the surface of foreign particles present in the circulation and make them easily recognizable by phagocytes that, through the process of phagocytosis, contribute to their removal from blood.

Hydrogel nanoparticles, NPs (recently referred to as nanogels) have been the point of convergence of a considerable amount of efforts devoted to the study of these systems dealing with drug delivery approaches. Interestingly, hydrogel nanoparticulate materials would demonstrate the features and characteristics hydrogels and NPs separately posses, at the same time. Therefore, it seems that the pharmacy world will benefit from the hydrophilicity, flexibility, versatility, high water absorptivity, and biocompatibility of these particles and all the advantages of the NPs, mainly long life span in circulation and the possibility of being actively or passively targeted to the desired biophase, e.g. tumor sites. Different methods have been adopted to prepare NPs of hydrogel consistency. Besides the commonly used synthetic polymers, active research is focused on the preparation of NPs using naturally occurring hydrophilic polymers. This text presents various types of nanogels prepared and characterized, using a classification based on the type of polymeric materials used in preparation of the NPs.

Nanometer-sized structures are gaining increasing interest for their unique properties and performance which result from their small size. There are a number of hard nanomaterials, including metals and ceramics, which have been extensively explored and characterized. Soft materials, such as polymer gels that exhibit mutability and responsiveness to their surroundings

can also be engineered to form nanostructured products. The mutability and responsiveness of these materials have led to a great deal of research interest for potential applications including drug delivery carriers [5], sensors [6], nanoreactors [7], and bio-mimetic mechanical devices [8] (e.g., artificial muscle), as are shown in Figure 3.

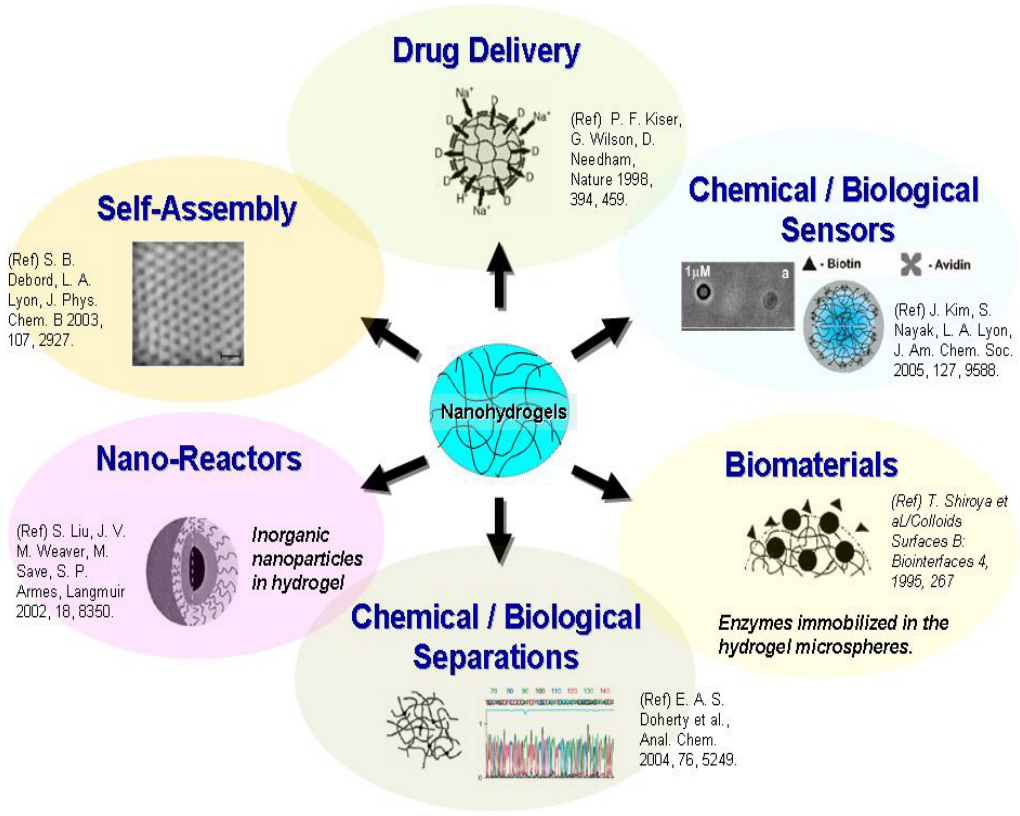

Figure 3. Applications of nanohydrogels.

Polymer gels may be categorized by their dimensions as either nano- or macroscopic gels, and each type may be selectively produced through the control of the gel-forming crosslinking reactions used to produce them. The inter-molecular crosslinking process which yields macroscopic gels has been extensively studied and is relatively well understood [9-12]. However, the radiation-induced synthesis of polymer nanogels, which is based on an intra-molecular crosslinking process, is less explored. An understanding of the mechanism of crosslink formation is very important in order to control the final, physical properties (e.g., size, conformation, molecular weight, crosslinking density, etc.) of the produced nanohydrogel materials.

Classification of nanoparticles

The classification of nanoparticles is fundamentally based on the constituent material of the same, and then they depend on the size and therefore the possible applications (Figure 4). In particular, are mentioned:

- SLNPs (Solid lipid nanoparticles). They consist of triglycerides, waxes and glycerides solids, both at ambient temperature to body temperature, stabilized by surfactants.
- CNPs (Ceramic nanoparticles). They are made with inorganic materials which in some cases have its therapeutic effects, but which do not show swelling or variations of porosity with the pH. The dimensions are very small (less than 50 nm).
- MNPs (Magnetic nanoparticles). It is a suspension of magnetic nanoparticles, functionalized surface with the drug, dispersed in an organic or inorganic fluid which acts as a carrier and which allows concentrating the drug at the site of interest through the application of magnetic fields.
- MBN (Metal based nanoparticles). Have extremely small size and high surface area allows them to deliver relatively high doses of the drug.
- Polymeric nanoparticles are biodegradable and biocompatible, also show high possibility of functionalization and derivatization with different compounds

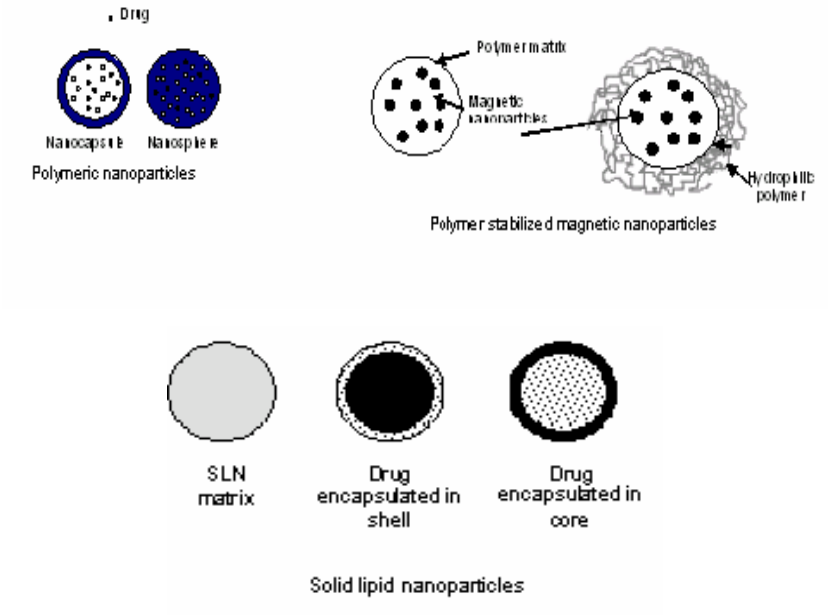

Figure 4. Schematic representation of the various types of NPs.

Methods of preparation NPs

The NPs, such as systems for drug delivery are carrier nanosized used as carrier for the release of drugs or biomolecules. Generally carriers include nanoscale particle sizes less than 1000 nm of different morphologies, including nanospheres, nanocapsules, nanomicelle, nanomedicines, etc.

The NPs are capable of:

- go through tiny capillaries to their small volume and avoid rapid clearance by phagocytes, so they remain in the blood stream is greatly prolonged.
- penetrate the cells and the intercellular spaces to get to organs such as liver, lymph nodes or spleen.
- show controlled release properties resulting from their properties such as biodegradability, sensitivity to T and the pH.
- increase the release of the drug and decrease its possible toxicity.

The NPs can be used for the controlled release of drugs, peptides, proteins, vaccines, nucleic acids, etc. Over time they have shown great potential in the field of biological, medical and pharmaceutical [13].

The materials used for the preparation of NPs for drug delivery must have properties of biocompatibility, biodegradability and lack of toxicity. For this purpose the methods of preparation of polysaccharide NPs can be classified according to four mechanisms of interaction:

1) Covalently crosslinked polysaccharide nanoparticles

In this type of preparation include various polysaccharides, including chitosan was previously used as crosslinker glutaraldehyde. Its toxicity has limited their use in the field of drug delivery [14]. Along with the use of biocompatible crosslinkers, biocompatible covalent crosslinking is promising. With the aid of water-soluble condensation agent of carbodiimide, natural di- and tricarboxylic acids, including succinic acid, malic acid, tartaric acid and citric acid, were used for intermolecular crosslinking of chitosan nanoparticles.

2) Ionically crosslinked polysaccharide nanoparticles

Compared with covalent crosslinking, ionic crosslinking has more advantages: mild preparation conditions and simple procedures. For charged polysaccharides, low MW of polyanions and polycations could act as ionic crosslinkers for polycationic and polyanionic polysaccharides, respectively. To date, the most widely used polyanion crosslinker is tripolyphosphate (TPP). TPP

is non-toxic and has multivalent anions. It can form a gel by ionic interaction between positively charged amino groups of chitosan and negatively charged counterions of TPP [15].

3) Polysaccharide nanoparticles by polyelectrolyte complexation (PEC)

Polyelectrolyte polysaccharides can form PEC with oppositely charged polymers by intermolecular electrostatic interaction. Polysaccharide based PEC nanoparticles can be obtained by means of adjusting the MW of component polymers in a certain range. In theory, any polyelectrolyte could interact with polysaccharides to fabricate PEC nanoparticles. However, in practice, these polyelectrolytes are restricted to those water-soluble and biocompatible polymers in view of safety purpose. In this sense, chitosan is the only natural polycationic polysaccharide that satisfies the needs. There are many negative polymers complexed with chitosan to form PEC nanoparticles, which can be divided into negatively charged polysaccharides [16], negatively charged peptides [17], polyacrylic acids [18].

4) Self -assembly of hydrophobically modified polysaccharides

When hydrophilic polymeric chains are grafted with hydrophobic segments, amphiphilic copolymers are synthesized. Upon contact with an aqueous environment, polymeric amphiphiles spontaneously form micelles or micelle like aggregates via undergoing intra- or intermolecular associations between hydrophobic moieties, primarily to minimize interfacial free energy. These polymeric micelles exhibit unique characteristics, depending on hydrophilic/hydrophobic constituents, such as unusual rheological feature, small hydrodynamic radius (less than microsize) with core-shell structure, and thermodynamic stability. In particular, polymeric micelles have been recognized as a promising drug carrier, since their hydrophobic domain, surrounded by a hydrophilic outer shell, can serve as a preservatory for various hydrophobic drugs [19]. In recent years, numerous studies have been carried out to investigate the synthesis and the application of polysaccharide-based self-aggregate nanoparticles as drug delivery systems.

APPLICATION OF NANOPARTICLES

The possible applications of nanoparticles are extremely numerous: from antineoplastic therapy to the antimicrobial, the channeling of vaccines to that of vectors for gene therapy, not to mention the possibility of reducing the side effects of drugs in common use. Were carried multifunctional nanoparticles, particularly versatile in gene therapy and as therapeutic agents? Many nanoparticles are useful for their antimicrobial properties and many others are finding use

in molecular diagnostics and imaging, especially of tumors. Some chemotherapeutic agents such as carboplatin, paclitaxel, doxorubicin, etoposide, were introduced in the nanoparticles and nanosystems these have proved very effective in anticancer therapy [20]. A particularly interesting aspect is represented by the influence of NPs on multidrug resistance (MDR), which makes it one of the prime causes of failure of cancer therapy: it can be explained by a reduction in the drug concentration in the tumor tissue, due to the possibility of P-glycoprotein membrane to accelerate the active efflux of the same from the cell.

3.2.References

1. Peppas N A, Bures P, Leobandung W, Ichikawa H. Eur J Pharm BioPharm. 2000; 10:27.
2. Bawa P, Pillay V, Choonara Y E, Du Toit LC. Biomedical Materials. 2009; 4:1.
3. Dee K C, Puleo D A, Bizios R. An introduction to tissue-biomaterial interactions, Wound healing. Hoboken J Wiley & Sons inc. (New Jersey). 2002:165.
4. Owens DE 3rd, Peppas N A. Int J Pharm. 2006; 307:93.
5. Kiser P F, Wilson G, Needham D A. Nature. 1998; 394: 459.
6. Kim B S, Qiu J M. Wang J P, Taton T A. Nano Letters 2005; 5: 1987.
7. Liu S Y, Weaver J V M, Save M, Armes S P. Langmuir. 2002; 18: 8350.
8. Van der Linden H, Herber S, Olthuis W, Bergveld P. Sensors Materials. 2002:14: 129.
9. Kim S W, Bae Y H, Okano T. Pharm Res.1992; 9: 283.
10. Rosiak J M. J Control Release. 1994; 31: 9.
11. Ulanski P, Bothe E, Hildenbrand K, Rosiak J M, VonSonntag C. J Chemical Society-Perkin Transactions II.1996;1: 13.
12. Safrany A.Radiation processing: Synthesis and modification of biomaterials for medical use. Nuclear Instruments & Methods in Physics Research Section B-Beam Interactions with Materials and Atoms.1997; 131:376.

13. Illum L. J Pharm Sci. 2007; 96:473.

14. Zheng Y L, Wu Y, Yang W L, Wang C C Fu S K, Shen X Z J. Pharm Sci. 2006 ;95:181.

15. Jain D, Banerjee R. J Biomed Mater Res. 2008; 86:105.

16. Cui Z R, Mumper R J. J Control Release. 2001;75:409.

17. Lin Y H,Chung C K, Chen C T, Liang H F, Chen S C, Sung H W. Biomacromolecules. 2006;6:1104.

18. Sajeesh S, Sharma C P. J Biomed Mater Res. 2006; 76:298.

19. Zheng F, Shi X W, Yang G F, Gong L L, Yuan H Y, Cui Y J, Wang Y, Du Y M, Li Y. Life Sci. 2007; 80:388.

20. Park J H, Kwon S G, Nam J O, Park R W, Chung H, Seo S B, Kim I S, Kwon I C,Jeong S Y. J Control Release. 2004;95:579.

4. Drug delivery mechanisms

Drug release kinetics may be affected by many factors such as polymer swelling, polymer erosion, drug dissolution/diffusion characteristics, drug distribution inside the matrix, drug/polymer ratio and system geometry (cylinder, sphere, etc.). With only few exceptions (e.g., ophthalmic matrices, due to the dosing together with the physical and chemical stability of the system), matrix systems are stored in dry, shrunken state, i.e. without any liquid phase inside. In this condition, the drug, present in the dry polymeric network, in the form of microcrystals, nanocrystals or in an amorphous state, cannot diffuse through the network meshes. Upon contact with the release fluids (water or physiological media), the polymer chains mobility increases, the network meshes enlarge so that the drug can dissolve and diffuse through the gel layer. Of course, drug diffusion through the swelling network depends on polymer/drug physical and chemical characteristics (a drug adsorption/desorption phenomenon can take place on polymer chains during diffusion) and on the ratio between diffusion and mesh size. Additionally, drug diffusion can be heavily affected by a particular aspect of the matrix topology. Matrix systems can be considered as fractal media for their internal high disorder degree due to complex network topology. If wide network meshes are defined as accessible sites for the diffusing drug and small network meshes as forbidden sites, and if forbidden sites approach a threshold value, the entire network can be seen as a percolative network (fractal network). It can be demonstrated that the diffusion on percolative (fractal) networks, and consequently the release kinetics, significantly differs from diffusion in non-fractal networks. Furthermore, also the drug distribution profile within the matrix (i.e., drug concentration profile) can heavily affect drug release kinetics [1, 2].
Lee [3-5] demonstrated that very different release kinetics can be achieved by properly selecting uniform, sigmoidal, steps or parabolic drug distribution. Additionally, in the case of an uniform drug distribution in a tablet, the dissolution of the drug present at the matrix/release environment interface can give origin to a burst effect in the release profile followed by a slower release. A very clear approach for the representation of polymer swelling/erosion and drug delivery from matrix systems is to observe that three main fronts appear during the release process (Figure 1).

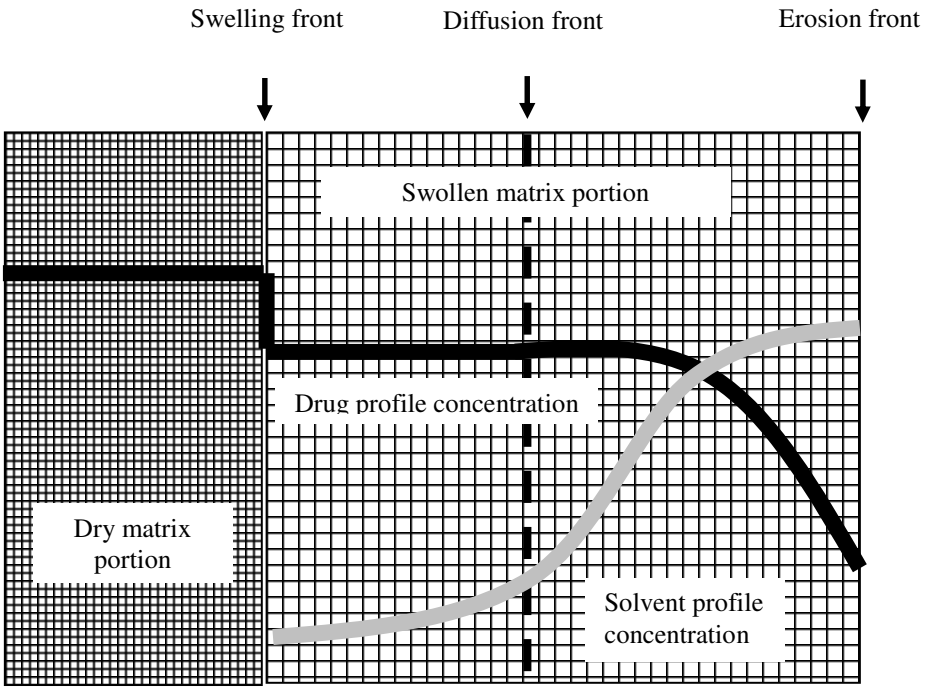

Figure 1. Polymer hydration and drug dissolution/diffusion give origin to the formation of three moving fronts: the swelling front, the erosion front and the diffusion front.

The eroding front separates the release environment from the matrix (it moves outwards when swelling kinetics is predominant on the erosion process, while it moves inwards in the opposite case) and its position depends on the combination of release environment hydrodynamic conditions and on matrix cross-linking strength. In other words, matrix erosion is function of the tensions applied by the release environment and network connectivity. The swelling front, separating the dry glassy core from the swollen matrix portion, moves inward and its speed depends on polymer/solvent characteristics (namely, on the viscoelastic properties of the polymer/solvent couple) in non-porous matrices, while it depends also on matrix porosity for porous systems. Additionally, in the case of sparingly soluble drugs, a third front, the diffusion front, can appear between the outer portion of the swollen matrix, where the drug is completely dissolved, and the inner part, where the drug is not yet dissolved despite the rubbery state of the polymer. This is a simplified vision of reality, as numerical simulations show that, with the few exceptions, both solvent and drug concentration profile in the matrix during release have not a step profile but, rather, a sigmoidal profile. Nevertheless, the drug release profile greatly enables the understanding of the complex drug delivery and solvent uptake processes. Obviously, drug

release from porous matrices is mainly influenced by drug dissolution and diffusion in the pore-filling liquid. This becomes more and more important when dealing with non-swelling porous hydrophobic matrices. Finally, it is also worth mentioning that matrix geometry (planar, spherical, cylindrical, etc.) highly influences drug release kinetics [1].

4.1. Mathematical modelling

The first example of a mathematical model aimed to describe drug release from a matrix system is the one proposed by Higuchi in 1961. Initially conceived for planar systems, it was then extended to different geometries and porous systems. This model is based on the hypotheses that (i) initial drug concentration in the matrix is much higher than drug solubility, (ii) drug diffusion takes place only in one dimension (edge effects must be negligible), (iii) drug particles are much smaller than system thickness, (iv) matrix swelling and dissolution is negligible, (v) drug diffusivity is constant and (vi) perfect sink conditions are always attained in the release environment. Accordingly, model expression is given by:

$$M_t = A\sqrt{D(2C_0 - C_s)C_s t} \qquad C_0 > C_s \qquad (1)$$

where M_t is the amount of drug released until time t, A is the release area, D is the drug diffusion coefficient, C_0 is the initial drug concentration in the matrix while C_s is drug solubility. Interestingly, this model shows an M_t square root dependence on time as exact Fick's solution predicts when the amount released is less than the 60 percent.

Although there is a high degree of approximation, for its simplicity, this model is still widely used.

Another simple and useful empirical equation is the so-called power law equation:

$$\frac{M_t}{M_\infty} = Kt^n \qquad (2)$$

where M_∞ is the amount of drug released after an infinite time, K is a constant and n is the

exponent characterising the release process.

If a Fickian diffusion takes place, *n* is equal to 0.5, 0.45 and 0.43 for a thin film, a cylinder and a sphere, respectively. When *n* exceeds these thresholds, the so-called non-Fickian release takes place.

Eq. (2) has to be used with great care for the classification of the release nature on the basis of *n* values. Indeed, it is well known that, despite Fickian diffusion in the matrix, boundary conditions such as the presence of a stagnant layer or a net faced on the release surface give origin to a release kinetics characterised by *n* greater than 0.5 [6].

Peppas and Sahlin [7] couple the Fickian diffusional contribute with the non-Fickian one in a linear manner:

$$\frac{M_t}{M_\infty} = K_1 t^n + k_2 t^{2n} \qquad (3)$$

Where *m*, k_1 and k_2 are constants related, respectively, to the Fickian and non Fickian diffusional contribute.

Analytical solutions to Fick's law are not available when more complex geometries or non-constant drug diffusivities are incorporated into the model descriptions. Except in extremely dilute systems, drug diffusion coefficients will be a function of drug concentration. Additionally, for hydrogel systems diffusivities of encapsulated molecules will depend on the degree of swelling and crosslinking density of the gels. Therefore the diffusion coefficient used to describe drug release will be sensitive to environmental changes or degradation of the polymer network and may vary over the timescale of release. Several theoretical models have been developed to relate molecule diffusion coefficients to fundamental hydrogel characteristics. Generally, theoretical models for predicting molecule diffusion coefficients have the following general form:

$$\frac{D_g}{D_o} = f(r_s, \nu_{2,s}, \xi) \qquad (4)$$

Here, D_g and D_o are the drug diffusion coefficients in the swollen hydrogel network and in pure solvent, respectively and r_s is the size of the drug to be delivered. This general expression takes into account factors affecting drug release such as the structure of the gel, the polymer

composition, the water content, and the size of the molecules. For a degradable hydrogel, D_g changes as the network degrades due to an increase in the gel mesh size (ξ) and a decrease in the polymer volume fraction ($\nu_{2,s}$) over time (Figure 2) [8].

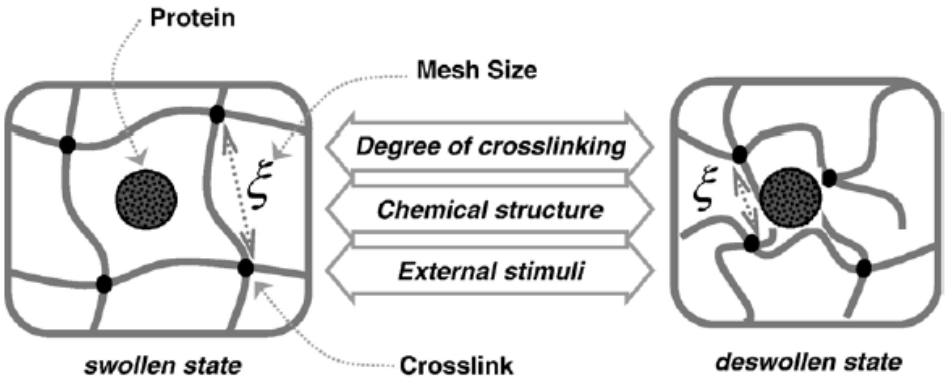

Figure 2. Schematic representation of mesh sizes in hydrogels at swollen or shrunken states.

4.2. References

1. Grassi M, Grassi G. Current Drug Deliv. 2005; 2:97.

2. Grassi M, Grassi G, Lapasin R, Colombo I. Understanding Drug Release and Adsorption Mechanism, a physical and mathematical approach. CRC press Taylor & Francio Group, 2007.

3. Lee P I, Polym. 1984; 25: 973.

4. Lee P I, J Pharm Sci. 1984; 73:1344.

5. Lee P I, J Control Release.1986; 4:1.

6. Peppas N A, Bures P, Leobandung W, Ichikawa H, Eur J Pharm Biopharm. 2000; 50:27.

7. Peppas N A, Sahlin J J. Int J Pharm. 1989; 57:169.

8. Lin C C, Metters A T. Adv Drug Deliv Reviews. 2006; 58:1379.

5. Viscometry

Introduction

Viscosity of a polymer solution depends on concentration and size (i.e., molecular weight) of the dissolved polymer. By measuring the solution viscosity we should be able to get an idea about molecular weight. Viscosity techniques are very popular because they are experimentally simple. They are, however less accurate and the determined molecular weight, the viscosity average molecular weight, is less precise. For example, Mv depends on a parameter which depends on the solvent used to measure the viscosity. Therefore the measured molecular weight depends on the solvent used. Despite these drawbacks, viscosity techniques are very valuable.

Viscosity and Viscosity Nomenclature

Figure 1 shows a piece of a liquid moving at a strain rate $\dot{\gamma}$ under an applied shear stress of τ. The viscosity of the liquid is the ratio of the applied shear stress to the resulting strain rate (or equivalently, the ratio of the shear stress required to move the solution at a fixed strain rate to that strain rate).

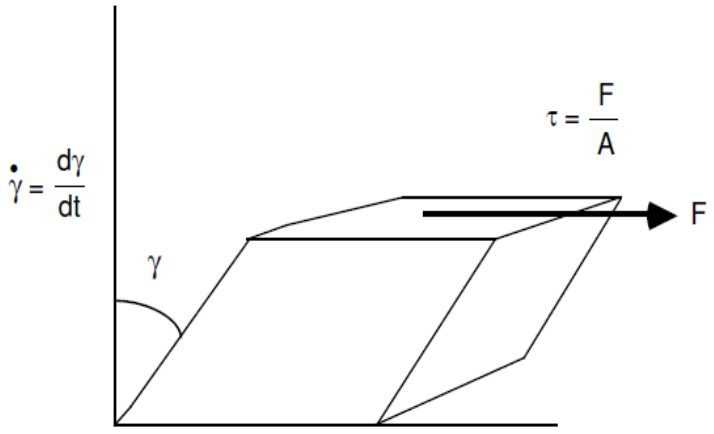

Figure 1. A piece of a liquid moving at shear rate $\dot{\gamma}$ under an applied shear stress of τ.

The shear strain in (Figure 1) is

$$\gamma = \frac{du}{dy} \tag{1}$$

where u is displacement in the x direction. The strain rate is therefore:

$$\dot{\gamma} = \frac{d}{dt}\frac{du}{dy} = \frac{d}{dy}\frac{du}{dt} = \frac{dv_x}{dy} \qquad (2)$$

where v_x is velocity in the x direction. The relations between viscosity (η), shear stress (τ), and shear rate ($\dot{\gamma}$) are:

$$\tau = \eta\,\dot{\gamma} \quad \text{or} \quad \dot{\gamma} = \frac{\tau}{\eta} \quad \text{or} \quad \eta = \frac{\tau}{\dot{\gamma}} \qquad (3)$$

A Newtonian fluid is one in which the viscosity is independent of the shear rate. In other words a plot of shear stress versus shear strain rate is linear with slope η. In Newtonian fluids all the energy goes into sliding molecules by each other. In non-Newtonian fluids, the shear stress/strain rate relation is not linear. Typically the viscosity drops at high shear rates a phenomenon known as shear thinning. Plots of shear force vs. shear rate for Newtonian and non-Newtonian fluids are given in Figure 2.

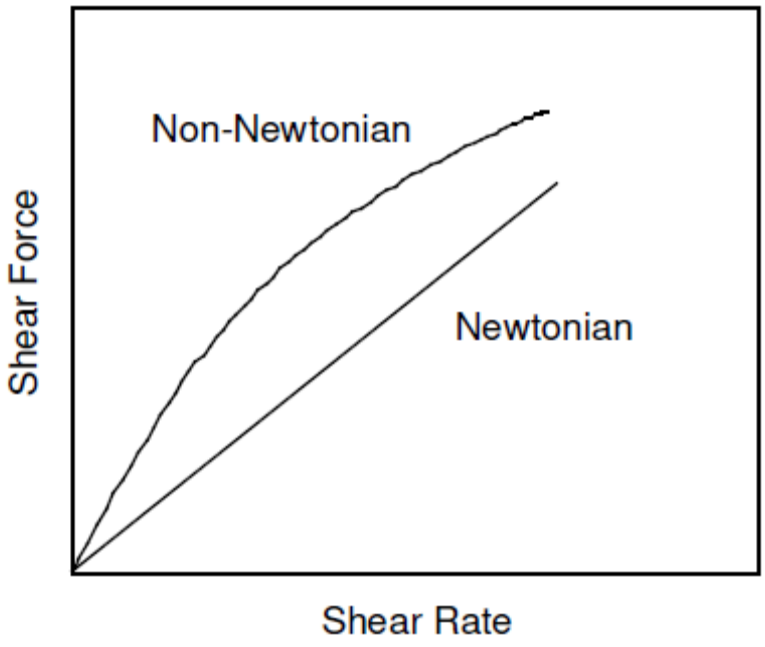

Figure 2. Schematic plots of shear force vs. shear rate for Newtonian and non-Newtonian fluids.

We let η_0 be the viscosity of the pure solvent and η be the viscosity of a solution using that solvent. Several methods exist for characterizing the solution viscosity, or more specifically, the capacity of the solute to increase the viscosity of the solution. That capacity is quantified by using one of several different measures of solution viscosity. The most common solution viscosity terms are:

1. Relative viscosity

$$\eta_r = \frac{\eta}{\eta_0} \tag{4}$$

2. Specific viscosity

$$\eta_{sp} = \frac{\eta - \eta_0}{\eta_0} = \eta_r - 1 \tag{5}$$

3. Inherent Viscosity

$$\eta_i = \frac{\ln \eta_r}{c} \tag{6}$$

4. Intrinsic Viscosity

$$[\eta] = \lim_{c \to 0} \frac{\eta_{sp}}{c} \tag{7}$$

In these equations, η is solution viscosity, η_0 is viscosity of the pure solvent, and c is concentration. Relative viscosity is self-explanatory. Specific viscosity expresses the incremental viscosity due to the presence of the polymer in the solution. Normalizing η_{sp} to concentration gives η_{sp}/c which expresses the capacity of a polymer to cause the solution viscosity to increase; i.e., the incremental viscosity per unit concentration of polymer. As with other polymer solution properties, the solutions used for viscosity measurements will be non ideal and therefore η_{sp}/c will depend on c. As with osmotic pressure, it will probably be useful to extrapolate to zero concentration. The extrapolated value of η_{sp}/c at zero concentration is known as the intrinsic viscosity $[\eta]$. $[\eta]$ will be shown to be a unique function of molecular weight (for a given polymer-solvent pair) and measurements of $[\eta]$ can be used to measure molecular weight.

The remaining form for the viscosity is the inherent viscosity. Like η_{sp}, ln η_r is zero for pure solvent and increases with increasing concentration, thus ln η_r also expresses the incremental viscosity due to the presence of the polymer in the solution. Normalizing ln η_r to concentration or ln η_r/c gives the inherent viscosity. In the limit of zero concentration, η_i extrapolates the same as $\eta sp/c$ and becomes equal to the intrinsic viscosity. This can be proved by:

$$\lim_{c\to 0} \frac{\ln \eta_r}{c} = \lim_{c \to 0} \frac{\ln(1+\eta_{sp})}{c} = \lim_{c \to 0} \frac{\eta_{sp}}{c} = [\eta] \qquad (8)$$

We can thus find [η] be extrapolating either η_{sp}/c or η_i to zero concentration. When c is not equal to zero the specific viscosity and inherent viscosities will be different, even for an ideal solution. In ideal solutions η_{sp}/c will be independent of concentration, but η_i will depend on concentration.

Viscometer

The presence of polymer molecules in a particular solvent may give rise to an increase in viscosity that is much higher than that found for equivalent concentrations of low molecular weight solute. This effect is due to the enormous difference between the size of the solvent molecules and the polymer and, in a good solvent, the effect is even greater, as "coils" polymeric form are even more. In general, the viscosity increase depends on:

- Nature of the solvent
- Type of polymer
- Molar mass of the polymer
- Concentration of the polymer
- Temperature

The viscosity is measured in (newtons/m^2) s = Pa.s.

Where N is Newton and Pa is Pascal,

The viscosity of a polymer solution is determined using the Ubbelohde viscometer (Figure 3).

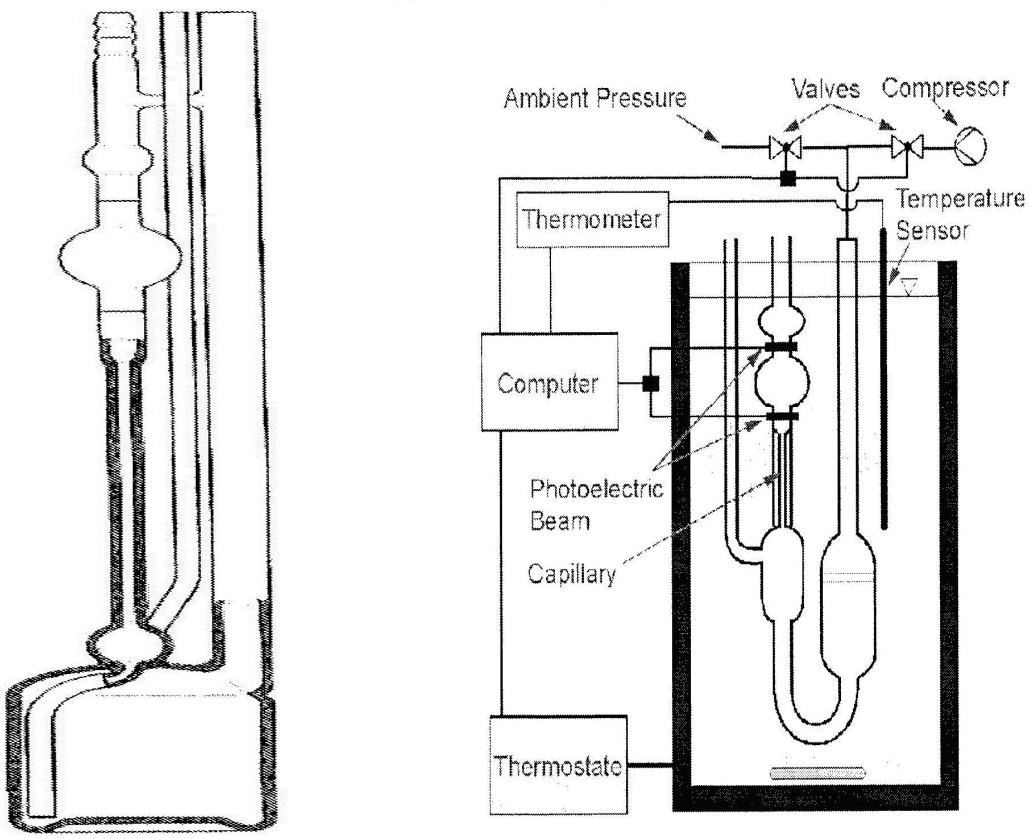

Figure 3. (left) Ubbelohde viscometer for dilutions. (right) Schematic representation of a viscometer in a thermostatic bath.

5.1. Ubbelohde capillary viscometer

The most useful kind of viscometer for determining intrinsic viscosity is the "suspended level" or Ubbelohde viscometer, is sketched below:

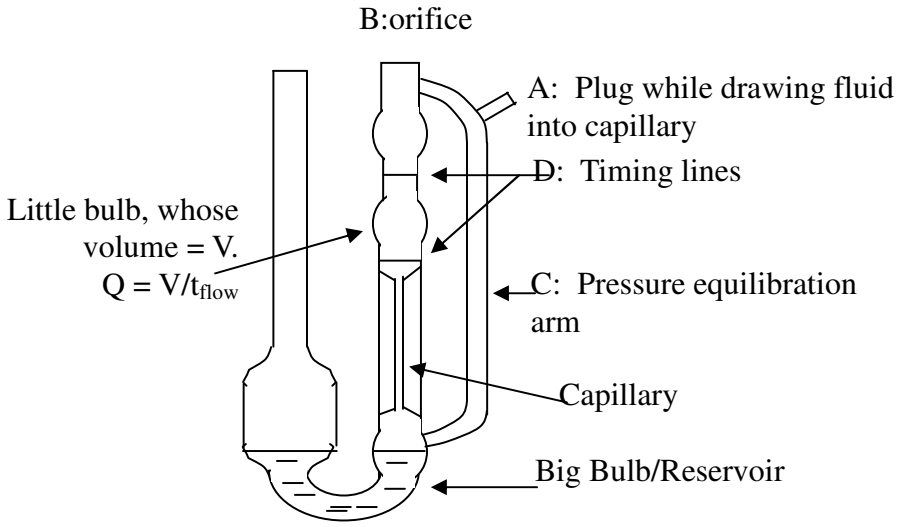

Figure 4. Schematic representation of a Ubbelohde capillary viscometer.

The viscometer is called "suspended level" because the liquid initially drawn into the small upper bulb is not connected to the reservoir as it flows down the capillary during measurement. The capillary is suspended above the reservoir. In conjunction with the pressure-equalization tube, this ensures that the only pressure difference between the top of the bulb and the bottom of the capillary is that due to the hydrostatic pressure i.e., the weight of the liquid. Other designs, e.g., the Cannon-Fenske viscometer, do not provide for this, and will give erroneous results in an intrinsic viscosity determination.

The units of $[\eta]$ are inverse concentration. Intrinsic viscosity has "grown up" around some fairly unconventional units regarding concentration. The most commonly used concentration is g/dL (grams per 100 mL) so $[\eta]$ is usually expressed as dL/g. As suggested by the units, $[\eta]$ represents essentially the volume occupied by a polymer per unit mass.

$$[\eta] \propto \frac{R^3}{M} \tag{9}$$

where M is the polymer molecular weight. Thus, $[\eta]^{-1}$ is approximately the concentration within the polymer, or the "overlap concentration". At concentrations exceeding about $[\eta]^{-1}$ polymer

molecules will touch and interpenetrate. The "semidilute" regime of polymers begins here. Furthermore, an important scaling relationship between $[\eta]$ and molecular weight holds:

$$[\eta] = KM^{a} \quad \text{“Mark-Houwink-Sakurada” relationship} \qquad (10)$$

Thus, log-log plots of $[\eta]$ against molecular weight have the intercept log(K) and slope a [1]. The slope contains information about the shape of the molecules (Table 1).

Table 1. Values of the parameters a for aqueous solutions of polysaccharides.

Type	**Relation between [η] and M**
1) flexible polymer chain in "ideal" solvent	$[\eta] \propto M^{0.5}$
2) partially random coil. “permeable” flexible polymer chain in "good" solvent (excluded volume limit)	$[\eta] \propto M^{a}$ $(0.5 < a < 0.8)$
3) rigid rod	$[\eta] \propto M^{1.8}$
4) thin disk	$[\eta] \propto M^{1.0}$
5) rigid sphere	$[\eta]$ does not depend on M

A given chain in any good solvent will have the same $[\eta]$. In that sense, $[\eta]$ really is a property intrinsic to the chain but only in as much as the polymer conformation is partly determined by the solvent. The intrinsic viscosity of a given chain will also be the same in all its Theta solvents [2]. However, the $[\eta]$ value of a chain in a Theta solvent will differ from that in a good solvent. If a polymer is measured in two solvents that induce very different conformations (e.g., a helix in one solvent and a random coil in another) then $[\eta]$ may differ dramatically.

5.2. References

1. Cantor C R, Schimmel P R. Biophysical Chemistry Part III: The Behaviour of Biological Macromolecules. W.H. Freeman and Company, San Francisco. 1980: 1019.

2. Cheng Y, Brown K M, Prud homme R K. Biomacromolecules. 2002; 3:456.

6. Oscillatory rheology

The basic principle of an oscillatory rheometer is to induce a sinusoidal shear deformation in the sample and measure the resultant stress response; the tested time scale is determined by the frequency of oscillation, ω, of the shear deformation. In a typical experiment, the sample is placed between two plates, as shown in Figure 1(a).

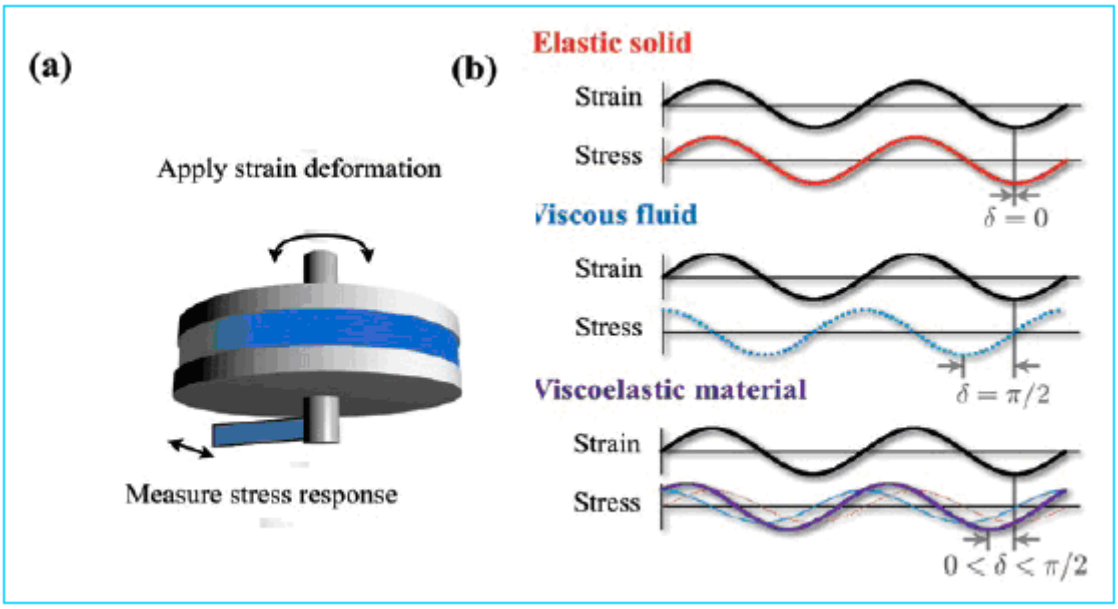

Figure 1. (a) Schematic representation of a typical rheometry setup, with the sample placed between two plates. (b) Schematic stress response to oscillatory strain deformation for an elastic solid, viscous fluid and viscoelastic material.

While the bottom plate remains stationary, a motor rotates the top plate, thereby imposing a time dependent strain $\gamma(t) = \gamma \cdot \sin(\omega t)$ on the sample. Simultaneously, the time dependent stress $\sigma(t)$ is quantified by measuring the torque that the sample imposes on the bottom plate. Measuring this time dependent stress response at a single frequency immediately reveals key differences between materials, as shown schematically in Figure 1(b). If the material is ideal elastic solid, then the sample stress is proportional to the strain deformation, and the proportionality constant is the shear modulus of the material. In this case the stress is always exactly in phase with the

applied sinusoidal strain deformation. On the other side, if the material is a purely viscous fluid, the stress in the sample is proportional to the rate of strain deformation, where the proportionality constant is the viscosity of the fluid. The applied strain and the measured stress are out of phase, with a phase angle $\delta=\pi/2$, as shown in Figure 1(b) in the middle.

Viscoelastic materials show a response that contains both in-phase and out-of-phase contributions, as shown in the bottom graph of Figure 1(b); these contributions reveal the extents of solid-like (red line) and liquid-like (blue dotted line) behaviour. As a consequence, the total stress response (purple line) shows a phase shift δ with respect to the applied strain deformation that lies between that of solids and liquids, $0<\delta<\pi/2$. The viscoelastic behaviour of the system, at a fixed ω, is characterised by the storage modulus, G' (ω), and the loss modulus, G'' (ω), which correspond to the solid-like and fluid-like contributions. In fact, for a sinusoidal strain deformation $\gamma(t) = \gamma_0 \sin(\omega t)$, the stress response of a viscoelastic material is given by $\sigma(t) = G'(\omega)\gamma_0 \sin(\omega t) + G''(\omega)\gamma_0 \cos(\omega t)$.

6.1. Linear and Nonlinear rheology

It is important to note that the frequency-dependent moduli G' and G'' are mostly recorded in the linear regime, i.e. when the applied strain deformations are sufficiently small and thus not able to affect the material properties. Many soft materials show a strikingly nonlinear stress response as the strain deformation is increased; this behaviour suggests a fundamental change of the material properties under shear from the equilibrium properties at rest. Such nonlinear data are often disregarded because the physical origins of this behaviour remain poorly understood [1, 2].

6.2. References

1. Ferry J D. Viscoelastic properties of polymers (3rd ed.), Wiley (New York). 1980.

2. Lapasin R, Pricl S. Rheology of industrial polysaccharides: Theory and applications, Blackie Academic & Professional, London. 1995.

7. Dynamo-mechanical studies

Texture analysis is a technique that has been extensively employed in the mechanical characterization of food materials and in the last few years it has emerged also as a useful technique in the field of pharmaceutical studies [1]. A TA-XT2*i* instrument may be used (Figure 1). It is easy to handle and to calibrate, very flexible and versatile. Obtained results are accurate and reproducible.

Figure 1. Texture analyzer TA-XT2*i*.

In the case of drug release formulations, different measurements (compression, puncture/penetration, tension, fracture/bending, extrusion, cutting/shearing) can be used for their characterization in order to improve their use in biomedical applications. Some of the derived mechanical parameters are:

Adhesion for tablet coating and transdermal delivery patch;

Bioadhesion/mucoadhesion for buccal/gastric drug delivery;

Hardness, rupture force and elasticity for stents and polymer implants;

Mechanical strength/hardness for tablets, granules, microspheres and capsules;

Extrusion force and syringability for injectable materials.

Mechanical puncture strength and elongation percentage for thin films.

Different probes may be used for each analysis and for specific sample types (Table 1):

Table 1. List of different types of probe and their typical applications.

Probe type	Typical application
Cylinder	For well defined samples, with uniform surfaces; general purposes
Sphere	Samples with small scale variations on surface; general purposes
Cone	Samples with rigid outer layer; often used for penetrometry
Wire	Required for cutting samples
Extrusion cell	Samples that can flow; general purposes

Within a probe category, variations of geometry can be significant: it is required a larger force to drive a cone of shallow angle in comparison to a cone of steep angle. Similarly, a cylinder of large diameter may require a larger force than a cylinder of small diameter. The selection of the probe (type and size) will affect the test result.

Penetration tests

Penetration testing is extensively employed in the mechanical characterization of polymeric materials, i.e. polysaccharidic hydrogels. A penetration experiment is based on recording the deformation curve when a material is subjected to a controlled force. From the resultant force-time curve, the following mechanical parameters may be derived (Figure 2):

- Hardness: maximum positive force required to attain a given deformation (maximum peak in the force-time plot, b)

- Cohesiveness: the work needed to overcome the internal bonds of the material (positive dashed area under the force-time curve, between a and b)

- Adhesiveness: the work necessary to overcome the attractive force between the surface of the hydrogel and the surface of the probe with which the sample comes into contact (total "negative" area over the force-time curve, between c and e)

- Adhesive force: force required to "pull" the probe from the sample (minimum peak in the force-time plot, d).

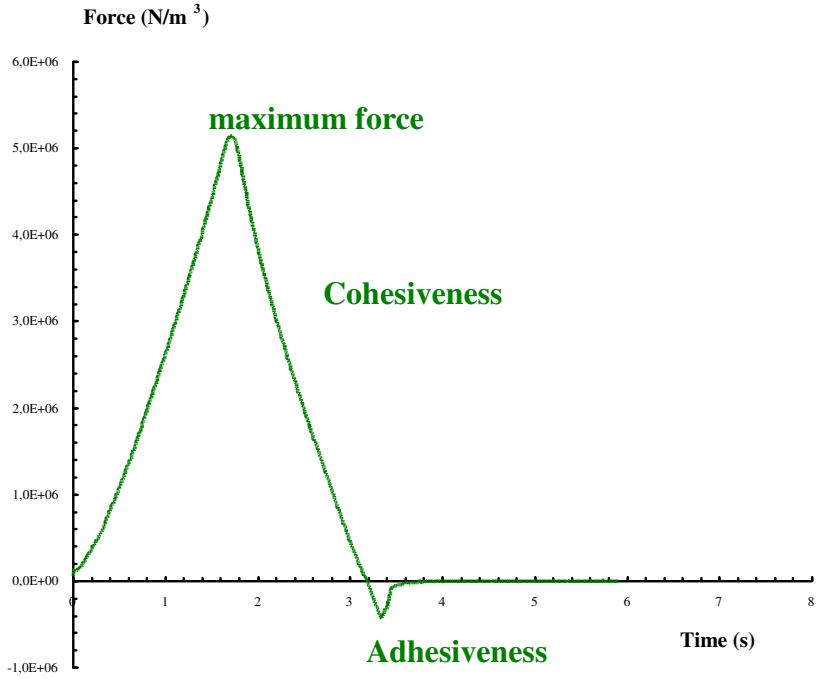

Figure 2. Profiles of penetration of the force in function of time.

Mechanical properties of polymeric films

For the mechanical characterization of the samples, a software-controlled dynamometer, TA-XT2*i* (Stable Micro Systems, UK), with a 5-kg load cell was used, and puncture strength tests were carried out. The film was placed in a holder with a cylindrical hole (d = 8.50 mm) and the diameter of the spherical probe was 6.35 mm (Figure 3). The pre-test and post-test speeds were fixed at 2.00 mm/s, the test speed at 1.00 mm/s and the trigger force at 0.098 N.

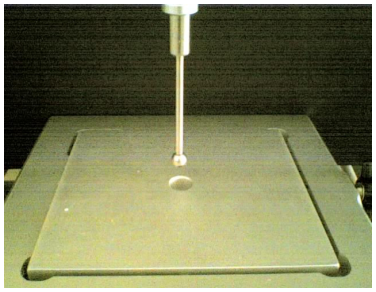

Figure 3. Set up for a puncture strength test.

Puncture Strength Test

Puncture strength tests are used to determine the puncture or rupture characteristics of a material. During a puncture test a material is penetrated by a probe or other type of device until the material ruptures or until an elongation limit is achieved.

Puncture testing is commonly used to determine the strength of a material such as film, rubber or membrane. It is also often used in the food processing industry to determine the texture of ripeness of a product. Puncture testing may be used in medical applications for determining the sharpness of a syringe, scalpel or blade or to measure the resistance and pliability of synthetic skin.

The force required to penetrate the film by the probe was determined by means of the puncture strength test. The table below shows the parameters used for the analysis:

Table 1. Parameters set for the penetration test

Pre-test speed	2.0 mm/s
Test speed	1.0 mm/s
Post-test speed	2.0 mm/s
Distance	5 mm
Temperature	25 °C
Trigger Type	Auto
Trigger Force	0.098 N

Pre-test speed: the speed with which the probe moves from the moment the run button is pressed, and until the trigger point is reached. The initial setting of the instrument is 2.0 mm/sec.

Speed test: the speed at which the probe moves after contact with the sample.

Post- test speed: the speed at which the probe returns to the starting point at the end of the test.

Distance: the distance can be expressed in mm or Strain percentage. With the first mode the distance that the probe has to travel after contact with the sample is set, while with the second mode the distance is expressed as the percentage of the length of the sample.

Temperature: the experiments are conducted at room temperature, 25 ° C.

Mode and trigger force: the data acquisition begins when the probe starts to move at the set speed. In particular, in Auto mode the instrument recognizes the point of contact with the surface of the sample. The surface of the product is the zero distance and the distance is recorded over time indicating how far the probe has moved away from that point. If the trigger value is set to 0.098 N, a force at least equal to that value, and exerted on the probe, will be interpreted as the surface of the sample which will be activated for the conditions set for the test. The point at which the trigger value is reached is called trigger point.

The following parameters are calculated from a puncture test:

$$\text{- Puncture strength at break} = F_{\max} \big/ ACS$$

where Fmax is the maximum applied force at film break, ACS the cross-sectional area of the edge of the film located in the path of the cylindrical hole of the film holder, with ACS =2$r\delta$, where r is the radius of the hole and δ is the thickness of the film.

$$\text{- Elongation (\%) at break} = \left[\frac{\left[\left(r^2 + D^2 \right) \right]^{1/2} - r}{r} \right] \times 100$$

Where r is the radius of the film exposed in the cylindrical hole of the film holder and D represents the displacement of the probe from the point of contact to the point of puncture.

The maximum load and the maximum displacement of films were measured, and then converted to puncture strength, and elongation at break.

7.1. Reference

1. Mesut C, Roland B. Int J Pharm. 2005; 303:62.

8. Gel Permeation Chromatography

Gel permeation chromatography (GPC) (Figure 1), sometimes called size-exclusion chromatography (SEC), is a relatively new technique for fractionating polymers, but it has become the premier characterization method for homopolymers, condensation polymers, and strictly alternating copolymers. Today, GPC is one of the most powerful instrumental tools available to polymer scientists. It has been used extensively to characterize high-molecular-mass polymers and oligomers of various polymer classes. It also permits determination of the molecular-weight distribution of polymers.

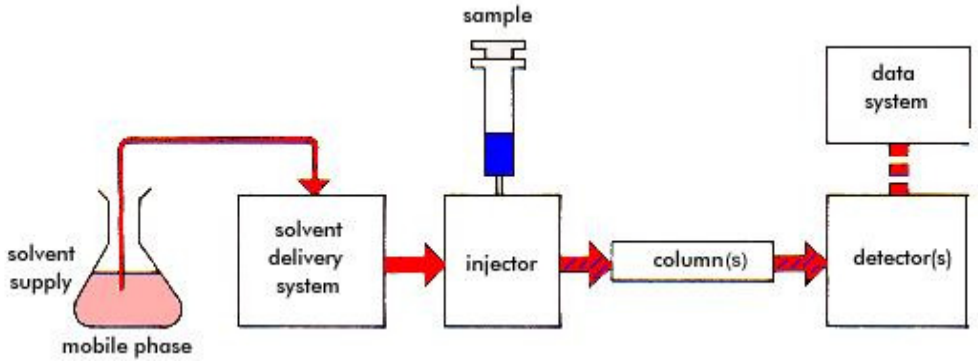

Figure 1. Scheme of a basic gel permeation chromatograph.

As a technique, SEC was first developed in 1955 by Lathe and Ruthven [1]. The term gel permeation chromatography can be traced back to J.C. Moore of the Dow chemical company who investigated the technique in 1964 and the proprietary column technology was licensed to Water Corporation who subsequently commercialized this technology in 1964 [2]. When characterizing polymers, it is important to consider the polydispersity index (PDI) as well as the molecular weight. Polymers can be characterized by a variety of definitions for molecular weight including the number average molecular weight (M_n), the weight average molecular weight (M_w) the size average molecular weight (M_z), or the viscosity molecular weight (M_v). GPC allows for the determination of PDI as well as M_v and based on other data, the M_n, M_w, and M_z can be determined.

How GPC works

GPC separates based on the size or hydrodynamic volume (radius of gyration) of the analytes. This differs from other separation techniques which depend upon chemical or physical interactions to separate analytes [3]. Separation occurs *via* the use of porous beads packed in a column (Figure 2).

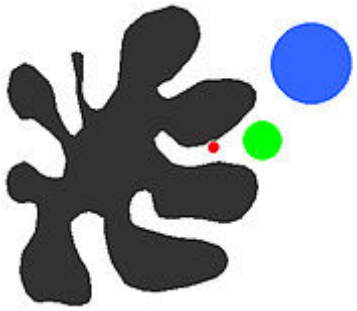

Figure 2. Schematic of pore vs. analyte size.

The smaller analytes can enter the pores more easily and therefore spend more time in these pores, increasing their retention time. Conversely, larger analytes spend little if any time in the pores and are eluted quickly (Figure 3). All columns have a range of molecular weights that can be separated.

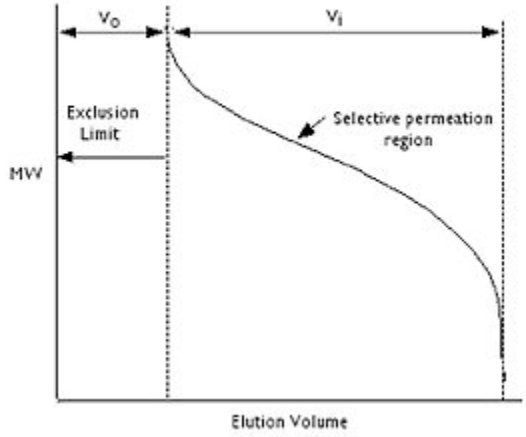

Figure 3. Range of molecular weights that can be separated for each packing material.

If an analyte is either too large or too small it will be either not retained or completely retained respectively. Analytes that are not retained are eluted with the free volume outside of the

particles (V_o), while analytes that are completely retained are eluted with volume of solvent held in the pores (V_i). The total volume can be considered by the following equation, where V_g is the volume of the polymer gel and V_t is the total volume [3]:

$$V_t = V_g + V_i + V_o$$

As can be inferred, there is a limited range of molecular weights that can be separated by each column and therefore the size of the pores for the packing should be chosen according to the range of molecular weight of analytes to be separated. For polymer separations the pore sizes should be on the order of the polymers being analyzed. If a sample has a broad molecular weight range it may be necessary to use several GPC columns in tandem with one another to fully resolve the sample.

Applications

GPC is often used to determine the relative molecular weight of polymer samples as well as the distribution of molecular weights. What GPC truly measures is the molecular volume and shape function as defined by the intrinsic viscosity. If comparable standards are used, this relative data can be used to determine molecular weights within ± 5% accuracy. Polystyrene standards with PDI of less than 1.2 are typically used to calibrate the GPC [4]. Unfortunately, polystyrene tends to be a very linear polymer and therefore as a standard it is only useful to compare it to other polymers that are known to be linear and of relatively the same size.

Gel

Gels are used as stationary phase for GPC. The pore size of a gel must be carefully controlled in order to be able to apply the gel to a given separation. Other desirable properties of the gel forming agent are the absence of ionizing groups and, in a given solvent, low affinity for the substances to be separated. Commercial gels like Sephadex, Bio-Gel (cross-linkes polyacrylamide), agarose gel and Styragel are often used based on different separation requirements [5].

Eluent

The eluent (mobile phase) should be a good solvent for the polymer, should permit high detector response from the polymer and should wet the packing surface. The most common eluents for

polymers that dissolve at room temperature are tetrahydrofuran (THF), *o*-dichlorobenzene and trichlorobenzene at 130–150 °C for crystalline polyalkynes and *m*-cresol and *o*-chlorophenol at 90 °C for crystalline condensation polymers such as polyamide and polyesters.

Separation

In GPC, a dilute polymer solution is injected into a solvent stream, which then flows under pressure through a chromatography column filled with porous gel packing, typically composed of silica beads and/or a polymeric gel. GPC separates the polymer molecules according to the size of the polymer chain in the elution solvent. The separation depends on the ability of the solute molecules to penetrate into the gel. It utilizes the partition equilibrium of polymer chains between common solvent phases located at the interstitial space and the pores of the column packing materials, typically in the form of uniform-size porous beads. Given the relationship between the chain size and the molecular weight of polymers, especially linear and chemically homogeneous polymers, GPC retention is well correlated with molecular weight.

Pump

There are two types of pumps available for uniform delivery of relatively small liquid volumes for GPC: piston or peristaltic pumps.

Instrumentation

The GPC instrument has twin pumps with voltage stabilization, thermostatting on the refractometer optical bench, and incorporates a non-servo-system refractometer with smaller cells. Samples are made up as solutions in solvent drawn from the main supply. The solutions then are filtered prior to injection to remove particles of gel or dirt which would otherwise block the GPC column.

The recorder sensitivity is kept constant, and the column set is calibrated using materials with known molar volumes of solute. The column set used consists of a known plate count.

Calibration of the columns is carried out with a series of well-characterized polystyrenes and poly (propylene glycols). Sometimes the viscosity molecular weights determined from the intrinsic viscosities are checked against viscosity molecular weights calculated from the GPC curves.

Calibration

According to the Einstein viscosity law, one can write

$$[\eta] = K\left(\frac{V}{M}\right) \qquad (1)$$

Where [η] is the limiting viscosity index, V is the hydrodynamic volume of the particles, M is their molecular weight, and K is a constant.

Calibration means primarily establishing a relationship between the molecular weight of a monodisperse species (or very narrow fraction) and the emergence volume V corresponding to the peak maximum of the chromatogram, although the questions of peak broadening due to statistical effects and column imperfections require quantitative answers. A tentative approach to the first part of the problem can be based on the assumption that for a given set of experimental conditions, flexible-coil molecules of the same statistical dimensions will exhibit the same emergence volume, provided no specific interaction with the gel takes place. The following considerations support this assumption.

Column Packing

Columns to be used in a separation are calibrated by examining the elution volume of materials with very narrow molecular-weight distributions. A graph is prepared from the results showing the elution volume to sample peak versus the theoretical extended chain length of a molecule of the solute.

Porous glass is a material with excellent mechanical properties for gel permeation chromatography, and is capable of resolving polymers over a wide molecular-weight range. Columns may be packed easily and require no special precautions to exclude air. Physical properties such as pore-size distributions may be measured by conventional methods.

Detector

In GPC, the concentration by weight of polymer in the eluting solvent may be monitored continuously with a detector. There are many detector types available and they can be divided into two main categories. The first is concentration sensitive detectors which include UV

absorption, differential refractometer (DRI) or refractive index (RI) detectors, infrared (IR) absorption and density detectors. Molecular weight sensitive detectors include low angle light scattering detectors (LALLS), multi angle light scattering (MALLS) [6]. The resulting chromatogram is therefore a weight distribution of the polymer as a function of retention volume (Figure 4).

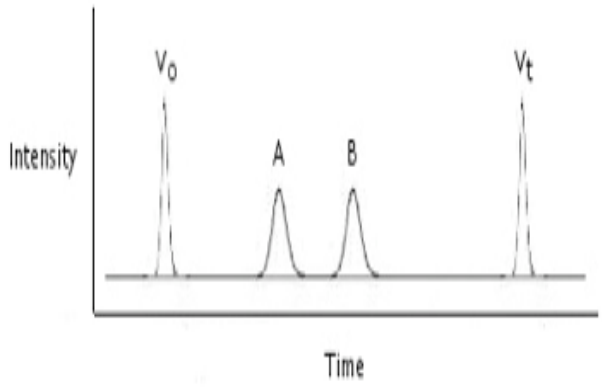

Figure 4. GPC Chromatogram; V_O= no retention, V_t = complete retention, A and B = partial retention.

The most sensitive detector is the differential UV photometer and the most common detector is the differential refractometer (DRI).

GPC experimental set up was used to determine Guar Gum (GG) molecular weight (M_w):

Weight molecular weight (M_w) and polydispersity index (M_w/M_n) were determined by GPC on a bank of TSK gel GMPWXL columns (Tosoh Bioscience, Tokyo,Japan). A Varian 210 HPLC system with a 356-LC refractive index detector was used. The eluant was 55mM Na_2SO_3 and 0.02 NaN_3 in double distilled water; the flow rate and temperature were maintained at 0.6ml/min and 40°C,respectively.All guar samples were diluted to 0.15%(w/v) and filtered through a 0.45 µm filter prior to analysis. The bank of columns was calibrated using pullulan standards [7, 8].

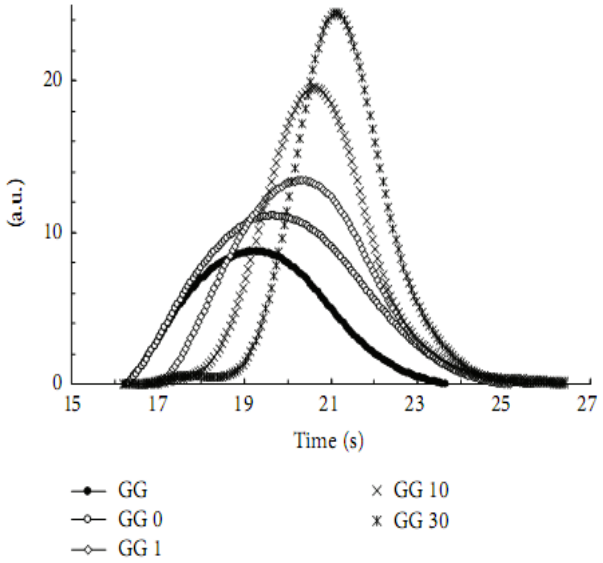

Sample	M_w/M_n
GG	4.65
GG 0	5.82
GG 1	3.9
GG 10	2.65
GG 30	2.06

Figure 5. Molar mass distributions of the guar samples and table of Polydispersity Index

GPC Measurements of guar gum. Molecular weight distributions of GG and sonicated GG samples by GPC are shown in Figure 5. It is apparent that depolymerization of GG by sonic irradiation causes degradation of the polysaccharide to give different fractions of lower molecular weight, each fraction having a narrow molecular weight distribution. In absence GG of external stimuli (GG and GG 0), the distribution curves are very broad while by applying sonication for different period of time, the peaks become sharper. The molecular weight distribution is in fact somehow more important for characterising the samples than just their M_w only. In Figure 5, typical chromatograms of GG samples are shown, together with the polydispersity index (M_w/M_n). From the table of Figure 5,it is evident how the sonication process reduces significantly the polydispersity index leading for an irradiation of 30min, towards the value expected for the most probable distribution in a random chain scission (M_w/M_n =2).

Advantages of GPC

As a separation technique GPC has many advantages. First of all, it has a well-defined separation time due to the fact that there is a final elution volume for all unretained analytes. In addition, since the analytes do not interact chemically or physically with the column, there is a lower chance for analyte loss to occur [3].

GPC provides a more convenient method of determining the molecular weights of polymers. In

fact most samples can be thoroughly analyzed in an hour or less [9].

8.1.References

1. Lathe G H, Ruthven C R J. Biochem J. 1956; 62:665.
2. Moore J C. J Polym Sci.1964; 2:835.
3. Skoog D A. Principles of Instrumental Analysis. Thompson Brooks/Cole Belmont C A.2006; 6th ed: Chapter 28.
4. Sandler S R, Karo W, Bonesteel J. Pearce E M. Polymer Synthesis Characterization: A laboratory Manual;Academic Press San Diego.1998.
5. Helmut D, Gel Chromatography, Gel Filtration, Gel Permeation, Molecular Sieves. A Laboratory Handbook Springer-Verlag. 1969.
6. Trathnigg B. Prog Polym Sci. 1995;20:615.
7. Cheng Y, Brown K M, Prud'homme R K. Biomacromolecules.2002;3:456.
8. Tayal A, Kelly R M, Khan S A. Macromolecules.1999;32:294.
9. Cowie J M G, Arrighi V. Polym Chem and Phys of Modern Materials, 3rd ed. CRC Press, 2008.

9. Sonication

Sonication is the act of applying sound energy to agitate particles in a sample, for various purposes. Ultrasonic frequencies (>20 kHz) are usually used, leading to the process also being known as ultrasonication [1].

In the laboratory, it is usually applied using an ultrasonic bath or an ultrasonic probe, colloquially known as a sonicator

Historical Background

Most modern ultrasonic (US) devices rely on transducers (energy converters), which are composed of piezoelectric materials. The basis for present-day generation of US devices was established around 1880, with the discovery of the piezoelectric effect by the brothers Pierre and Jacques Curie. Piezoelectric materials respond to the application of an electrical potential across opposite faces with a small change in dimension. If the potential is alternated at high frequencies, the crystal converts the electrical energy to mechanical vibration energy; at sufficiently high alternating potential, high frequency sound (ultrasound) is generated.

However, cavitation as a phenomenon was first identified and reported in 1895 by John Thornycroft and Sidney Barnaby [2]. During field tests of high-speed torpedo boats, they observed that the formation and collapse of large bubbles caused erosion of the ship's propeller. In 1927, Richards and Loomis (1927) noticed the first chemical effects of US frequencies.

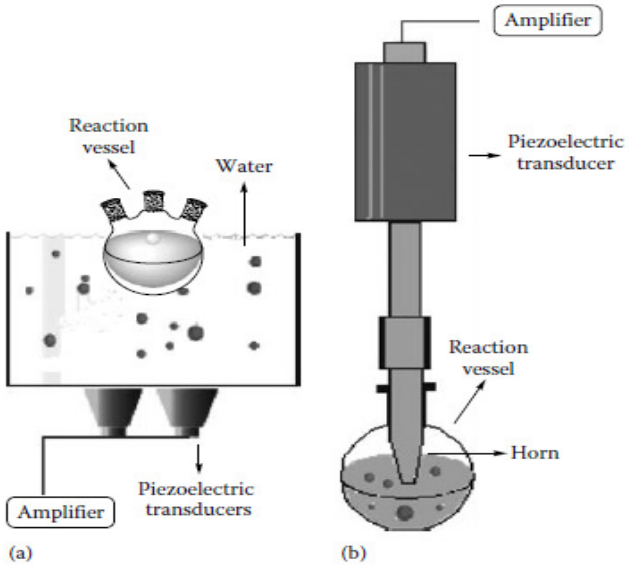

Figure 1. (a) Ultrasonic cleaning bath. (b) Ultrasonic probe.

With some exceptions, the field was quite forgotten for nearly 60 years. However, in the 1980s, sonochemistry was reborn and began to be widely used in many different areas. The reason for this growth was the availability of inexpensive and appropriate laboratory equipment, such as ultrasonic cleaning baths (low intensity) or ultrasonic probes (high intensity) (Figure 1).

Effects

Sonication has numerous effects, both chemical and physical. The chemical effects of ultrasounds are concerned with understanding the effect of sonic waves on chemical systems. The chemical effects of ultrasounds do not come from a direct interaction with molecular species. Studies have shown that no direct coupling of the acoustic field with chemical species on a molecular level can account for sonochemistry [2] or sonoluminescence [3]. Instead, sonochemistry arises from acoustic cavitation: the formation, growth, and implosive collapse of bubbles in a liquid [4].

Power of sound

Sound is transmitted through a medium by inducing vibrational motion of the molecules through which it is travelling. This motion can be visualised as rather like the ripples produced when a pebble is dropped into a pool of still water. The waves move but the water molecules which constitute the wave revert to their normal positions after the wave has passed. An alternative representation is provided by the effect of a sudden twitch of the end of a horizontal stretched spring. Here the vibrational energy is transmitted through the spring as a compression wave which is seen to traverse its whole length. This is just a single compression wave and it does not equate to sound itself which is a whole series of such compression waves separated by rarefaction (stretching) waves in between. The pitch (or note) of the sound produced by this series of waves depends upon their frequency i.e. the number of waves which pass a fixed point in unit time. In physics sound waves are often shown as a series of vertical lines or shaded colour where line separation or colour depth represent intensity or as a sine wave where intensity is shown by the amplitude (Figure 2)**.**

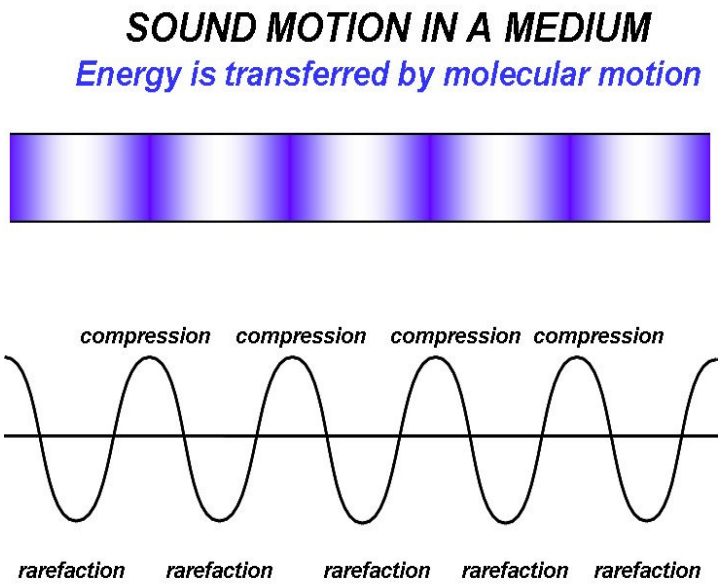

Figure 2. Sound transmission through a medium.

The physical effects of sound vibrations are most easily experienced by standing in front of a loudspeaker playing music at high volume. The actual sound vibrations are transmitted through the air and are not only audible but can also be sensed by the body through the skin. The bass notes are felt through the body more easily than the high notes and this is connected with the frequency of the pressure pulse creating the sound. Low frequency sound becomes audible at around 18 Hz (1 Hz = 1 Hertz = 1 cycle per second) but as the frequency of the sound is raised (becoming more treble) it becomes more difficult for the body to respond and that sensation is lost.

High frequency sound, while not noticeably affecting the body does cause severe annoyance to hearing e.g. feedback noise from a microphone through a loud speaker. At even higher frequencies the ear finds it difficult to respond and eventually the human hearing threshold is reached, normally around 18-20 kHz for adults, sound beyond this limit is inaudible and is defined as ultrasound. The hearing threshold is not the same for other animal species, thus dogs respond to ultrasonic whistles (so called "silent" dog whistles) and bats use frequencies well above 50 kHz for navigation (Figure 3).

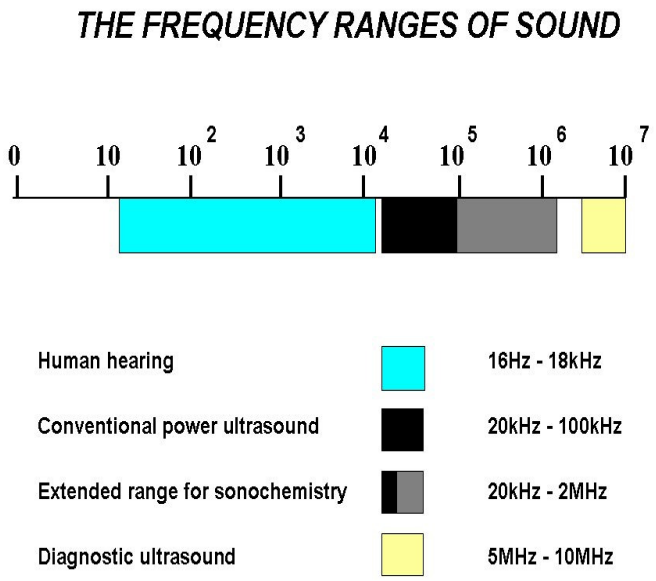

Figure 3. Frequency ranges of sound.

The broad classification of ultrasounds as sounds above 20 kHz and up to 100 MHz can be subdivided into two distinct regions: Power and Diagnostic. The former is generally at lower frequency end where greater acoustic energy can be generated to induce cavitation in liquids, the origin of chemical effects. Sonochemistry normally uses frequencies between 20 and 40 kHz simply because this is the range employed in common laboratory equipment. However since acoustic cavitation in liquids can be generated well above these frequencies, recent researches into sonochemistry use a much broader range (Figure 3). High frequency ultrasound from around 5 MHz and above does not produce cavitation and this is the range used in medical imaging.

A whistle which generates a frequency of 20 kHz is inaudible to humans but perfectly audible to a dog and produces no physical harm to either. It is however in the correct frequency range to affect chemical reactivity (Power Ultrasound). Yet such a whistle blown in a laboratory will not influence chemical reactions in any way. This is because the whistle is producing sound energy in air and airborne sound cannot be transferred into a liquid.

Acoustic Cavitations

Power ultrasound enhances chemical and physical changes in a liquid medium through the generation and subsequent destruction of cavitation bubbles. Like any sound wave ultrasound is propagated via a series of compression and rarefaction waves induced in the molecules of the medium through which it passes. At sufficiently high power the rarefaction cycle may exceed the

attractive forces of the molecules of the liquid and cavitation bubbles will form. Such bubbles grow by a process known as rectified diffusion i.e. small amounts of vapour (or gas) from the medium enters the bubble during its expansion phase and is not fully expelled during compression. The bubbles grow over the period of a few cycles to an equilibrium size for the particular frequency applied. It is the fate of these bubbles when they collapse in succeeding compression cycles which generates the energy for chemical and mechanical effects (Figure 4). Cavitation bubble collapse is a remarkable phenomenon induced throughout the liquid by the power of sound. In aqueous systems at an ultrasonic frequency of 20 kHz each cavitation bubble collapse acts as a localised "hotspot" generating temperatures of about 4,000 K and pressures in excess of 1000 atmospheres [5-7].

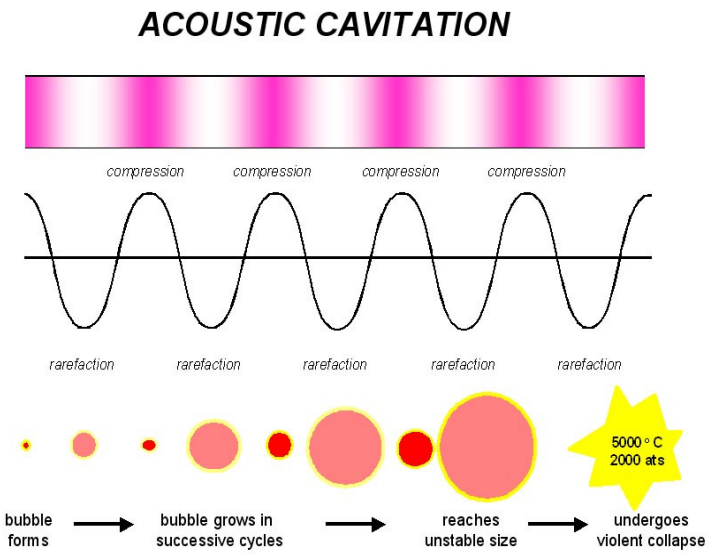

Figure 4. Generation of an acoustic bubble.

The cavitation bubble has a variety of effects within the liquid medium depending upon the type of system in which it is generated. These systems can be broadly divided into homogeneous liquid, heterogeneous solid/liquid and heterogeneous liquid/liquid. Within chemical systems these three groupings represent most processing situations.

Homogeneous liquid phase reactions

(i) In the bulk liquid immediately surrounding the bubble where the rapid collapse of the bubble generates shear forces which can produce mechanical effects and

(ii) In the bubble itself where any species introduced during its formation will be subjected to extreme conditions of temperature and pressure on collapse leading to chemical effects. (Figure 5).

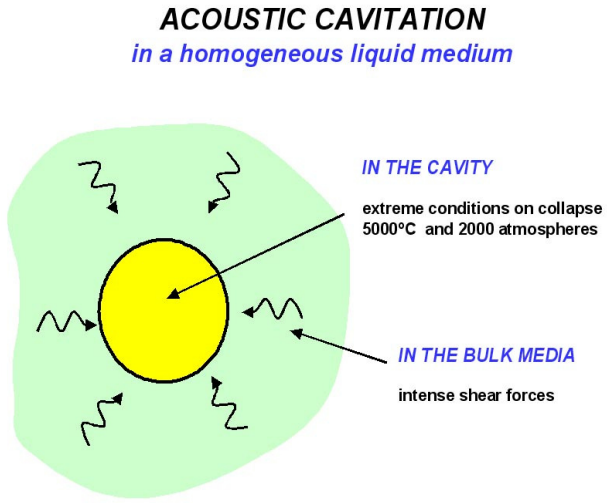

Figure 5. Acoustic cavitation in a homogeneous liquid.

Cavitation near a surface

Unlike cavitation bubble collapse in the bulk liquid, collapse of a cavitation bubble on or near to a surface is unsymmetrical because the surface provides resistance to liquid flow from that side. The result is an inrush of liquid predominantly from the side of the bubble remote from the surface resulting in a powerful liquid jet being formed, targeted at the surface (Figure 6).

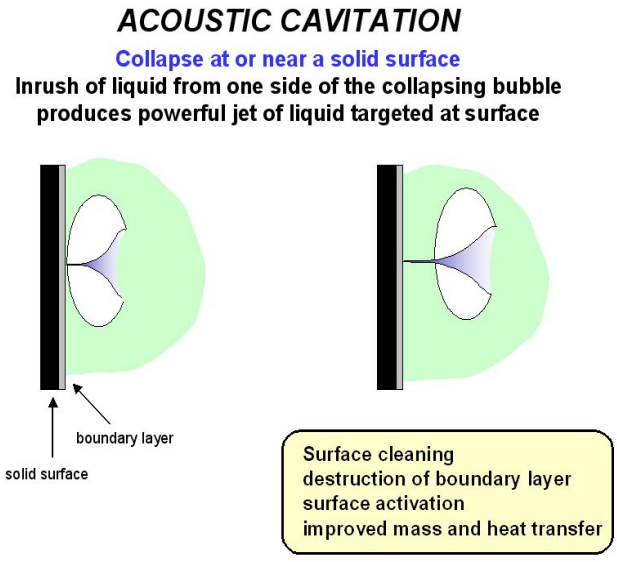

Figure 6. Cavitation bubble collapse at or near a solid surface.

The effect is equivalent to high pressure jetting and is the reason that ultrasound is used for cleaning. This effect can also activate solid catalysts and increase mass and heat transfer to the surface by disruption of the interfacial boundary layers.

Heterogeneous power liquid reaction

Acoustic cavitation can produce dramatic effects on powders suspended in a liquid (Figure 7).

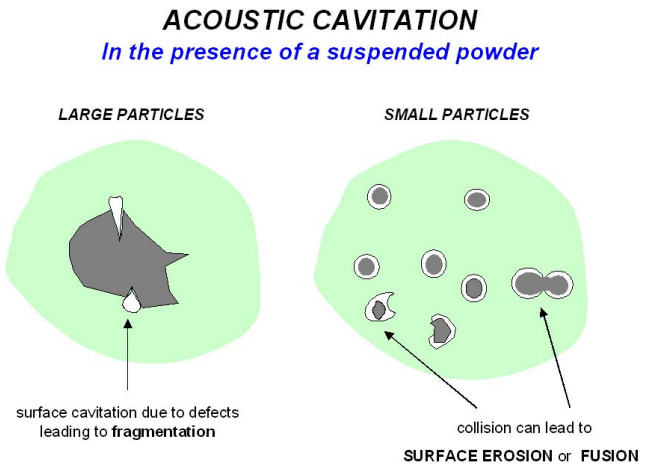

Figure 7. Acoustic cavitations in a liquid with a suspended powder.

Surface imperfections or trapped gas can act as the nuclei for cavitation bubble formation on the surface of a particle and subsequent surface collapse can then lead to shock waves which break the particle apart. Cavitation bubble collapse in the liquid phase near to a particle can force it into rapid motion. Under these circumstances the general dispersive effect is accompanied by interparticle collisions which can lead to erosion, surface cleaning and wetting of the particles and particle size reduction.

In heterogeneous liquid/liquid reactions, cavitational collapse at or near the interface will cause disruption and mixing, resulting in the formation of very fine emulsions (Figure 8).

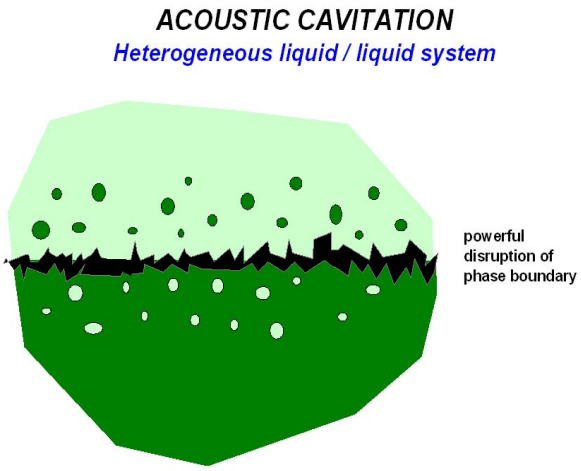

Figure 8. Cavitation effects in a heterogeneous liquid/liquid system.

Applications

Sonication can be used for the production of nanoparticles, such as nanoemulsion [8], nanocrystals, liposomes and wax emulsions, as well as for wastewater purification, degassing, extraction of plant oil, production of biofuels, crude oil desulphurization, cell disruption, polymer and epoxy processing, adhesive thinning, and many other processes. It is applied in pharmaceutical, cosmetic, water, food, ink, paint, coating, wood treatment, metalworking, nanocomposite, pesticide, fuel, wood product and many other industries.

Sonication can be used to speed dissolution, by breaking intermolecular interactions. It is especially useful when it is not possible to stir the sample, as with NMR tubes. It may also be used to provide the energy for certain chemical reactions to proceed. Sonication can be used to remove dissolved gases from liquids (degassing) by sonicating the liquid while it is under a vacuum. This is an alternative to the freeze pump thaw and sparing methods.

In biological applications, sonication may be sufficient to disrupt or deactivate a biological material. For example, sonication is often used to disrupt cell membranes and release cellular contents. This process is called sonoporation. Sonication is also used to fragment molecules of DNA, in which the DNA subjected to brief periods of sonication is sheared into smaller fragments. Sonication is commonly used in nanotechnology for evenly dispersing nanoparticles in liquids.

Sonication is the mechanism used in ultrasonic cleaning loosening particles adhering to surfaces. In addition to laboratory science applications, sonicating baths have applications including

cleaning objects such as spectacles and jewlry. Sonication is also used to extract microfossils from rock [6]. Sonication can also refer to buzz pollination the process that bees use to shake pollen from flowers by vibrating their wing muscles.

Equipment

Ultrasonication offers great potential in the processing of liquids and slurries, by improving the mixing and chemical reactions in various applications and industries. The effects of cavitation are used for the deagglomeration and milling of micrometre and nanometre-size materials as well as for the disintegration of cells or the mixing of reactants. In this aspect, ultrasonication is an alternative to high-speed mixers and agitator bead mills.

Ultrasonic foils under the moving wire in a paper machine will use the shock waves from the imploding bubbles to distribute the cellulose fibres more uniformly in the produced paper web, which will make a stronger paper with more even surfaces. Furthermore, chemical reactions benefit from the free radicals created by the cavitation as well as from the energy input and the material transfer through boundary layers. For many processes, this sonochemical effect leads to a substantial reduction in the reaction time, like in the transesterification of oil into biodiesel.

Substantial intensity of ultrasound and high ultrasonic vibration amplitudes are required for many processing applications, such as nano-crystallization, nano-emulsification [9], deagglomeration, extraction, cell disruption, as well as many others. Commonly, a process is first tested on a laboratory scale to prove feasibility and establish some of the required ultrasonic exposure parameters. After this phase is complete, the process is transferred to a pilot (bench) scale for flow-through pre-production optimization and then to an industrial scale for continuous production. During these scale-up steps, it is essential to make sure that all local exposure conditions (ultrasonic amplitude, cavitation intensity, time spent in the active cavitation zone, etc.) stay the same. If this condition is met, the quality of the final product remains at the optimized level, while the productivity is increased by a predictable "scale-up factor". The productivity increase results from the fact that laboratory, bench and industrial-scale ultrasonic processor systems incorporate progressively larger ultrasonic horns, able to generate progressively larger high-intensity cavitation zones and, therefore, to process more material per unit of time. This is called "direct scalability". It is important to point out that increasing the power capacity of the ultrasonic processor alone does *not* result in direct scalability, since it may

be (and frequently is) accompanied by a reduction in the ultrasonic amplitude and cavitation intensity. During direct scale-up, all processing conditions must be maintained, while the power rating of the equipment is increased in order to enable the operation of a larger ultrasonic horn [10-12].

POLYMER degradation

Since the hydrophobic derivatization of the native Scleroglucan (Sclg) and Guar Gum (GG) did not lead to nanhydrogel formation, probably due to the rigidity and the high molecular weight of the polymer chains, we undertook a depolymerization strategy to improve the nanhydrogel size and morphology. The Sclg & GG molecular weight was reduced by sonication and the obtained polymer was then hydrophobically modified, yielding a novel polymeric amphiphile. It is noteworthy that the solutions of native Sclg and GG exhibited much higher viscosities than the corresponding solutions of the sonicated polymer. Moreover, the native polymer could be solubilized in distilled water only at high temperatures while the corresponding ‘‘sonicated’’ polymer was easily solubilized in distilled water at room temperature. These features represent a great advantage in the polymer treatments during nanhydrogel preparation steps and influence nanhydrogel properties.

We chose ultrasonic treatment to reduce the polymer molecular weight because it allowed to avoid the use of chemicals or enzymes and the ultrasonic radiation splits the most susceptible chemical bonds in the polymer chains without causing any changes in the chemical structure of the macromolecule [13].

(a)

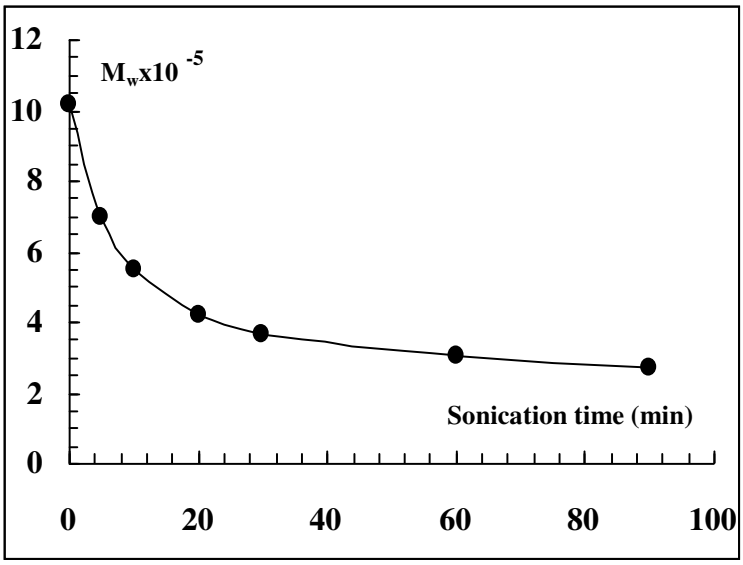

(b)

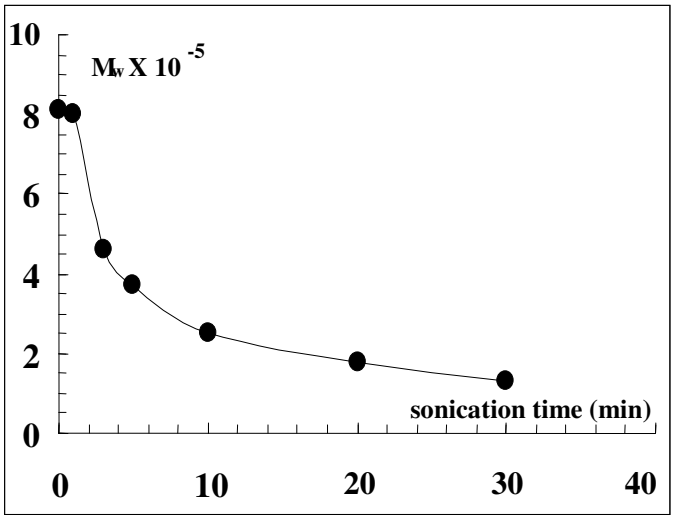

Figure 9. Weight dependence on the sonication time for Sclg and GG shown in (a) and (b)

The decrease of the molecular weight of native Sclg was strongly dependent on the ultrasound treatment time. For up to 1 h of sonication time the Mw decreased (Figure. 9a) and then remained at a stable value for up to 100 min. The Mw of Sclg, starting from about 10.0 x 10^5, was thus reduced to 3.07 x 10^5, by applying ultrasounds for 1 h. The Mw of GG, starting from about 8.0 x 10^5, was thus reduced to 1.32 x 10^5, by applying ultrasound for 30 min.

9.1. Refefences

1. http://www.rsc.org/publishing/journals/prospect/ontology.asp?id=CMO:0001708
2. Suslick K S. Sonochem Sci. 1990; 247:1439.
3. Suslick K S, Flannigan D J. Annual Rev Phys Chem. 2008; 59:659.
4. Suslick K S. Scientific American. 1989; 62:62.
5. Neppiras E A. Ultrasonic*s*. 1984; 22: 25.
6. Henglein A.Ultrasonics.1987; 25:6.
7. Suslick K S. Sci.1990; 247:1439.

8. Peshkovsky A S, Peshkovsky S L, Bystryak S. Chemical Engineering and Processing Process Intensification. 2013; 69:77.

9. Gensel P G, Johnson N G, Strother P K. Early Land Plant Debris Hooker's Waifs and Strays PALAIOS. 1990; 5:520.

10. Peshkovsky S L, Peshkovsky A S. Ultrason Sonochem. 2007; 14:314.

11. Peshkovsky A S, Peshkovsky S L. Industrial-scale processing of liquids by high intensity acoustic cavitation the underlying theory and ultrasonic equipment design principles In Nowak F.M. ed, Sonochemistry Theory Reactions and Syntheses and Applications Hauppauge NY Nova Science Publishers. 2010.

12. Peshkovsky A S, Peshkovsky S.L. Acoustic Cavitation Theory and Equipment Design Principles for Industrial Applications of High-Intensity Ultrasound Book Series Physics Research and Technology, Hauppauge NY Nova Science Publishers. 2010.

13. Heymach G J, Jost D E, J Polym Sci. Part C Polym Symp. 1968; 25:145.

10. Aim of the thesis

The aim of the thesis was the preparation of polysaccharide chains at low molecular weight by means of a non-toxic method. The obtained polysaccharides were characterized in terms of rheological properties. Furthermore, the effect of addition of borax on the new samples was investigated by recording the mechanical spectra, the flow curves and the swelling behaviour of tablets prepared with the sonicated polymers. Actually, a well-defined knowledge of these systems can improve their use as drug delivery carriers and for biomedical applications.
The GG and Sclg at lower molecular weights were then used for derivatization reactions in order to prepare new substrates for self-assembling nanoparticles for modified drug delivery. The possible use of Sclg for new topical delivery system was also tested.

10.1. Outline

In **Chapter 1** a general and very schematic overview of the main thesis topics is given. In particular, a short introduction on polysaccharides, especially on those used in this thesis, Scleroglucan and Guar Gum, was reported. Information on a specific kind of hydrogels, the nanohydrogels, was included, together with some comments on the drug delivery mechanism. Finally, some details on the technique applied during the research work (viscometry, rheology, texture analysis, GPC, sonication) were also added.

In **Chapter 2** the variations of properties after reduction of Scleroglucan molecular weight were reported. Thus, the effect of sonication on two different polymer concentrations and for different period of time was investigated. Molar mass, estimated by viscometric measurements, was drastically reduced already after a sonication for a few min. Sonicated samples were used for the preparation of gels in the presence of borate ions. The effect of borax on the new samples was investigated by recording the mechanical spectra and the flow curves. A comparison with the system prepared with the dialysed polymer was also carried out. The anisotropic elongation, observed with tablets of scleroglucan and borax, was remarkably reduced when the sonicated samples were used for the preparation of the gels. The sonication process did not change the basic repeating units of Sclg, as evidenced by means of NMR spectra. Thus, sonication appeared a rather easy and suitable method to reduce the molecular weight of Sclg without destroying the structural characteristic of the polymeric chains.

Chapter 3 reports the sonication of Guar Gum for different periods of time, and the characterization of the obtained fractions at lower molecular weight. Viscoelasticity range, flow curves, and mechanical spectra were recorded together with an estimation of molecular weight by mans of viscometric measurements. Sonicated samples were used for the preparation of gels in the presence of borate ions. The effect of borax on the new samples was investigated: the anisotropic elongation, observed in previous studies with tablets of Guar Gum and borax, was remarkably reduced when the sonicated samples were used for the preparation of the gels. As evidenced in the NMR spectra, sonication does not destroy the structural characteristics of the polymeric chains. Thus, sonication appears to be a rather easy method suitable to reduce the molecular weight of polysaccharides without the use of chemicals allowing more easily acceptable applications in the field of pharmaceutics, cosmetics, and food industry.

Chapter 4 reports the different chemical approaches carried out in order to derivatize the Sclg and GG polymeric chains for the final formation of self-assembled structures in the form of nanohydrogels suitable for modified drug delivery systems.

Chapter 5 reports the preparation of Sclg films loaded with tioconazole, a drug usually used for dermal therapies. Preliminary “in vitro” studies showed the noticeable fungal activity of the new formulation against Candida Albicans infections. A dynamo-mechanical characterization and swelling studies of the novel delivery system were carried out.

Chapter 2

EVALUATION OF RHEOLOGICAL PROPERTIES AND SWELLING BEHAVIOUR OF SONICATED SCLEROGLUCAN SAMPLES

Molecules **2012**, *17*, 2283-2297; doi:10.3390/molecules17032283

OPEN ACCESS

molecules

ISSN 1420-3049

www.mdpi.com/journal/molecules

Article

Evaluation of Rheological Properties and Swelling Behaviour of Sonicated Scleroglucan Samples

Siddique Akber Ansari, Pietro Matricardi, Chiara Di Meo, Franco Alhaique and Tommasina Coviello *

Department of Drug Chemistry and Technologies, University "La Sapienza", 00185 Rome, Italy; E-Mails: siddiqueakber.ansari@uniroma1.it (S.A.A.); pietro.matricardi@uniroma1.it (P.M.); Chiara.Dimeo@uniroma1.it (C.D.M); franco.alhaique@uniroma1.it (F.A.)

* Author to whom correspondence should be addressed; E-Mail: tommasina.coviello@uniroma1.it; Tel.: +39-06-4991-3557; Fax: +39-06-4991-3133.

Received: 16 January 2012; in revised form: 9 February 2012 / Accepted: 16 February 2012 / Published: 24 February 2012

Abstract: Scleroglucan is a natural polysaccharide that has been proposed for various applications. However there is no investigation on its property variations when the molecular weight of this polymer is reduced. Scleroglucan was sonicated at two different polymer concentrations for different periods of time and the effect of sonication was investigated with respect to molecular weight variations and rheological properties. Molar mass, estimated by viscometric measurements, was drastically reduced already after a sonication for a few min. Sonicated samples were used for the preparation of gels in the presence of borate ions. The effect of borax on the new samples was investigated by recording the mechanical spectra and the flow curves. A comparison with the system prepared with the dialysed polymer was also carried out. The anisotropic elongation, observed with tablets of scleroglucan and borax, was remarkably reduced when the sonicated samples were used for the preparation of the gels.

Keywords: scleroglucan; sonication; rheology; polymer gels; swelling

1. Introduction

Scleroglucan (Sclg) is a homopolysaccharide, produced by fungi of the genus *Sclerotium*, consisting of a main chain of (1→3)-linked β-D-glucopyranosyl units bearing, every three units, a

single β-D-glucopyranosyl unit linked (1→6). The commercial polymer is produced by various companies (e.g., Cargill, Mero-Rousselot-Satia, Degussa, CarboMer) with slightly differences in the application features.

Because of its peculiar rheological properties, its resistance to hydrolysis, temperature and electrolytes, Sclg has several industrial applications, in the oil industry, for water colours, printing inks, animal feed, *etc*. Several Japanese patents proposed the use of Sclg for the improvement of food quality. The polymer has been used also in cosmetic industry as well as in the field of pharmaceutics [1–3]. In the last few years, several studies have been carried out for the possible use of Sclg and its derivatives as new matrices for sustained drug delivery purposes [4–12]. Furthermore, Sclg shows antitumor, antiviral and antimicrobial activities as well as immune stimulatory effects [13–16].

X-ray diffraction studies indicate that Sclg has a triple-helical backbone conformation in the solid state that is maintained also in aqueous solutions [17]. In the presence of borax Sclg, like other polysaccharides, gives a weak gel that shows a higher capability to keep its shape when a stress is applied [18]. It is interesting to point out that when tablets were prepared with this Sclg/borax network, swelling induced a peculiar anisotropic elongation and, at the same time, also an uncommon enhanced diffusion of water molecules was found by means of NMR studies [19–24].

The Sclg/borax gel can be described in terms of soft nanochannels made up by Sclg triple helix aggregates. The triple helices are organized in domains with an intrinsic ordered structure that leads to an anisotropic arrangement of the chains along the compression direction during the tablet preparation. This kind of arrangement deeply influences the diffusion properties of water molecules (during the swelling experiments), which show an enhanced diffusion that may play an important role on the release performance of the gels. Actually, a deeper knowledge of the mechanisms involved in drug release also depends on matrix swelling and water molecules diffusion.

The commercially available Sclgs have molecular weights of the order of 10^6. This high molecular weight often is not suitable for specific applications, e.g., for the preparation of micro- or nano-systems suitable for drug delivery. In order to get a more versatile polymer, the decrease of the molar mass was suggested.

In this paper the preparation of various batches of Sclg (provided by Cargill) with reduced molecular weight, obtained by sonication, is described. The molecular weight was estimated by capillary viscometric measurements. The rheological properties of the new samples were investigated and a comparison with Sclgs purified by means of dialysis or centrifugation was carried out. Furthermore, the swelling behaviour of tablets prepared with Sclg obtained from different companies (samples already used for previous studies by the authors and, in some cases, no longer on the market or produced by companies acquired by other industries) and with different trade names and borax, together with tablets prepared with the sonicated samples, was studied in order to test the possible differences in water uptake and in anisotropic elongation among all tested samples.

2. Results and Discussion

2.1. Rheological Measurements

Sclg solutions were first prepared at two different polymer concentrations, cp = 0.1 and 0.5 (w/v), in order to test the influence of this parameter on the sonication process. Furthermore, the sonication

process was carried out for different periods of time: from a minimum of 5 min up to 120 min. After sonication, the samples were centrifuged. The flow curves for the different batches of polymer sonicated for different periods of time at two different cp (cp = 0.1 and 0.5%) are shown in Figure 1.

Figure 1. (A) Flow curves of Sclg samples sonicated at cp = 0.1% (open symbols) and cp = 0.5% (full symbols) for different periods of time. (B) Flow curves of Sclg sonicated for 10 and 120 min at cp= 0.1 and 0.5%. For comparison, also the flow curves recorded for the dialysed Sclg and the centrifuged Sclg, are reported (cp = 0.7%, T = 25 °C).

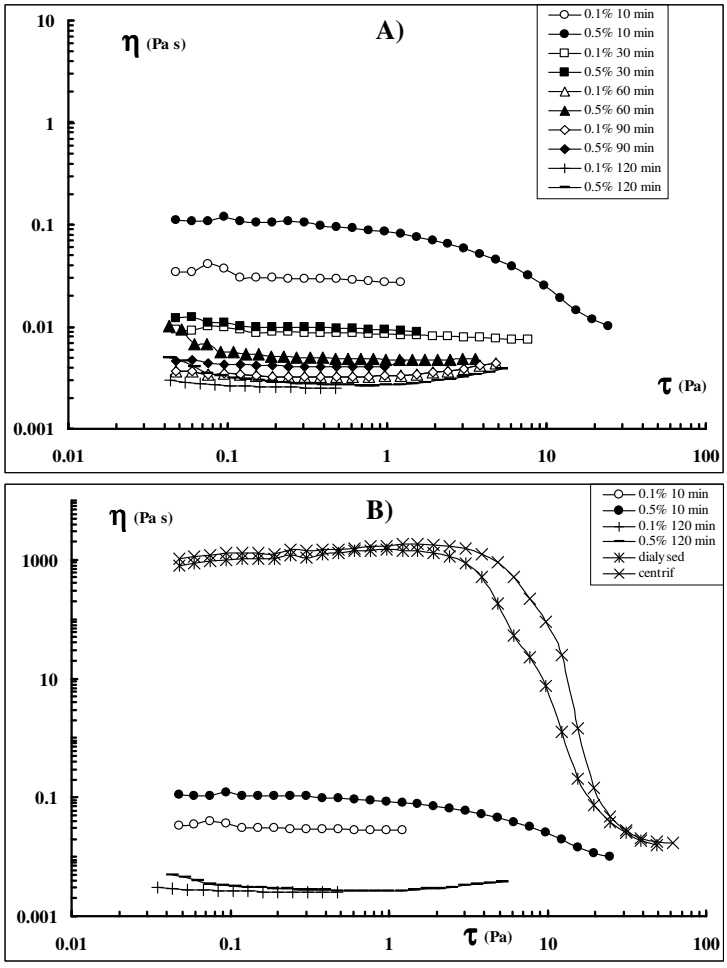

As a comparison, also the flow curves of the Sclg purified by dialysis, and the centrifuged Sclg, are reported. For the rheological measurements, all samples, regardless of the concentration used for the sonication process, were tested at cp = 0.7%. It can be noted that the Sclg dialysed and the centrifuged one, show similar flow curve profiles. It can be observed that a sonication of 30 min is sufficient to reduce drastically the viscosity of the polymer: at $\tau = 5 \times 10^{-2}$ (Pa) the viscosity drops from 1,000 to 0.01 (Pa s) for both systems, (*i.e.*, the polymer that was sonicated at cp = 0.1% and the one that was sonicated at cp = 0.5%) indicating that polymer concentration during the sonication process is not a crucial parameter. A slight difference between the two set of cp could be appreciated only after a sonication of 10 min, being the viscosity of the polymer sonicated at cp = 0.5% slightly higher than

that of the polymer sonicated at cp = 0.1%. Anyhow, ten min of sonication were sufficient to break significantly the Sclg chain backbones and to reduce to one half the molecular weight (see Section 3.2).

Increasing the sonication time, a further breakdown of the polymeric chains occurs without damaging the repeating unit structure, as evidenced by NMR analysis (Figure 2).

Figure 2. ^{1}H-NMR spectra at 600.13 MHz and 27 °C (DMSO-d_6 + 10% v/v of D_2O) of dialysed Sclg (green), Sclg sonicated 30 min (red) and Sclg sonicated 60 min (black).

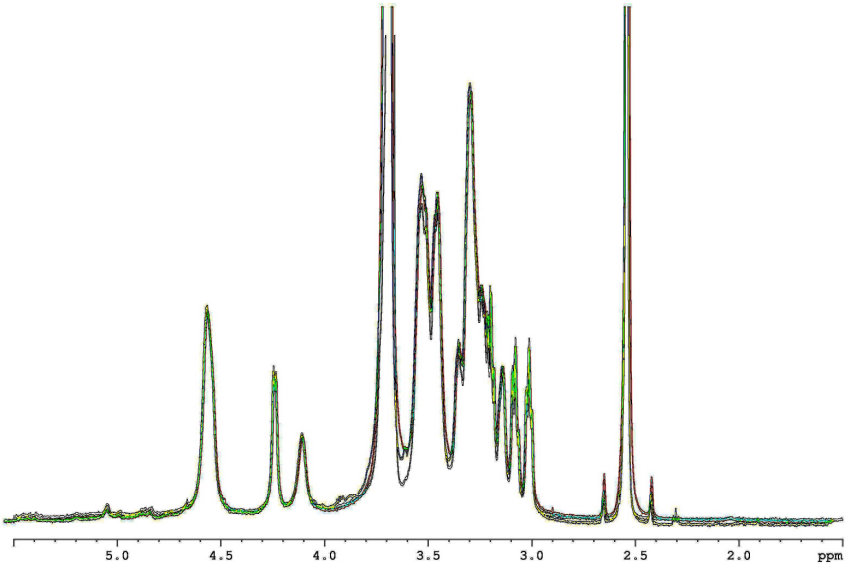

NMR was carried out in DMSO-d_6, in order to separate the Sclg triple helices in single chains, thus obtaining sharp signals of the polymer; the addition of 10% v/v D_2O allowed a further spectrum simplification by suppressing all hydroxyl proton resonances. As shown in Figure 2, the spectra of the dialysed sample, of the Sclgs sonicated for 30 and 60 min, are superimposable. In particular, the ratio between the anomeric β (1→3) protons at 4.571 ppm and the anomeric β (1→6) protons at 4.245 ppm remains constant and equal to 3 for all tested samples. Thus, the sonication process can be proposed as a valid method for the Sclg molecular weight reduction. In fact, by means of sonication, it is possible to prepare Sclg with a wide range of molecular weights but keeping intact the molecular structure as supported by the experimental conditions that prevent disentanglements of the triple helices: temperature below 135 °C (melting temperature of the triple helix), because of the ice bath; environmental pH well below 13 and absence of DMSO (solvent capable to breakdown the Sclg triple helix). This is a crucial point, especially with reference to possible industrial and biomedical applications of Sclg, since the rheological properties of the polymeric solutions prepared with the sonicated samples show remarkable variations in comparison to the dialysed polymer.

The addition of borax to the various samples was also investigated (Figure 3). Addition of borate ions to Sclg samples led to the formation of a network with a higher flow resistance (in comparison to the polymer alone) that was also capable to keep its shape (*i.e.*, a self-sustaining gel is formed).

Critical stresses, τ_c = 2 and τ_c = 4 were found for Sclg and Sclg/borax respectively (using the dialysed Sclg) and τ_c = 3 and τ_c = 6 were found for Sclg and Sclg/borax (using the centrifuged Sclg), where τ_c represents the stress value corresponding to 95% of the viscosity plateau value. On the other

side, for all sonicated samples, no appreciable variations were detected in the flow curves, regardless of the presence or absence of the borate ions. Thus, in these samples, the key parameter for the flow characteristics is only represented by the molecular weight of the polymer.

Figure 3. Flow curves of Sclg samples (cp = 0.7%), previously sonicated at cp = 0.1% and cp = 0.5%, with (full symbols) and without borax (empty symbols) (A). Flow curves of Sclg sonicated (cp = 0.5%) for 10 and 90 min with and without borax: for comparison, also the flow curves recorded for the dialysed and the centrifuged Sclgs, are reported (B).

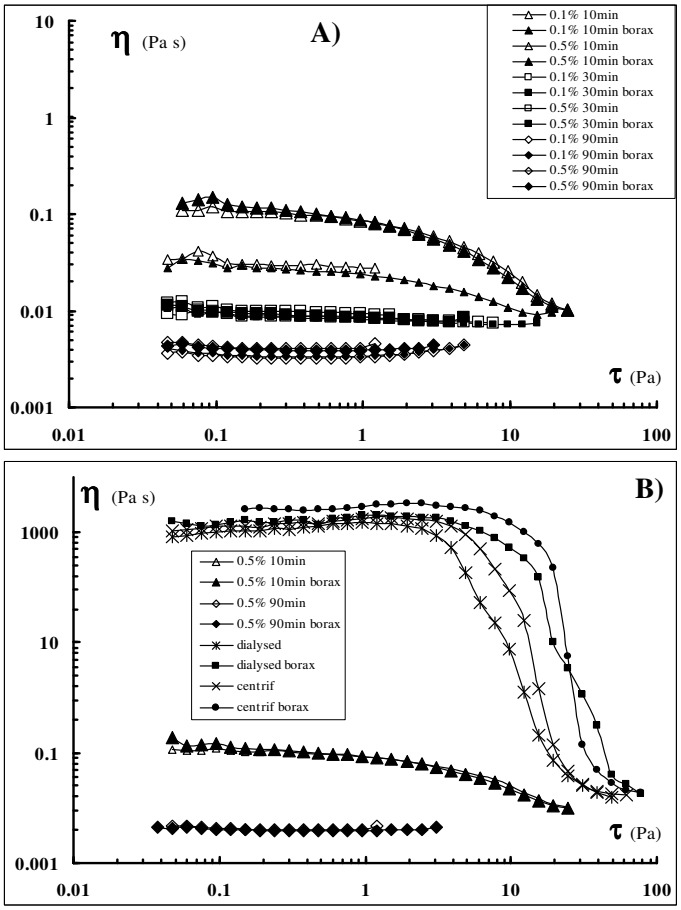

Interestingly, the modulus variations in the stress sweep experiments also show the noticeable effect of the sonication process on the supramolecular structure. Actually, in order to acquire meaningful data for the sonicated samples, a sonication of only 5 min was applied (Figure 4). In fact, for higher sonication times, it was not possible to detect the sample moduli. The effect of 5 min sonication on the storage modulus is rather impressive: for G': a drastic reduction of ten times was observed while the decrease in the loss modulus, G", was much smaller. Thus, the breakdown of the polymeric chains mainly influences the elastic component of the system, *i.e.*, the chains, becoming shorter and shorter, are not capable any longer to give entanglements with effective elastically crosslinking points which are responsible for the increase of G' in the gel system. On the other side, also the viscous component is influenced by the molecular weight decrease with a corresponding lowering (even smaller) of G" that is comparable and almost the same of G'.

Figure 4. Viscoelasticity plot for dialysed Sclg (●, ○) and for Sclg sonicated for 5 min (■, □); cp = 0.7%, T = 25 °C (G' = full symbols; G" = empty symbols).

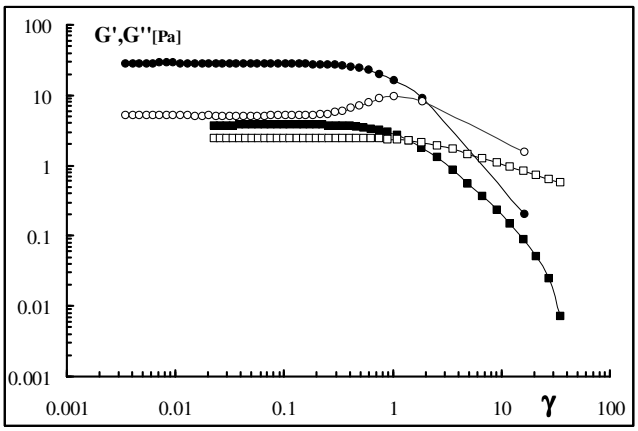

Interesting was also the comparison between the two mechanical spectra (Figure 5). While the dialysed Sclg showed the typical weak gel behaviour, the sample sonicated for 5 min showed the characteristic sol-gel transition. This means that a significant reduction in the molecular weight (see also the viscosity measurements section) dramatically influences also the mechanical properties of the sample.

Figure 5. Mechanical spectra of dialysed Sclg (●, ○) and of Sclg sonicated for 5 min (■, □); cp = 0.7%, T = 25 °C (G' = full symbols; G" = empty symbols).

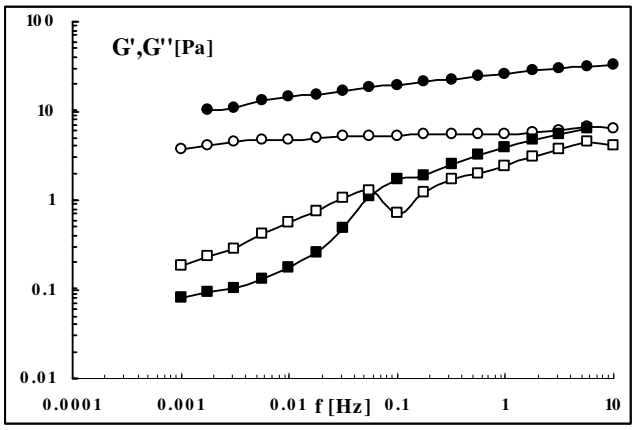

For frequencies lower than 0.05 the system is liquid-like while for higher frequencies the system is solid-like. A sonication prolonged for 10 min or higher leads to liquid-like systems with moduli too low to be experimentally recorded.

2.2. Viscosity Measurements

Solutions of the sonicated polymer were prepared in 0.01 N NaOH in order to break the possible aggregates still present in solution [25,26]. Viscosity measurements were carried out at 25 °C and the results are shown in Figure 6.

Figure 6. Plot of $\eta_{specific}/c$ *vs.* polymer concentration for Sclg samples sonicated for different periods of time (NaOH = 0.01 N, T = 25 °C).

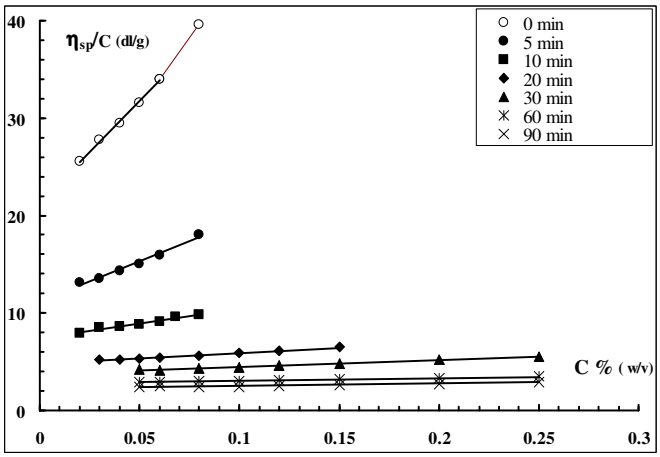

From the intercepts, *i.e.*, from the intrinsic viscosities [η] of the samples, according to the Mark-Houwink-Sakurada equations valid for Sclg [27]:

$$[\eta] = KM_w^{1.7} \text{ for } M_w < 5 \times 10^5$$

$$[\eta] = KM_w^{1.2} \text{ for } M_w > 5 \times 10^5$$

where K = 1,3 × 10^{-7} cm^3 g^{-1}, the molecular weights of the various fractions were estimated and reported in Figure 7. It is possible to observe that, applying the sonication for only 10 min, the molecular weight of the polymer was reduced to one half. The reduction was further increased by increasing the sonication process for longer time. The values of the Huggins constant (see Table in Figure 7) calculated for all samples from the slope of the linear trend of viscosity data are 0.5 ± 0.1 indicating that, in the applied experimental conditions (0.01 N NaOH), no significant aggregation of the polymeric chains occurs.

Figure 7. Sclg molecular weight dependence on sonication time (NaOH = 0.01 N, T = 25 °C), together with the calculated Huggins constants (k_H).

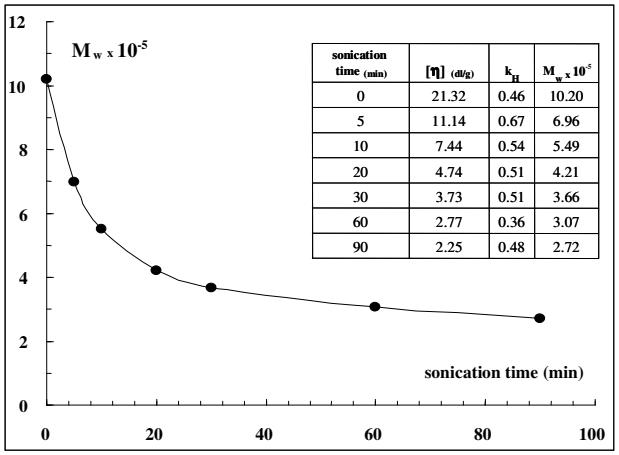

sonication time (min)	[η] (dl/g)	k_H	$M_w \times 10^{-5}$
0	21.32	0.46	10.20
5	11.14	0.67	6.96
10	7.44	0.54	5.49
20	4.74	0.51	4.21
30	3.73	0.51	3.66
60	2.77	0.36	3.07
90	2.25	0.48	2.72

2.3. Water Uptake and Dimensional Increase Studies

It is known [19–24] that tablets, prepared with the Sclg/borax freeze-dried hydrogel, undergo an anomalous peculiar swelling essentially along one direction. New tablets were then prepared with the sonicated samples and the water uptake and the elongation behaviour were followed as a function of time. As a comparison, the experiments were carried out also on tablets prepared with Sclg produced (in some cases not marketed anymore) by different companies, *i.e.*, Degussa, CarboMer, and Mero-Rousselot-Satia (Actigum CS11).

The results, reported in Figure 8 (in distilled water at 37 °C), clearly show that both, the water uptake and the anisotropic elongation of the tablets, observed for the Sclg/borax system, were dramatically reduced when the sonicated samples were tested.

Figure 8. Water uptake ($(w-w_0)/w_0$; (A) and relative height increase ($(h-h_0)/h_0$; (C) from tablets of Sclg/borax prepared with Sclg of different brands (Cargill dialysed, Cargill centrifuged, Actigum CS11, CarboMer and Degussa) and with Sclg sonicated for different periods of time (Cargill sonicated for 5, 10, 20, 30 and 60 min). (A) and (C): as a function of time; (B) and (D): as a function of the square root of time. Experiments were carried out in triplicate and the obtained values always laid within 10% of the mean.

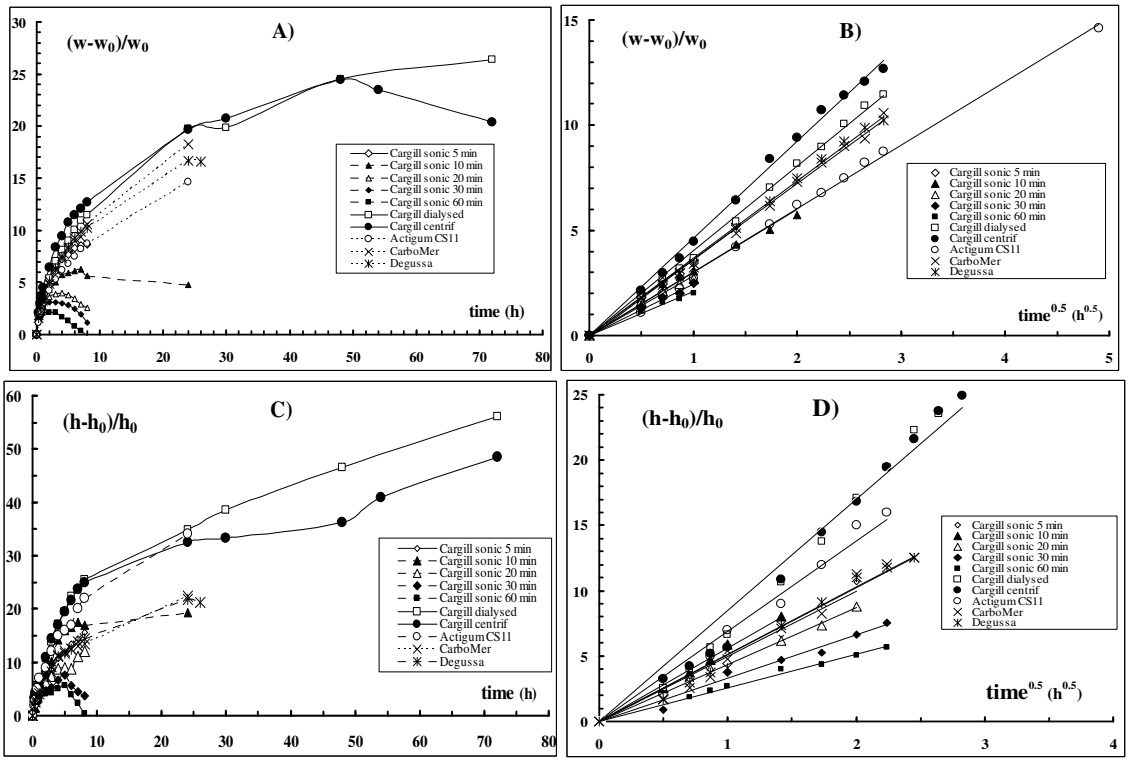

While the tablets prepared with the untreated polymer increased their weight and elongated even after 3 days, those prepared with Sclg sonicated for 5 min started to dissolve in the medium already after 8 hours. This phenomenon occurred earlier and earlier as the applied sonication time increased: the tablets prepared with Sclg sonicated for 1 hour ($M_w = 3.07 \times 10^5$) started to loose their weight

already after 1 hour and the anomalous elongation could be detected only up to 5 hours. After 8 hours the tablets dissolved completely in the swelling medium.

In Figure 9 the pictures of tablets prepared with different types of Sclg and swelled for different periods of time are shown. Both processes, the uptake of water and the height increase, obey, during the first hours, the fickian law in all tested systems (Figure 8). Thus, the reduction of the polymeric chain lengths did not change the diffusional character of water molecules behaviour during the imbibition of the tablet matrices.

Figure 9. Pictures of Sclg/borax tablets, prepared with Cargill Sclg dialysed, centrifuged and sonicated for 10 and 60 min, after swelling for different periods of time in distilled water at 37 °C (the height of the tablets before the swelling process was $h_0 \approx 1.05$ mm).

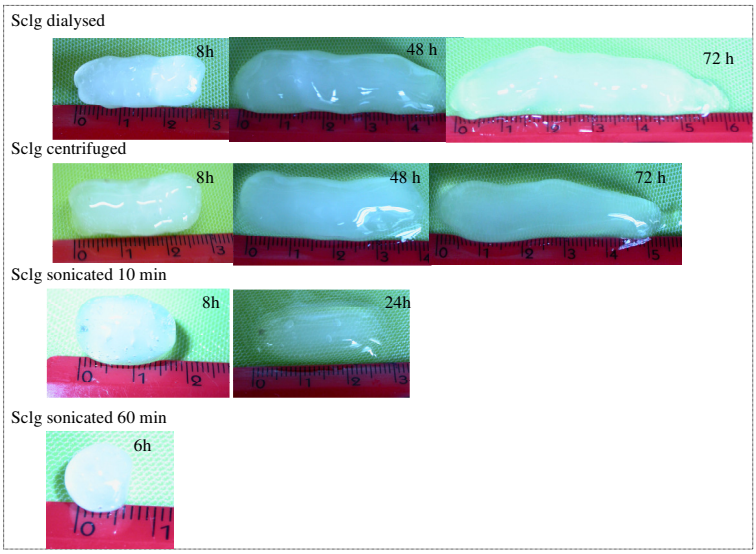

In Figure 10 the rates of water uptake and tablet elongation processes (*i.e.*, the slope of Figure 8 linear trends) *vs.* the sonication time are reported. For comparison, the dependence of M_w on sonication time is also shown. It is clear that the highest rate in anisotropic elongation is observed for tablets prepared with Sclg with $M_w = 6.96 \times 10^5$. Also in the profile describing the M_w *vs.* the sonication time the biggest effect is observed after a sonication of 5 min. On the other hand, the weight increase showed a slower kinetic in comparison to the height increase and a reduced dependence on the sonication time. As a comparison the rates calculated for the swelling of tablets prepared with the dialysed Sclg are also reported. Both rates are almost superimposable to those of centrifuged Sclg. Thus, the water uptake and anisotropic elongation phenomena mainly depend on the polymeric molar mass, both for the extent of the processes and for the rate. On the other side for the raw polymer, the dialysis purification (in order to eliminate the low mass fraction of the polymer and impurities, if present, of low molecular weight) or the centrifugation process (to eliminate the large and rough aggregates) did not influence significantly the swelling behaviour.

Figure 10. Slopes of the fickian linear trends for the water uptake and height increase (left) together with the molecular weight dependence on the sonication time (right).

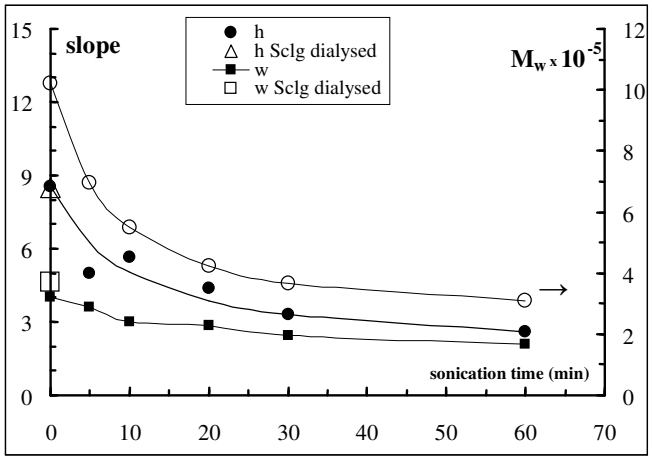

3. Experimental

3.1. Materials

Sclg was provided by Cargill (Minneapolis, USA), while borax and NaOH Normex were Carlo Erba (Italy) products. For the sample preparations distilled water was always used, except for NMR experiments, where deuterium oxide (D_2O) (Cambridge Isotope Laboratories, USA) was used. All products and reagents were of analytical grade.

For an appropriate comparison, also scleroglucans provided in the past by different companies, were tested: in particular the Sclg provided by Mero-Rousselot-Satia (France, molecular weight = 1.4×10^6 from viscometric measurements), named Actigum CS11 (no more in the market), the Sclg provided by CarboMer (USA, degree of polymerization = 800), and the Sclg provided by Degussa (Germany, molecular weight = 1.1×10^6, from viscometric measurements).

3.1.1. Purification of Scleroglucan

A given amount of polymer was dissolved in distilled water (polymer concentration, cp = 0.5% w/v), and then kept under magnetic and mechanical stirring at room temperature for 24 h. The obtained solution was exhaustively dialysed at 7 °C against distilled water and then freeze-dried.

3.1.2. Hydrogel and Tablet Preparation

For the preparation of the tablets, an appropriate amount of polymer (about 200 mg) was magnetically stirred in water for 24 h. Then, the calculated amount (*i.e.*, moles of borax = moles of repeating units of polymer) of 0.1 M borax solution was added and the system was left under magnetic stirring for 5 min The obtained sample (cp = 0.7%, w/v) was kept overnight at 7 °C for gel-setting and then freeze-dried. Tablets were prepared from the freeze-dried sample with an IR die (Perkin Elmer hydraulic press) using a force of 5.0 kN for 30 s. The weight of the Sclg/borax tablets was 230 ± 10 mg, the diameter was 13.0 ± 0.1 mm, and the thickness was 1.05 ± 0.02 mm.

3.2. Methods

3.2.1. Sonication

To reduce the Sclg molecular weight a High Intensity Ultrasonic Processor (750 Watt model, probe type sonicator–Vibra Cell–VC 750, Cole-Parmer, USA) was used, working at 20 kHz, with a 6.5 mm microtip, applying an amplitude of 30% and pulser cycles of 30 s ON and 30 s OFF. Aqueous solutions (50 mL) of Sclg, prepared at two different polymer concentrations, cp = 0.1 and 0.5% w/v, were kept in an ice bath during sonication. All samples (cp = 0.1 and 0.5% w/v), after sonication, were centrifuged for 20 min at 18,000 rpm and 20 °C in order to remove the probe-tip residues from the polymer solutions. Freeze-drying procedure was then carried out.

3.2.2. Ultracentrifugation

Sclg samples were also prepared by centrifugation, in order to separate the aggregates from the polymer solutions (cp = 0.5% w/v). For this purpose a centrifuge Sorvall WX 80 ULTRA (Thermo Scientific, USA) was used (20 min at 18,000 rpm and 20 °C). Freeze-drying procedure was then carried out.

3.2.3. NMR Analysis

Samples of dialysed Sclg, Sclg sonicated 30 min and Sclg sonicated 60 min, about 4 mg, were solubilized in 630 μL of DMSO-d_6 + 70 μL D_2O. ^{1}H-NMR experiments were performed at 27 °C on a Bruker AVANCE AQS 600 spectrometer operating at 600.13 MHz and equipped with a Bruker multinuclear, *z*-gradient probe head. A soft presaturation of the HOD residual signal was applied before the spectra acquisition [28].

3.2.4. Rheological Measurements

The rheological characterization of the Sclg and Sclg/borax samples was performed by means of a controlled stress rheometer (Haake Rheo-Stress RS300; Thermo Haake DC50 water bath); a cross-hatch plate device (Haake PP35 TI: diameter = 35 mm) was used in order to reduce the extent of wall slippage phenomena [29]. To perform the measurements, the samples were transferred in the rheometer and the upper plate was then lowered until it reached the sample surface. Gap-setting optimizations have been undertaken according to the procedure described elsewhere [30]. Samples were loaded at fixed temperature (25 °C), and coated around their periphery with light silicone oil to minimize loss of water. Rheological properties were studied under small and large deformations, as well as in flow conditions, by applying different procedures: stress (ν = 1 Hz, $\omega = 2\pi\nu$ = 6.28 rad/s) and frequency sweep (in the linear viscoelastic region; constant deformation γ = 0.01).

3.2.5. Viscosity Measurements

For the viscosity measurements an automatic viscometer (Instrument Schott AVS 370, Lauda, Germany) with a water bath (Lauda 0.15 T) allowing the temperature control to 0.1 °C was used. An Ubbelohde capillary viscometer (Type No 531 01, with a capillary diameter = 0.54 mm, Schott-Geräte)

for dilution sequences, with a flux time for the solvent (NaOH = 0.01 N) at 25 °C of 178.56 s, was used.

The polymer solutions (Sclg in 0.01 N NaOH), before measurements, were filtered two times with 1.2 μ Millipore filters. The solvent for the dilution was previously filtered three times with 0.22 μ Millipore filters. The flux time of the solution (η) was compared with that of the solvent (η_0) and the relative increase of fluxing time ($\eta/\eta_0 = \eta_{rel}$; $\eta_{rel} - 1 = t/t_0 - 1 = \eta_{specific}$) was evaluated at different polymer concentrations. In the range of viscosities up to about twice that of water (*i.e.*, $\eta_{rel} = 2$) the following Huggins equation is valid:

$$\eta_{specific}/c = [\eta] + k_H[\eta]^2 c$$

The limiting value of $\eta_{specific}/c$ for $c \rightarrow 0$ represents the intrinsic viscosity, $[\eta]$ (cm^3/g), while from the slope of the linear trend of viscosity data it is possible to calculate the Huggins constant, which gives an indication on the aggregation state of the polymer in the tested conditions of solvent and temperature [31]. The intrinsic viscosity is an important parameter being related, according to the Mark-Houwink-Sakurada equation, to the molar mass of the sample [32]: $[\eta] = KM_w^a$, where K and a are constants for each polymer-solvent system at a given temperature.

3.2.6. Water Uptake and Dimensional Increase Studies

The swelling of Sclg/borax tablets, prepared with different kinds of Sclg (*i.e.*, Cargill dialysed, Cargill centrifuged, Cargill sonicated for different times, Actigum CS11, CarboMer and Degussa), was carried out by soaking the tablets in distilled water at 37 °C. At fixed time intervals, the tablets were withdrawn, the excess of water was removed with soft filter paper for 5 s, and then the corresponding weights and dimensional variations along the longitudinal axis were determined by means of a screw gauge with an accuracy of ± 0.1 mm. No remarkable variations of cross-section dimensions were detected during the swelling process. All experiments were carried out in triplicate and the obtained values always laid within 10% of the mean.

4. Conclusions

The sonication process did not change the basic repeating units of Sclg, as evidenced by means of NMR spectra. Thus, sonication appeared a rather easy and suitable method to reduce the molecular weight of Sclg without destroying the structural characteristic of the polymeric chains. The effect of the M_w reduction on the rheological properties was studied. The flow curves were noticeably modified as a consequence of the polymeric chain reduction. Furthermore, it was possible to acquire the mechanical spectra only for the sample sonicated 5 min, the moduli of the other samples being too low to be detected. The sample sonicated for 5 min lost the characteristic of a weak gel (typical of Sclg samples) and showed the peculiar spectra of a system undergoing the sol-gel transition. Also the addition of borax, that usually increases the flow resistance in Sclg samples, did not affect the sonicated samples.

The Sclg molecular weight, as estimated by viscometric measurements, decreased very rapidly by applying ultrasounds to the polymeric solutions. The reduction to one half of M_w occurred already after 10 min of sonication.

The swelling behaviour of Sclg/borax tablets was also investigated. In this respect the reduced molecular weight of the polymer led to a noticeable difference in water uptake and anisotropic elongation in comparison to the dialysed Sclg. The tablets started to lose weight and to swell along one direction much earlier than the reference system showing the polymeric chain length as the most important parameter for these processes.

It has to be underlined that the possibility to modulate the mechanical properties of the Sclg solutions by changing the polymer molecular weight is very important in order to rationalize its behaviour in formulations to be used in various fields, as in drug delivery, for biomedical and cosmetics applications, and in food industry.

Acknowledgements

Sapienza University Grant C26A119N2S is acknowledged.

References and Notes

1. Coviello, T.; Palleschi, A.; Grassi, M.; Matricardi, P.; Bocchinfuso, G.; Alhaique, F. Scleroglucan a versatile polysaccharide for modified drug delivery. *Molecules* **2005**, *10*, 6–33.
2. Giavasis, I.; Harvey, L.M.; McNeil, B. Scleroglucan. In *Biopolymers Polysaccharides II*; De Baets, S., Vandamme, E.J., Steinbüchel, A., Eds.; Wiley-VCH: London, UK, 2002; Chapter 2, pp. 37–60.
3. Patachia, S.; Dobritoiu, R.; Coviello, T. Determination of the sorption efficiency of poly(vinyl alcohol)/scleroglucan cryogels, against Cu(2+) ions. *J. Environ. Eng. Manag.* **2011**, *10*, 193–198.
4. Coviello, T.; Grassi, M.; Rambone, G.; Santucci, E.; Carafa, M.; Murtas, E.; Riccieri, F.M.; Alhaique, F. Novel hydrogel system from Scleroglucan synthesis and characterization. *J. Control. Release* **1999**, *60*, 367–378.
5. Maeda, H.; Coviello, T.; Yuguchi, Y.; Urakawa, H.; Rambone, G.; Alhaique, F.; Kajiwara, K. Structural Characteristics of oxidized scleroglucan and its network. *Polym. Gels. Netw.* **1998**, *6*, 355–366.
6. Coviello, T.; Grassi, M.; Rambone, G.; Alhaique, F. A crosslinked system from Scleroglucan derivative preparation and characterization. *Biomaterials* **2001**, *22*, 1899–1909.
7. Maeda, H.; Rambone, G.; Coviello, T.; Yuguchi, Y.; Urakawa, H.; Alhaique, F.; Kajiwara, K. Low-degree oxidized scleroglucan and its hydrogel. *Int. J. Biol. Macromol.* **2001**, *28*, 351–358.
8. Coviello, T.; Grassi, M.; Lapasin, R.; Marino, A.; Alhaique, F. Scleroglucan/borax characterization of a novel hydrogel system suitable for drug delivery. *Biomaterials* **2003**, *24*, 2789–2798.
9. Coviello, T.; Alhaique, F.; Parisi, C.; Matricardi, P.; Bocchinfuso, G.; Grassi, M. A new polysaccharidic gel matrix for drug delivery preparation and mechanical properties. *J. Control. Release* **2005**, *102*, 643–656.
10. Coviello, T.; Alhaique, F.; Dorigo, A.; Matricardi, P.; Grassi, M. Two galactomannans and scleroglucan as matrices for drug delivery preparation and release studies. *Eur. J. Pharm. Biopharm.* **2007**, *66*, 200–209.

11. Coviello, T.; Matricardi, P.; Balena, A.; Chiapperino, B.; Alhaique, F. Hydrogels from Scleroglucan and ionic cross-linkers: Characterization and drug delivery. *J. Appl. Polym. Sci*. **2010**, *115*, 3610–3622.
12. Grassi, M.; Lapasin, R.; Coviello, T.; Matricardi, P.; Di Meo, C.; Alhaique, F. Scleroglucan/borax/drug hydrogels structure characterisation by means of rheological and diffusion experiments. *Carbohydr. Polym*. **2009**, *78*, 377–383.
13. Singh, P.; Wisler, R.; Tokuzen, R.; Nakahara, W. Scleroglucan, an antitumor polysaccharide from *Sclerotium glucanicum*. *Carbohydr. Res*. **1974**, *37*, 245–247.
14. Jong, S.; Donovick, R. Antitumor and antiviral substances from fungi. *Adv. Appl. Microbiol*. **1989**, *34*, 183–262.
15. Prets, H.; Eusley, H.; McNamee, R.; Jones, E.; Browder, I.; Williams, D. Isolation physicochemical characterisation and preclinical efficacy evaluation of a soluble scleroglucan. *J. Pharmacol. Exp. Ther*. **1991**, *257*, 500–510.
16. Patchen, L.; Bleicher, P. Mobilisation of peripheral blood precursor cells by beta (1,3)-glucan. U.S. Patent 6,117,850, 12 September 2000.
17. Palleschi, A.; Bocchinfuso, G.; Coviello, T.; Alhaique, F. Molecular dynamics investigations for the polysaccharide scleroglucan first study on the triple helix structure. *Carbohydr. Res*. **2005**, *340*, 2154–2162.
18. Coviello, T.; Coluzzi, G.; Palleschi, A.; Grassi, M.; Santucci, E.; Alhaique, F. Structural and rheological characterization of Scleroglucan/borax hydrogel for drug delivery. *Int. J. Biol. Macromol*. **2003**, *32*, 83–92.
19. Coviello, T.; Grassi, M.; Palleschi, A.; Bocchinfuso, G.; Coluzzi, G.; Banishoeib, F.; Alhaique, F. A new Scleroglucan/borax hydrogel anomalous swelling and drug release. *Int. J. Pharm*. **2005**, *289*, 97–107.
20. Palleschi, A.; Coviello, T.; Bocchinfuso, G.; Alhaique, F. Investigation of a new scleroglucan/borax hydrogel structure and drug release. *Int. J. Pharm*. **2006**, *322*, 13–21.
21. Coviello, T.; Bertolo, L.; Matricardi, P.; Palleschi, A.; Bocchinfuso, G.; Maras, A.; Alhaique, F. Peculiar behaviour of polysaccharide/borax hydrogel tablets a dynamo-mechanical characterization. *Colloid. Polym. Sci*. **2009**, *287*, 413–423.
22. Bocchinfuso, G.; Palleschi, A.; Mazzuca, C.; Coviello, T.; Alhaique, F.; Marletta, G. Theoretical and experimental study on a self-assembling polysaccharide forming nanochannels static and dynamic effects induced by a soft confinement. *J. Phys. Chem. B* **2008**, *112*, 6473–6483.
23. Bocchinfuso, G.; Mazzuca, C.; Sandolo, C.; Margheritelli, S.; Alhaique, F.; Coviello, T.; Palleschi, A. Guar Gum and Scleroglucan interactions with borax experimental and theoretical studies of an unexpected similarità. *J. Phys. Chem. B* **2010**, *114*, 13059–13068.
24. Di Meo, C.; Coviello, T.; Matricardi, P.; Alhaique, F.; Capitani, D.; La,manna, R. Anisotropic enhanced water diffusion in scleroglucan gel tablets. *Soft Matter* **2011**, *7*, 6068–6075.
25. Yanaki, T.; Kojima, T.; Norisuye, T. Triple helices in dilute aqueous sodium hydroxide. *Polym. J.* **1981**, *13*, 1135–1143.
26. Yanaki, T.; Norisuye, T. Triple helix and random coil Scleroglucan in dilute solution. *Polym. J.* **1983**, *15*, 389–396.

27. Yanaki, T.; Norisuye, T.; Fujita, H. Triple helix of *Schizophyllum commune* polysaccharide in dilute solution.3 Hydrodynamic properties in water. *Macromolecules* **1980**, *13*, 1462–1466.
28. Guerénon, M.; Plateau, P.; Decorps, M. Solvent signal suppression in NMR. *Prog. Nucl. Magn. Reson. Spectrosc*. **1991**, *23*, 135–109.
29. Lapasin, R.; Pricl, S. *Rheology of Industrial Polysaccharides Theory and Applications*; Blackie Academic & Professiona: London, UK, 1995.
30. Kuijpers, A.J.; Engbers, G.H.M.; Feijen, J.; De Smedt, S.C.; Meyvis, T.K.L.; Demeester, J.; Krijgsveld, J.; Zaat, S.A.J.; Dankert, J. Characterization of the network structure of carbodiimide cross-linked gelatin gels. *Macromolecules* **1999**, *32*, 3325–3333.
31. Tanford, C. *Transport Processes. Viscosity in Physical Chemistry of Macromolecules*; John Wiley & Sons, Inc.: New York, NY, USA, 1961; pp. 317–456.
32. Cantor, C.R.; Schimmel, P.R. *Elementary Polymer-Chain Hydrodynamics and Chain Dimensions in Biophys Chem, part III The Behaviour of Biological Macromolecules*; Freeman W.H. and Company: San Francisco, CA, USA, 1980; pp. 1019–1039.

Sample Availability: Contact the authors.

Chapter 3

SONICATION-BASED IMPROVEMENT OF THE PHYSICOCHEMICAL PROPERTIES OF GUAR GUM AS A POTENTIAL SUBSTRATE FOR MODIFIED DRUG DELIVERY SYSTEMS

Hindawi Publishing Corporation
BioMed Research International
Volume 2013, Article ID 985259, 11 pages
http://dx.doi.org/10.1155/2013/985259

Research Article

Sonication-Based Improvement of the Physicochemical Properties of Guar Gum as a Potential Substrate for Modified Drug Delivery Systems

Siddique Akber Ansari,[1] Pietro Matricardi,[1] Claudia Cencetti,[1] Chiara Di Meo,[1] Maria Carafa,[1] Claudia Mazzuca,[2] Antonio Palleschi,[2] Donatella Capitani,[3] Franco Alhaique,[1] and Tommasina Coviello[1]

[1] *Department of Drug Chemistry and Technologies, University "La Sapienza", 00185 Rome, Italy*
[2] *Department of Sciences and Chemical Technologies, University of Rome "Tor Vergata", 00133 Rome, Italy*
[3] *Magnetic Resonance Laboratory Annalaura Segre, Institute of Chemical Methodologies, CNR Research Area of Rome, Monterotondo Stazione, 00016 Rome, Italy*

Correspondence should be addressed to Tommasina Coviello; tommasina.coviello@uniroma1.it

Received 4 April 2013; Accepted 26 June 2013

Academic Editor: Rares Salomir

Guar Gum is a natural polysaccharide that, due to its physicochemical properties, is extensively investigated for biomedical applications as a matrix for modified drug delivery, but it is also used in the food industry as well as in cosmetics. A commercial sample of Guar Gum was sonicated for different periods of time, and the reduction in the average molecular weight was monitored by means of viscometric measurements. At the same time, the rheological behaviour was also followed, in terms of viscoelasticity range, flow curves, and mechanical spectra. Sonicated samples were used for the preparation of gels in the presence of borate ions. The effect of borax on the new samples was investigated by recording mechanical spectra, flow curves, and visible absorption spectra of complexes with Congo Red. The anisotropic elongation, observed in previous studies with tablets of Guar Gum and borax, was remarkably reduced when the sonicated samples were used for the preparation of the gels.

1. Introduction

It is well known that viscometric properties of macromolecules are significantly affected by their molecular weight. The aim of this study was to examine the effect of the reduction of Guar Gum (GG) molecular weight for an appropriate modulation of its flow and gelling properties, according to specific needs and possible applications in the field of pharmaceutics, cosmetics, and food industry. Furthermore, a reduced molecular weight should allow conjugation with hydrophobic moieties which should lead to self-assembled structures suitable as systems for drug delivery and targeting as previously proposed with gellan gum, which was sonicated and chemically linked to prednisolone [1]. Furthermore, following previous investigations carried out using another polysaccharide (i.e., scleroglucan) [2], we studied the effect of borax crosslinking on the rheological properties of GG solutions sonicated for different intervals of time and the corresponding anisotropic swelling and elongation of tablets obtained by compression of the GG/borax system. The helix conformation, assumed by the GG chains in the presence of borax [3], was tested to be stable even at high pH values by means of Congo Red complexation experiments. The chosen polysaccharide, GG, is a water-soluble galactomannan which consists of a linear β-D-(1,4)-mannose backbone irregularly substituted by uncharged α-D-(1,6)-linked galactose side groups [4]. This seed gum, generally recognised as safe (GRAS), because of its gelling, viscosifying, and thickening properties is used in pharmaceutics [5] for the stabilization of emulsions and suspensions; it is also employed in tablet manufacturing as a binder and disintegrating agent and for drug micr-encapsulation. Furthermore, GG is suitable as a food supplement [6]. It has been proposed in the therapy of hypercholesterolemia, hyperglycemia, and obesity [7], but also

in textile, paper, and paint industries, as well as in cosmetics. As pointed out, most practical applications of GG are related to its rheological and gelling properties; furthermore, GG is pable to form hydrogels when crosslinked with glutaraldehyde [8–11] and in the presence of borax [3]. For the reduction of GG molecular weight, the probe sonication approach was used because in such case no chemicals are needed, and such aspect represents an important prerequisite for the marketing approval of the obtained polymer.

2. Materials and Methods

2.1. Materials. GG was provided by CarboMer (USA), borax was a Carlo Erba (Italy) product, and Congo Red (CR) a Sigma Aldrich (USA) product. For the sample preparations distilled water was always used, except for NMR experiments, where deuterium oxide (D_2O) (Cambridge Isotope Laboratories, USA) was used. All products and reagents were of analytical grade. The Polysaccharide calibration kits, SAC-10 (Agilent Technologies, UK) were used as pullulan standards.

2.1.1. GG Purification. A given amount of polymer was dissolved in distilled water (polymer concentration, C_p = 0.5% w/v) and then kept under magnetic and mechanical stirring at 60°C for 24 h. The obtained solution was exhaustively dialysed at 7°C against distilled water and then freeze-dried. The molecular weight cut-off of dialysis tubing was 12,000–14,000. From now on, the sample purified by dialysis will be called GG.

2.1.2. Hydrogel and Tablet Preparation. For the preparation of the tablets, an appropriate amount of polymer (about 200 mg) was magnetically stirred in water for 24 h. Then, the calculated amount (i.e., moles of borax = moles of repeating units of polymer) of 0.1 M borax solution was added, and the system was left under magnetic stirring for 5 min. The obtained sample (C_p = 0.7%, w/v) was kept overnight at 7°C for gel setting and then freeze-dried. Tablets were prepared from the freeze-dried sample with an IR die (Perkin Elmer hydraulic press) using a force of 5.0 kN for 30 s. The weight of the GG/borax tablets was 230 ± 10 mg, the diameter was 13.0 ± 0.1 mm, and the thickness was 1.05 ± 0.02 mm.

2.2. Methods

2.2.1. Sonication. In order to reduce the GG molecular weight, a High Intensity Ultrasonic Processor (750 Watt model, probe type sonicator—Vibra Cell—VC 750, Cole-Parmer, USA) was used, working at 20 kHz, with a 6.5 mm microtip, applying an amplitude of 30% of the maximum power supplied by the instrument corresponding to 20 watts and pulser cycles of 30 s ON and 30 s OFF. Aqueous solutions (50 mL) of GG (0.5% (w/v)), prepared in glass beaker, were kept, during sonication, in an ice bath which allowed to keep an average temperature of the samples below 25°C. These experimental conditions allowed to maintain the structural characteristics of the polymeric chains as evidenced also in the case of other polysaccharides [2]. All samples, after sonication, were centrifuged for 20 min at 5,000 rpm and 20°C. The centrifuge speed was selected after several tests in order to find out the minimum rpm value capable of removing the probe-tip residues from the polymer solutions. The supernatant solutions were then dialysed and finally freeze-dried.

2.2.2. Ultracentrifugation. After sonication, all samples were centrifuged (Sorvall WX 80 ULTRA centrifuge (Thermo Scientific, USA)) for 20 min at 20°C and 5,000 rpm. For an appropriate comparison, GG samples (C_p = 0.5% w/v) were only centrifuged (without applying the sonication step). All GG samples were then dialysed and freeze-dried.

From now on, the dialysed sample will be called GG while the centrifuged and dialysed samples will be called, according to the minutes of sonication, GG 0 (no sonication), GG 1, GG 3, GG 5, GG 10, GG 20, and GG 30.

2.2.3. GPC. Weight molecular weight (M_w) and polydispersity index (M_w/M_n) were determined by GPC on a bank of TSK gel GMPWXL columns (Tosoh Bioscience, Tokyo, Japan). A Varian 210 HPLC system with a 356-LC refractive index detector was used. The eluant was 55 mM Na_2SO_3 and 0.02 NaN_3 in double distilled water; the flow rate and temperature were maintained at 0.6 mL/min and 40°C, respectively. All guar samples were diluted to 0.15% (w/v) and filtered through a 0.45 μm filter prior to analysis. The bank of columns was calibrated using pullulan standards [12, 13].

2.2.4. NMR Analysis. Samples of dialysed GG and GG 30, about 4 mg, were solubilized in 0.7 μL of D_2O. ^{1}H-NMR experiments were carried out at 45°C on a Bruker AVANCE AQS 600 spectrometer operating at 600.13 MHz and equipped with a Bruker multinuclear, z-gradient probe head. A soft presaturation of the HOD residual signal was applied before spectra acquisition [14].

2.2.5. Rheological Measurements. The rheological characterization of the GG and GG/borax samples was performed by means of a controlled stress Haake Rheo-Stress RS300 rotational rheometer, provided with a Haake DC50 thermostat. A cone plate device (Haake CP60Ti: diameter = 60 mm; cone = 1°; gap = 0.053 mm) was used for GG solutions while a grained plate-plate device (Haake PP35 TI: diameter = 35 mm) was employed for GG/borax samples in order to reduce the extent of wall slippage phenomena [15]. To perform the measurements, the samples were transferred in the rheometer, and the upper part of the selected device was then lowered until it reached the sample surface. Gap-setting optimizations were undertaken according to the procedure described elsewhere [16]. Stress sweep experiments were performed (25°C and 1 Hz) in the range γ = 0.001 ÷ 1000; frequency sweep experiments were carried out in the range 0.01 ÷ 10 Hz, in the linear viscoelastic region (usually γ = 0.01), preliminary assessed by stress sweep experiments; flow curves were performed in the range 0.001 ÷ 1000 s^{-1}, applying a stepwise increase of the stress. All measurements were made at 25°C.

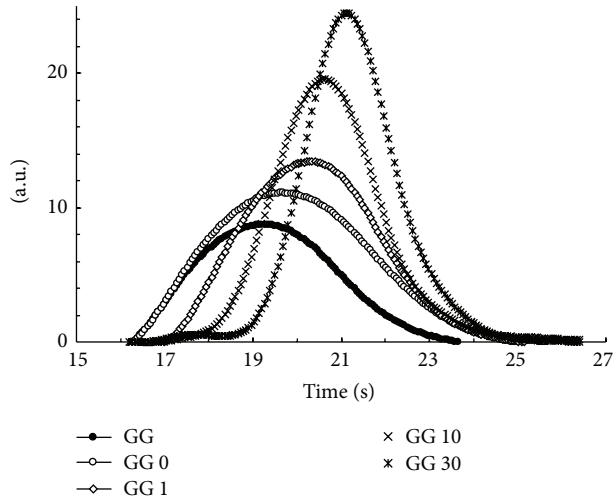

Sample	M_w/M_n
GG	4.65
GG 0	5.82
GG 1	3.9
GG 10	2.65
GG 30	2.06

Figure 1: Molar mass distributions of the guar samples and table of Polydispersity Index.

2.2.6. Dilute Solutions Viscometry. For the viscosity measurements, an automatic viscometer (Instrument Schott AVS 370, Lauda, Germany) with a water bath (Lauda 0.15 T) allowing the temperature control to 0.1°C was used. An Ubbelohde capillary viscometer (Type no 531 01, with a capillary diameter = 0.54 mm, Schott-Geräte) for dilution sequences, with a flux time for the solvent (distilled water) at 25°C of 178.28 s, was used. The distilled water for the sample preparations and for the dilutions was previously filtered three times with 0.20 μ Sartorius Biolab Products filters. The flux time of GG solutions (t) was compared with that of the solvent (t_0), and the relative increase of fluxing time ($t/t_0 = \eta/\eta_0 = \eta_{\text{rel}}; \eta_{\text{rel}} - 1 = t/t_0 - 1 = \eta_{\text{specific}}$) was evaluated at different polymer concentrations. In the range of viscosities up to about twice that of water (i.e., $\eta_{\text{rel}} = 2$), the following Huggins equation is valid:

$$\frac{\eta_{\text{specific}}}{C} = [\eta] + k_H[\eta]^2 C. \quad (1)$$

The limiting value of η_{specific}/C for $C \rightarrow 0$ represents the intrinsic viscosity, $[\eta]$ (cm^3/g), while from the slope of the linear trend of viscosity data it is possible to calculate the Huggins constant, k_H, which gives an indication on the aggregation state of the polymer in the tested conditions of solvent and temperature [17]. The intrinsic viscosity is a measure of the inherent ability of the polymer to increase the viscosity of the solvent at a given temperature, and it can be determined, according to Huggins equation, by measuring viscosity of solutions at low concentrations and extrapolating to infinite dilution. Furthermore, intrinsic viscosity $[\eta]$ is related to the viscosity average molecular mass of the polymer through the Mark-Houwink-Sakurada relationship (MHS), to the molar mass of the sample [18]: $[\eta] = KM_w^a$, where K and a are constants for each polymer-solvent system at a given temperature and are, both, related to the "stiffness" of the polymer. For flexible polymer coils, a is 0.5 in a θ solvent and 0.8 in a good solvent [12].

2.2.7. Conformational Transition Studies. The capability of sonicated GG to retain the helix conformation when linked with borax [3] was examined by characterising the Congo Red-GG complexes [19, 20]. Experimentally, aliquots of a NaOH stock solution were added to GG-borax samples (1 g/L) containing 10 μM CR, in order to obtain the desired pH values (9, 10, and 13).

The solutions were left to equilibrate until their UV-Vis spectra did not change with time. For a comparison, similar experiments were carried out on a 10 μM CR solution. The absorption spectra were recorded with a Cary 100 spectrophotometer (Varian, Palo alto, CA, USA) using a quartz cuvette with a path length of 1 cm.

2.2.8. Water Uptake and Dimensional Increase Studies. The swelling of GG/borax tablets, prepared with the different types of GG (i.e., dialysed GG, centrifuged and dialysed GG, and GG sonicated for different periods of time, centrifuged and then dialysed), was carried out by soaking the tablets in distilled water at 37°C. At fixed time intervals, the tablets were withdrawn, the excess of water was removed with soft filter paper for 5 s, and then the corresponding weights and dimensional variations along the longitudinal axis were determined by means of a screw gauge with an accuracy of ±0.1 mm. No remarkable variations of cross-section dimensions were detected during the swelling process. All experiments were carried out in triplicate, and the obtained values always lay within 10% of the mean.

3. Results and Discussion

3.1. GPC Measurements. Molecular weight distributions of GG and sonicated GG samples by GPC are shown in Figure 1. It is apparent that depolymerization of GG by sonic irradiation causes degradation of the polysaccharide to give different fractions of lower molecular weight, each fraction having a narrow molecular weight distribution. In absence

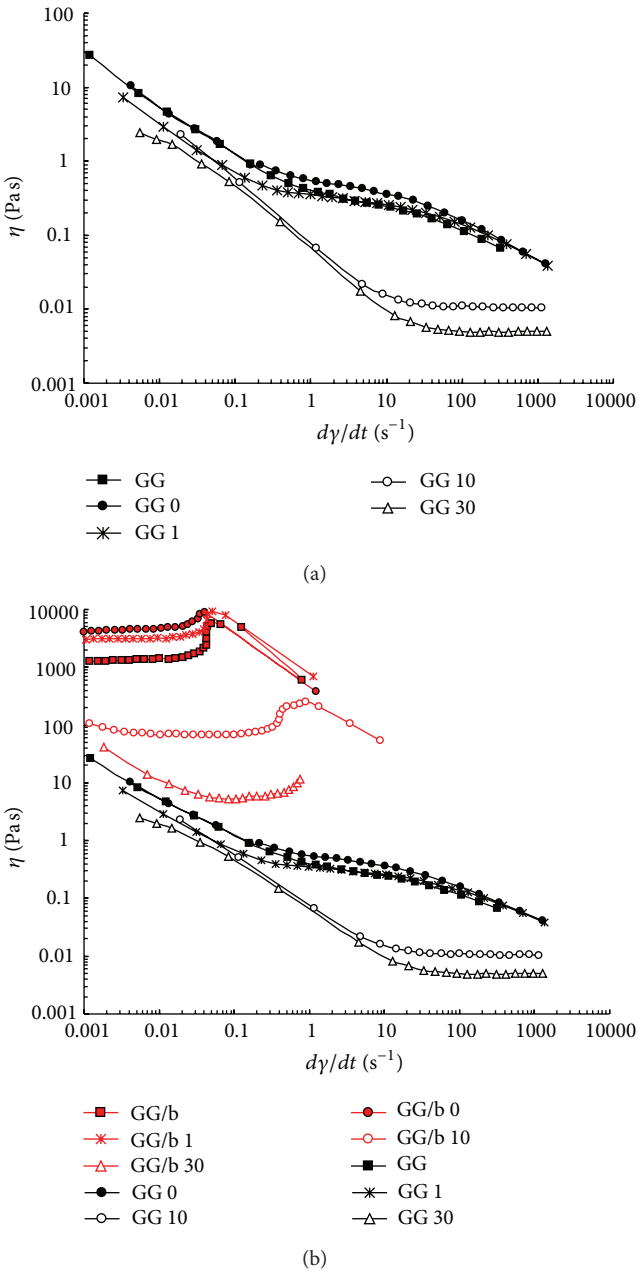

FIGURE 2: (a) Flow curves of GG samples sonicated (at C_p = 0.5%) for different periods of time (0, 1, 10, and 30 min). (b) Flow curves of GG samples, with (red symbols) and without borax (black symbols): for a comparison, the flow curves recorded for GG and GG 0 are also reported (C_p = 0.7%, T = 25°C).

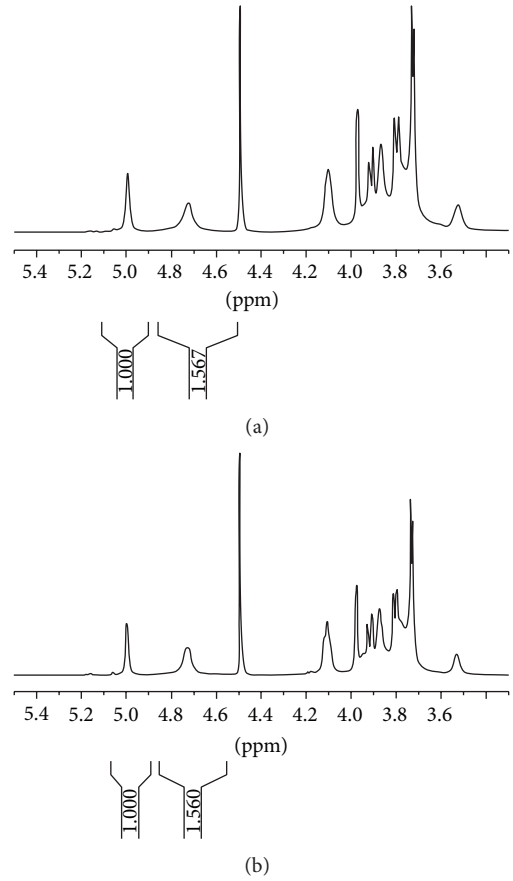

FIGURE 3: ^{1}H-NMR spectra at 600.13 MHz and at 45°C (D_2O) of dialysed GG (a) and GG 30 (b).

of external stimuli (GG and GG 0), the distribution curves are very broad while by applying sonication for different period of time, the peaks become sharper. The molecular weight distribution is in fact somehow more important for characterising the samples than just their M_w only. In Figure 1, typical chromatograms of GG samples are shown, together with the polydispersity index (M_w/M_n). It should be kept in mind that the sonicated samples are also centrifuged (and finally dialysed), and this procedure removes not only the tip dust but also the possible aggregates present in the samples. On the other hand, in the dialysed sample (GG), only the polymeric fractions of very small molecular weights (cut-off of dialysis tubing: 12.000–14.000) and impurities, if present, are removed. Thus, the dialysed samples lack the smallest molecular weight fractions while the sonicated ones lack also molecular aggregates, if present. The high polydispersity index detected for GG 0 sample may be due to the effect of centrifugation that breaks the aggregates leading to the dissolution of lower molecular weight fractions (though higher than 14.000); such effect obviously does not occur in the sample that was only dialysed. From the table of Figure 1, it is evident how the sonication process reduces significantly the polydispersity index leading for an irradiation of 30 min, towards the value expected for the most probable distribution in a random chain scission (M_w/M_n = 2).

3.2. Rheological Measurements. The flow curves for the sonicated samples are shown in Figure 2. As a comparison, the flow curves of GG and GG 0 are also reported. It can be noted that these two samples, together with GG 1, show almost superimposable profiles. The small differences in the three profiles can be attributed to the different molecular weight

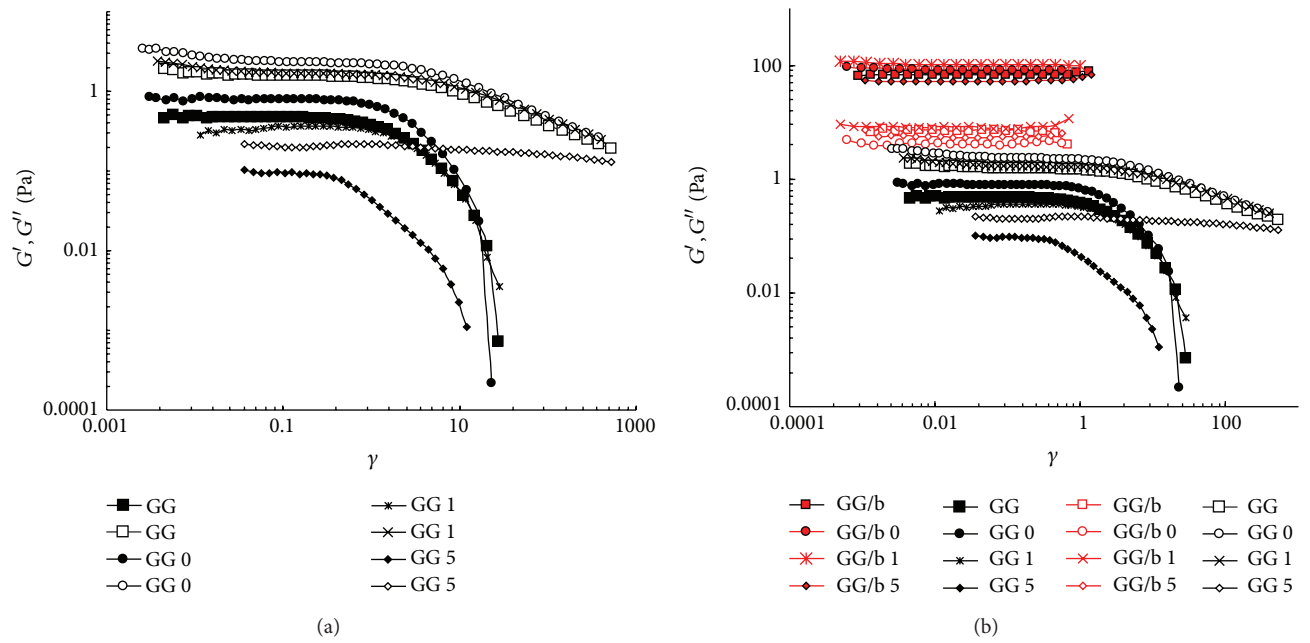

FIGURE 4: (a) Viscoelasticity plot of GG samples sonicated (at C_p = 0.5%) for different periods of time (0, 1, and 5 min). (b) Viscoelasticity curves of GG samples, with (red symbols) and without borax (black symbols): for comparison, the flow curves recorded for GG are also reported (G' = full symbols, G'' = empty symbols; C_p = 0.7%, T = 25°C).

distributions, as evidenced by the GPC measurements. The first Newtonian plateau is not detectable for any sample, and the drop of viscosity is quite significant until the second Newtonian plateau is reached with values of viscosity approximately less than 1 Pa s. By increasing the sonication time, drastic changes are observed in the flow curves. A sonication of ten min is sufficient to drastically reduce the viscosity of the polymer (at $d\gamma/dt$ = 10 (s^{-1})) which drops of one decade, from 0.3 (for GG and GG 1) to 0.02 (Pa s). Furthermore, the interval of the Newtonian plateau is remarkably shifted to a higher shear rates indicating that, by reducing the chain length, the viscosity continues to decrease while, for the native polymer or the polymer sonicated for 1 min, the viscosity values remain almost constant up to $d\gamma/dt$ = 100 (s^{-1})). Thus, ten minutes of sonication are sufficient to break significantly the GG chain backbones (the initial molecular weight was reduced to one third, see Section 3.3). Furthermore, by increasing the period of sonication, the range of the second Newtonian plateau is even more shifted towards higher shear rate values, and the macroscopic effect of a sonication of 30 min is that the viscosity approaches values only five times higher than those of water.

Increasing the sonication time, a further breakdown of the polymeric chains occurs without damaging the repeating unit structure, as evidenced by NMR analysis (Figure 3).

NMR was carried out in D_2O at 45°C, in order to separate the HOD residual signal from the anomeric signals. As shown in Figure 2, the spectra of GG and GG 30 are superimposable. In particular, the ratio between the anomeric β $(1 \rightarrow 4)$ mannose protons at 4.73 ppm and the anomeric α $(1 \rightarrow 6)$ galactose protons at 5.02 ppm remains constant and equal to 1.56 for the tested samples. This is a clear indication that the M/G ratio is not affected by the sonication process; that is, the repeating units of the polymer keep intact their chemical compositions.

Thus, the sonication process can be proposed as a suitable method for GG molecular weight reduction. Actually, by means of sonication, it is possible to prepare GG within a quite wide range of molecular weights without damaging the molecular structure. This is a crucial point, especially with reference to possible industrial applications of GG, because the rheological properties of the polymeric solutions prepared with the sonicated samples that show remarkable variations in comparison with the native polymer, can be appropriately tailored according to specific needs.

The effect on the rheological properties of the addition of borax to the various samples was also investigated (Figure 2). Addition of borate ions to the GG samples led to a dramatic change in the flow curve trends. Between the samples without borax and those with borax, a difference in the viscosity values of four decades is detected. A well-defined plateau is recorded at low shears, up to $d\gamma/dt$ = 0.1 (s^{-1}). After this value, GG and GG 0 undergo a rapid decrease in viscosity followed by the impossibility to further proceed with the measurements due to the brittle nature of the network. The presence of borax leads to a better discrimination among the different samples even after 1 min of sonication. Going from 1 to 10 min of sonication, the viscosity is strongly reduced and the plateau is extended up to $d\gamma/dt \approx 2$ (s^{-1}). Thus, the reduction in molecular weight induces a dramatic change in the polymeric network. When sonication is carried out for 30 min, the sample with borax starts to show a pseudoplastic behaviour. However, in no case the viscosities of the GG/b samples reach values below those recorded for the samples

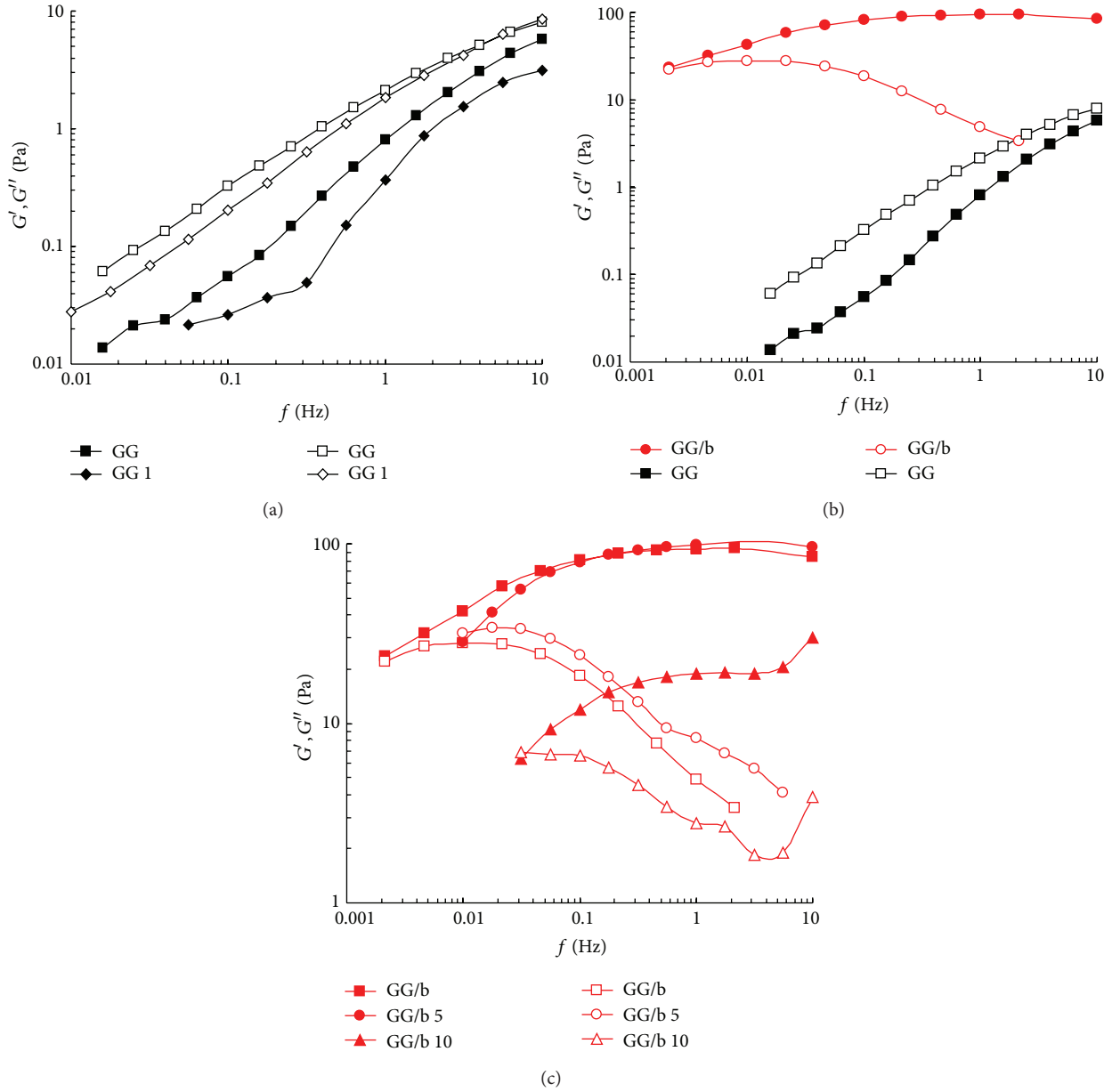

FIGURE 5: Mechanical spectra of GG samples, with (red symbols) and without borax (black symbols), sonicated (at C_p = 0.5%) for different periods of time. (a) Frequency sweep of GG and GG 1; (b) frequency sweep of GG and GG/b; (c) frequency sweep of GG/b and GG/b sonicated for 5 and 10 min; (c) comparison between the frequency sweep of GG and GG/b. (G' = full symbols, G'' = empty symbols; C_p = 0.7%, T = 25°C).

without borax. It is clear that both GG molecular weight and borax represent key parameters for the flow properties.

In Figure 4, the changes of the two moduli, G' (storage modulus) and G'' (loss modulus), as a function of the deformation are shown. As expected, the linear viscoelasticity interval is reduced by lowering the sample molecular weight. The addition of borax increases the G' values from about 1 to approximately 100 Pa and the stress/strain response is linear up to a 100% of deformation. The mechanical spectra were then recorded at γ = 0.01.

In Figure 5, the mechanical spectra of GG samples are reported. It is interesting to follow the modulus variations in the stress sweep experiments, which show the significant effect of sonication on the supramolecular structure.

In Figure 5(a), the effect on GG sample of 1 min sonication is reported: both mechanical spectra are those typical of a solution ($G'' > G'$), and a strong dependence of the two moduli on frequency can be detected. In the case of samples sonicated for a longer period of time, it was not possible to carry out the experiment, due to their predominant liquid-like characteristics. Figure 5(b) compares the dynamic rheological moduli, prior to degradation, of a GG solution with a GG-borax gel at the same polymer concentration (0.7% w/v). There is a dramatic effect on the shape of frequency sweep

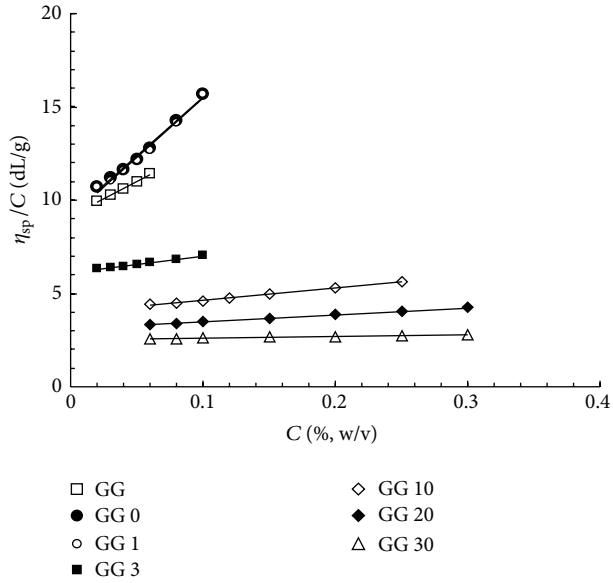

Figure 6: (a) η_{sp}/C versus polymer concentration for GG samples sonicated for different periods of time ($T = 25^{\circ}$C).

trend as a consequence of the addition of borax: a well-defined transition from a liquid-like to a gel-like behaviour is detected. Actually, the loss modulus (G'') dominates the solution response over most of the frequency domain, indicating the mainly viscous nature of the GG solution. Borax crosslinking causes an increase in both moduli, with the elastic modulus (G') being more strongly affected. A well-defined plateau is observed in the elastic modulus at intermediate frequencies (0.05–10 Hz), being G' higher than G'' within this interval. These features are characteristic of a network structure formed by the GG-borax crosslinks. Due to the labile nature of these linkages, the GG/b gel displays a terminal region similar to that of polymer solutions with a well-defined crossover between G' and G''. The frequency values at which the moduli inversion takes place increase as sonication time increases. Obviously, by reducing the GG molecular weight, the strength of the gel, formed in the presence of borax, correspondingly decreases. This is clearly evidenced by the reduction of the storage modulus values of the frequency interval where G' is independent of the applied frequencies and of the shift of the crossover towards higher frequency values. All these variations indicate the increasing weakness of the polymeric network as sonication proceeds with a widening of the mesh size (with the reduction of G' values) and a corresponding shortening of the longest relaxation time (the crossover frequency is shifted towards higher values).

In Figure 5(c), the effects of sonication on GG/b samples are evidenced. The addition of borax to GG 5 leads to a network very similar to that of GG/b. Nevertheless, it must be pointed out that the crossover between G' and G'' is appreciably shifted to higher frequencies in comparison to GG/b sample (from 0.002 Hz (GG/b) to 0.012 Hz (GG/b 5). In the case of sonicated samples, the sol-gel transition occurs at higher frequencies due to the reduced influence of the longest relaxation modes, as expected for a looser network. Furthermore, the maximum of G'' does not match with the crossing point: this discrepancy is reduced by increasing the sonication time. This means that, by reducing the chain length, the data can be fitted by using the generalized Maxwell model applying only a few or only one (in the case of coincidence between the G'' maximum and the crossing point) relaxation time. This is even more evident when GG undergoes a 10 min sonication. The mechanical spectra are still those of a gel system, but both moduli are lowered by a power of ten, and the crossover is further shifted to higher frequencies (≈0.3 Hz). Of course, in this last case a much weaker gel is obtained, being the G' plateau significantly reduced in comparison to that of the previous two systems.

Anyhow, in the case of GG, one min is the maximum sonication time that can be applied in order to record the mechanical spectra (a more prolonged sonication leads to liquid-like systems with moduli that are too low to be experimentally recorded). On the other side, the presence of borax, leading to the formation of a three-dimensional network, allowed to acquire mechanical spectra of a GG sample sonicated up to 10 min. When the sonication time is further increased to 30 min the linkages with borax are too few, due to the reduction of GG molecular weight ($M_w = 1.32 \times 10^5$) for the formation of a real gel network, and consequently the modulus values become too low to be recorded.

Table 1: Sonication times of the GG samples, the corresponding intrinsic viscosity, the Huggins constant and the average molecular weight calculated according to the MHS equation.

Sample	Sonication time (min)	$[\eta]$ (dL/g)	k_H	$M_w \times 10^{-5}$
GG	0	9.15	0.44	8.02
GG 0	0	9.23	0.74	8.13
GG 1	1	9.14	0.75	8.01
GG 3	3	6.13	0.43	4.60
GG 5	5	5.24	0.49	3.70
GG 10	10	3.97	0.42	2.52
GG 20	20	3.10	0.39	1.78
GG 30	30	2.50	0.15	1.32

3.3. Reduction of Guar Gum Solution Viscosity upon Sonication. Aqueous solutions of sonicated samples were prepared for the viscosity measurements, carried out at 25°C, and the results are shown in Figure 6. For an appropriate comparison, GG samples were also tested.

From the intercepts, that is, from the intrinsic viscosities $[\eta]$ of the samples, the molecular weights of the various fractions were estimated (and reported in Table 1) according to the Mark-Houwink-Sakurada (MHS) equations valid for galactomannans [21]:

$$[\eta] = KM_w^a, \tag{2}$$

where $K = 5.13 \times 10^{-4}$ and $a = 0.72$.

It is possible to observe that, by applying the sonication for only 5 min, the GG molecular weight was reduced to

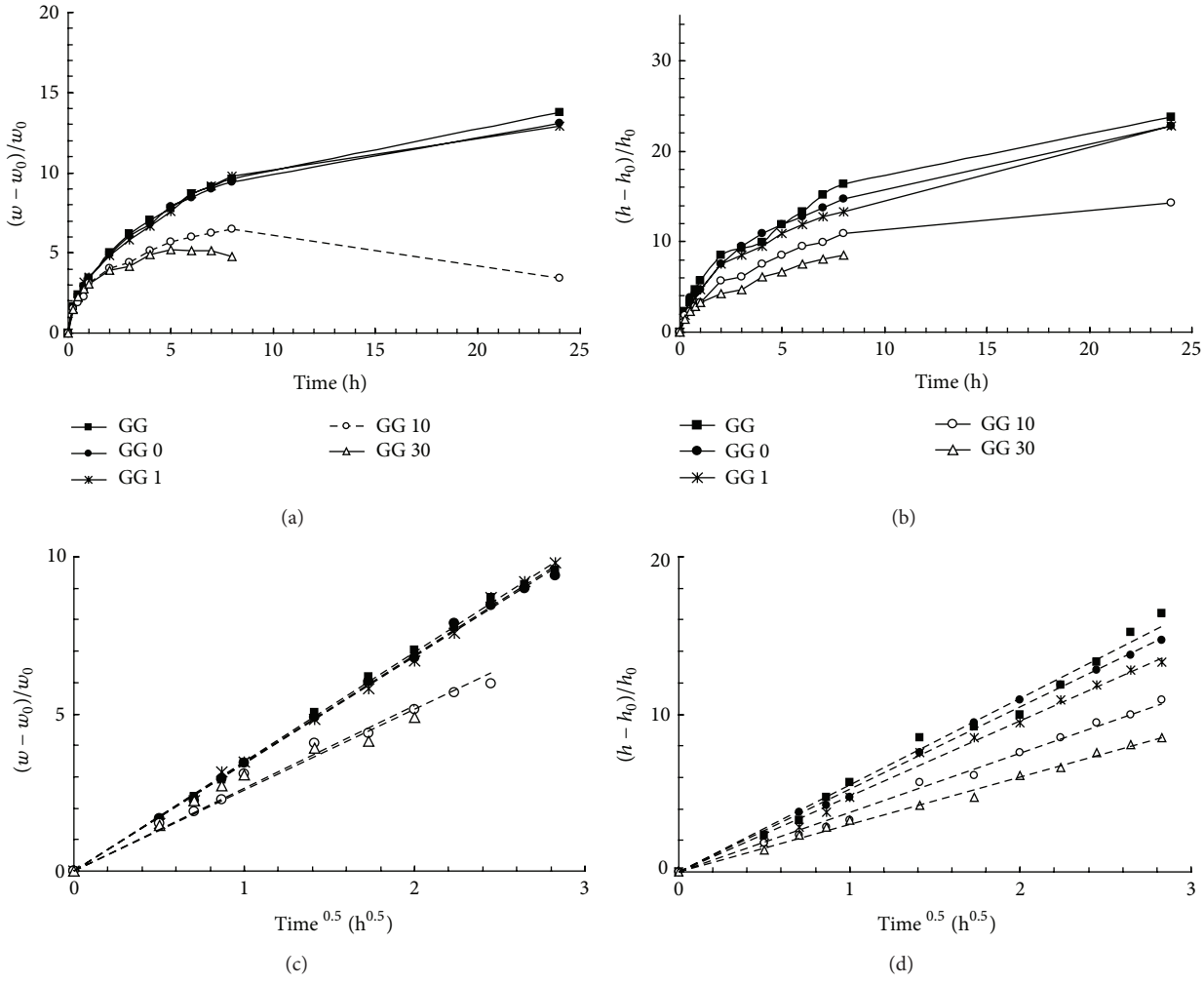

FIGURE 7: (a) Water uptake $(w - w_0)/w_0$ and (b) relative height increase $(h - h_0)/h_0$ from tablets of GG/borax (using GG samples sonicated for different periods of time) as a function of time. (c) and (d) the same data of (a) and (b) reported as a function of the square root of time. Experiments were carried out in triplicate, and the obtained values always lay within 10% of the mean.

more than one half. The reduction was further increased by increasing the sonication process for longer times. From the slope of the linear trend of viscosity data, the values of the Huggins constant, k_H, (see Table 1) were calculated for all samples. The Huggins coefficient is a measure of polymer-polymer interactions in solution (with values of roughly 0.30–0.40 in good solvents and 0.50–0.80 in θ solvents) and assumes high values when intermolecular associations exist [22]. Furthermore, it is known that water is a fairly good solvent for GG. However, k_H of GG in water is much higher than the regular value for a good solvent (0.3–0.4), which indicates the importance of polymer-polymer hydrogen bonding interactions among the GG molecules. When sonication is applied, the decrease in molecular weight reduces the number per chain of hydrogen bonding sites leading, at the same time, to a reduction of the intermolecular hydrogen bonding between polymer molecules, that is, the attractions between guar chains [12]. k_H is also very sensitive to the formation of molecular aggregates. In other words, the Huggins coefficient can provide additional information about the state of guar gum macromolecules in solution and can be a measure of the goodness of the solvent [23].

3.4. Water Uptake and Dimensional Increase Studies. In previous works [24], it was reported that tablets, prepared with the GG/borax freeze-dried hydrogel, undergo an anomalous peculiar swelling, essentially along one direction and very similar to that reported for the Scleroglucan/borax tablets [1, 25–27]. New tablets were then prepared with sonicated GG samples, and water uptake and elongation behaviour were followed as a function of time. As a comparison, the experiments on tablets prepared with GG (i.e., with the polymer that was only dialysed) were also carried out. The results, reported in Figure 7 (in distilled water at 37°C), clearly show that both, water uptake and anisotropic elongation of the tablets, observed for the GG/borax system, were significantly reduced when the sonicated samples were tested.

The tablets prepared with GG and GG 0 increased their weight and elongated for 24 hrs; those prepared with GG

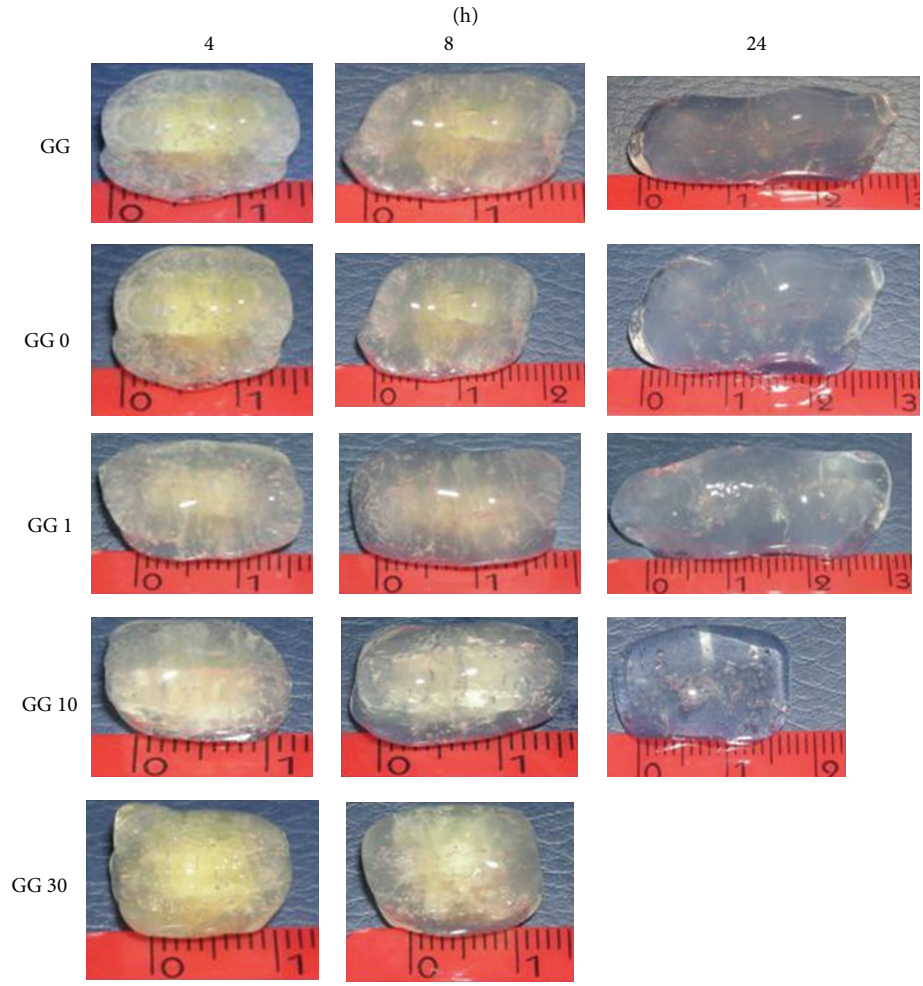

Figure 8: Pictures of swelled GG/borax tablets, prepared with GG sonicated for different periods of time in distilled water at 37°C (the height of the tablets before the swelling process was $h_0 \approx 1.05$ mm).

sonicated for 1 min follow the same trend while those prepared with GG 10 started to dissolve in the medium already after 8 hours. This phenomenon started even earlier for the sample sonicated for 30 min: the tablets started to loose their weight already after 5 hours, and the anomalous elongation could be detected only up to 5 hours. After 8 hours, the tablets dissolved completely in the swelling medium. Both processes, the uptake of water and the height increase, obey, during the first hours, the Fickian law (Figures 7(c) and 7(d)). Thus, the reduction of the polymeric chain lengths did not change the diffusional character of water molecules behaviour during the imbibition of the tablet matrices.

In Figure 8, the pictures of swelled tablets prepared with GG sonicated for different periods of time are shown.

3.5. Helix-Coil Transition Analysis. The conformational structures of GG-borax and sonicated GG/borax were investigated by means of the formation of CR-polymer complexes at various alkali concentrations. CR, indeed, tends to bind to polysaccharides in helical structures, and as a consequence, its visible absorption maximum shifts to higher values. By following its shift in the Vis spectra of the polymer-dye complex, it is possible to demonstrate the presence of helix conformation. As reported in Figure 9, the CR absorption maxima of GG/borax and GG/borax sonicated samples are red shifted in comparison to those of the dye alone, even at high pH values, indicating that the polymer at low molecular weight is still able to bind the dye, keeping a helix structure.

4. Conclusions

Sonication appears to be a rather easy method suitable to reduce the M_w of a polysaccharide such as GG without the use of chemicals (i.e., without producing side products that could contaminate the final product) thus allowing more easily acceptable applications in the field of pharmaceutics, cosmetics, and food industry. As evidenced in the NMR spectra, sonication does not destroy the structural characteristics of the polymeric chains; furthermore, obtained results showed that depolymerization of GG by sonic irradiation leads to different fractions of lower M_w, each fraction having a narrow molecular weight distribution. As expected, such

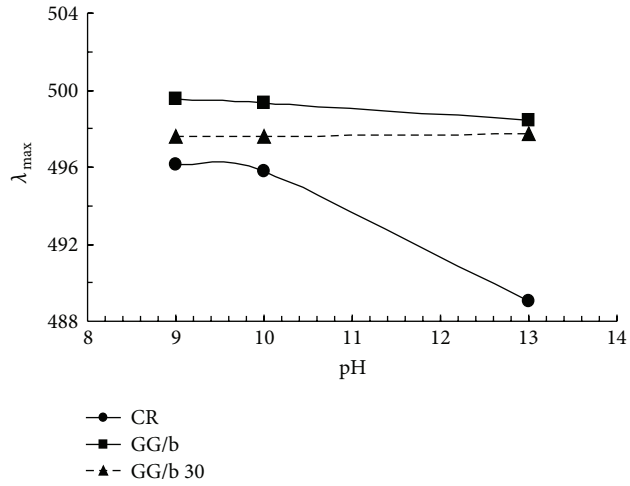

Figure 9: Absorption maximum shifts, at different pH values, for CR and GG/b systems with GG sonicated 0 and 30 min.

M_w reduction dramatically affects the rheological properties of the polysaccharide, leading to significantly modified flow curves. In this sense, it must be pointed out that it was possible to acquire the mechanical spectra only for the sample sonicated for 1 min because the moduli of the other samples, obtained after sonication was carried out for a longer period of time, were too low to be detected. As in the case of other polysaccharides (3), the addition of borax changed completely the rheological properties from liquid-like systems to gel-like systems, and this behaviour, although to a less extent, was observed for all sonicated samples. Only when the molecular weight was decreased to $M_w = 1.32 \times 10^5$, the GG chains were no more able to build up a three-dimensional gelled network, and the rheological moduli were too low to be experimentally detected. Actually, the GG molecular weight, as estimated by viscometric measurements, decreased very rapidly by applying ultrasounds to the polymeric solutions, leading to a reduction to one-half of the initial M_w already after a sonication of 3 minutes.

The swelling behaviour of GG/borax tablets was also investigated. In this respect, the reduced molecular weight of the polymer led to a significant difference in water uptake and anisotropic elongation in comparison to the starting GG sample.

In conclusion, the use of a simple method, such as sonication, for the reduction of GG M_w, represents an important approach for an appropriate tailoring of the mechanical properties of GG solutions in consideration of a more suitable and rational utilization of such polysaccharide in the various and wide fields of practical uses. In particular, as far as innovative drug formulations are concerned, an optimized reduction of the GG M_w will allow an easy conjugation of the obtained shorter chains with a hydrophobic drug that should then lead to the formation of self-assembled structures, in the form of nanohydrogels, that are suitable for modified drug delivery systems, as already successfully carried out and reported in the case of sonicated gellan gum chemically linked to prednisolone [1].

Acknowledgment

Sapienza University Grant no. C26A119N2S is acknowledged.

References

[1] G. D'Arrigo, C. Di Meo, E. Gaucci et al., "Self-assembled gellan-based nanohydrogels as a tool for prednisolone delivery," *Soft Matter*, vol. 8, pp. 11557–11564, 2012.

[2] S. A. Ansari, P. Matricardi, C. Di Meo, F. Alhaique, and T. Coviello, "Evaluation of rheological properties and swelling behaviour of sonicated scleroglucan samples," *Molecules*, vol. 17, no. 3, pp. 2283–2297, 2012.

[3] G. Bocchinfuso, C. Mazzuca, C. Sandolo et al., "Guar gum and scleroglucan interactions with borax: experimental and theoretical studies of an unexpected similarity," *Journal of Physical Chemistry B*, vol. 114, no. 41, pp. 13059–13068, 2010.

[4] I. S. Dierckx and I. K. Dewettinck, "Seed gums," in *Biopolymers Polysaccharides II*, S. De Baets, E. J. Vandamme, and A. Steinbüchel, Eds., pp. 321–343, Wiley-VCH, London, UK, 2002.

[5] T. Shaikh and S. Sasi Kumar, "Pharmaceutical and pharmacological profile of guar gum an overview," *International Journal of Pharmacy and Pharmaceutical Sciences*, vol. 3, supplement 5, pp. 38–40, 2011.

[6] K. T. Roberts, "The physiological and rheological effects of foods supplemented with guar gum," *Food Research International*, vol. 44, no. 5, pp. 1109–1114, 2011.

[7] M. S. Butt, N. Shahzadi, M. K. Sharif, and M. Nasir, "Guar gum: a miracle therapy for hypercholesterolemia, hyperglycemia and obesity," *Critical Reviews in Food Science and Nutrition*, vol. 47, no. 4, pp. 389–396, 2007.

[8] T. Coviello, F. Alhaique, A. Dorigo, P. Matricardi, and M. Grassi, "Two galactomannans and scleroglucan as matrices for drug delivery: preparation and release studies," *European Journal of Pharmaceutics and Biopharmaceutics*, vol. 66, no. 2, pp. 200–209, 2007.

[9] C. Sandolo, P. Matricardi, F. Alhaique, and T. Coviello, "Dynamo-mechanical and rheological characterization of guar gum hydrogels," *European Polymer Journal*, vol. 43, no. 8, pp. 3355–3367, 2007.

[10] C. Sandolo, T. Coviello, P. Matricardi, and F. Alhaique, "Characterization of polysaccharide hydrogels for modified drug delivery," *European Biophysics Journal*, vol. 36, no. 7, pp. 693–700, 2007.

[11] C. Sandolo, P. Matricardi, F. Alhaique, and T. Coviello, "Effect of temperature and cross-linking density on rheology of chemical cross-linked guar gum at the gel point," *Food Hydrocolloids*, vol. 23, no. 1, pp. 210–220, 2009.

[12] Y. Cheng, K. M. Brown, and R. K. Prud'homme, "Characterization and intermolecular interactions of hydroxypropyl guar solutions," *Biomacromolecules*, vol. 3, no. 3, pp. 456–461, 2002.

[13] A. Tayal, R. M. Kelly, and S. A. Khan, "Rheology and molecular weight changes during enzymatic degradation of a water-soluble polymer," *Macromolecules*, vol. 32, no. 2, pp. 294–300, 1999.

[14] M. Guéron, P. Plateau, and M. Decorps, "Solvent signal suppression in NMR," *Progress in Nuclear Magnetic Resonance Spectroscopy*, vol. 23, no. 2, pp. 135–209, 1991.

[15] R. Lapasin and S. Pricl, *Rheology of Industrial Polysaccharides, Theory and Applications*, Chapman & Hall, London, UK, 1995.

[16] A. J. Kuijpers, G. H. M. Engbers, J. Feijen et al., "Characterization of the network structure of carbodiimide cross-linked gelatin gels," *Macromolecules*, vol. 32, no. 10, pp. 3325–3333, 1999.

[17] C. Tanford, "Transport processes, viscosity," in *Physical Chemistry of Macromolecules*, pp. 317–456, John Wiley & Sons, New York, NY, USA, 1961.

[18] C. R. Cantor and P. R. Schimmel, "Elementary polymer-chain hydrodynamics and chain dimensions," in *Biophysical Chemistry, Part III—The Behaviour of Biological Macromolecules*, pp. 1019–1039, W. H. Freeman, San Francisco, Calif, USA, 1980.

[19] K. Ogawa, T. Dohmaru, and T. Yui, "Dependence of complex formation of (1–>3)-beta-D-glucan with congo red on temperature in alkaline solutions," *Bioscience, Biotechnology, and Biochemistry*, vol. 58, no. 10, pp. 1870–1872, 1994.

[20] J. I. Fariña, F. Siñeriz, O. E. Molina, and N. I. Perotti, "Isolation and physicochemical characterization of soluble scleroglucan from *Sclerotium rolfsii*. Rheological properties, molecular weight and conformational characteristics," *Carbohydrate Polymers*, vol. 44, no. 1, pp. 41–50, 2001.

[21] D. R. Picout and S. B. Ross-Murphy, "On the Mark-Houwink parameters for galactomannans," *Carbohydrate Polymers*, vol. 70, no. 2, pp. 145–148, 2007.

[22] M. Bohdanecky and J. Kovar, *Viscosity of Polymer Solutions*, Elsevier Scientific Publishing Company, Amsterdam, The Netherlands, 1982.

[23] X. Ma and M. Pawlik, "Intrinsic viscosities and Huggins constants of guar gum in alkali metal chloride solutions," *Carbohydrate Polymers*, vol. 70, no. 1, pp. 15–24, 2007.

[24] T. Coviello, L. Bertolo, P. Matricardi et al., "Peculiar behavior of polysaccharide/borax hydrogel tablets: a dynamomechanical characterization," *Colloid and Polymer Science*, vol. 287, no. 4, pp. 413–423, 2009.

[25] T. Coviello, M. Grassi, A. Palleschi et al., "A new scleroglucan/borax hydrogel: swelling and drug release studies," *International Journal of Pharmaceutics*, vol. 289, no. 1-2, pp. 97–107, 2005.

[26] A. Palleschi, T. Coviello, G. Bocchinfuso, and F. Alhaique, "Investigation on a new scleroglucan/borax hydrogel: structure and drug release," *International Journal of Pharmaceutics*, vol. 322, no. 1-2, pp. 13–21, 2006.

[27] C. Di Meo, T. Coviello, P. Matricardi, F. Alhaique, D. Capitani, and R. Lamanna, "Anisotropic enhanced water diffusion in scleroglucan gel tablets," *Soft Matter*, vol. 7, no. 13, pp. 6068–6075, 2011.

Chapter 4

SYNTHESIS AND CHARACTERIZATION OF POLYSACCHARIDE NANOHYDROGELS

Preparation and characterization of Scleroglucan nanohydrogels

Introduction

In recent years, significant efforts have been devoted to the development of amphiphilic polymers consisting of hydrophilic polysaccharides and hydrophobic moieties because of their ability to form nanohydrogels (NHs) self-assemblies in aqueous media. The intermolecular interactions between the hydrophilic and hydrophobic segments allow the creation of a hydrophilic shell that faces towards the solvent and an inner hydrophobic core with minimal interactions with the aqueous medium [1-4]. In recent years, a variety of self-assembled nanoparticles (NPs) have been developed for their potential application as drug delivery systems (DDS) and their ability to increase the therapeutic efficacy of the drugs and to reduce drug side effects. Numerous examples of NPs have been proposed as anticancer drug carriers because they exhibit prolonged systemic circulation time and can accumulate in the tumour masses (EPR, Enhanced Permeability and Retention effect). The NPs surface can then be functionalized to improve targeting to the site of action of the drug, thereby reducing non-specific distribution. In particular, surface functionalization can address the drug release, avoid NP aggregation, and reduce the rapid clearance of the drug. As applied to DDS, natural polysaccharides have the advantages of their abundance in nature, low cost, safety, general biocompatibility, biodegradability, and high stability. Among all natural polysaccharides, Sclg is a promising candidate for biomedical applications because of its peculiar physicochemical properties and its biocompatibility [5-7].

Herein, we prepared Sclg nanohydrogels (NHs) by self-assembling of the polymer chains, after an appropriate chemical derivatization with Penicillin-G. Sclg was sonicated to reduce the molecular weight thus obtaining a reliable and suitable polymer system for NH formation. Penicillin-G, a poorly water-soluble antimicrobial drug, was chemically conjugated to the Sclg sonicated for 60 min (Sclg60–Penicillin G). Penicillin-G are a group of antibiotics derived from *Penicillium fungi* among which benzylpenicillin commonly known as Penicillin-G, represents the gold standard type.

Another drug that was tested is Levofloxacin, a broad spectrum antibiotic of the fluoroquinolone drug class. Its spectrum of activity includes most strains of bacterial pathogens responsible for respiratory, urinary tract, gastrointestinal, and abdominal infections.

The proposed approach allowed us to combine the advantages of nanotechnology, such as high stability, high carrier capacity, and feasibility of different routes of administration.

Synthesis and characterization of Scleroglucan derivatives:

Materials

Sclg was provided by Cargill (Minneapolis, USA). For the sample preparations distilled water was always used, except for NMR experiments, where deuterium oxide (D_2O) (Cambridge Isotope Laboratories, USA) was used. 4-bromobutyric acid, N-(3-imethylaminopropyl)-N'-ethylcarbodiimide hydrochloride (EDC.HCl), 4-dimethylamino pyridine (DMAP), Penicillin-G sodium salt and Levofloxacin were Sigma products. All products and reagents were of analytical grade.

Purification of Scleroglucan

A given amount of polymer was dissolved in distilled water (polymer concentration, cp = 0.5% w/v), and then kept under magnetic and mechanical stirring at room temperature for 24 hr. The obtained solution was exhaustively dialysed at 7 °C against distilled water and then freeze-dried.

Methods

Scleroglucan controlled depolymerization

Probe Sonication

In order to reduce the Sclg molecular weight, a High Intensity Ultrasonic Processor (750 Watt model, probe type sonicator—Vibra Cell—VC 750, Cole- Parmer, USA) was used, working at 20 kHz, with a 6.5 mm microtip, applying an amplitude of 30% of the maximum power supplied by the instrument (corresponding to 20 watts) and pulser cycles of 30 s ON and 30 s OFF. Aqueous solutions (50 ml) of Sclg (0.5% (w/v)), prepared in glass beaker, were kept, during sonication, in an ice bath which allowed to keep an average temperature of the samples below 25°C.

Bath sonicator

A second source of ultrasound used was an ultrasonic bath "Starsonic 35 Basic-Liarre", with the following characteristics:

- Frequency: 28-34 kHz
- Voltage: 230 VAC / 50-60 Hz
- Power: 80-180 W
- Heating Power Supply: 100 W

The samples were sonicated in a water bath for 5 min at room temperature in order to get uniform NHs.

Ultracentrifugation used after probe sonication

Sclg samples were also prepared by centrifugation in order to separate the aggregates from the polymer solutions (cp = 0.5% w/v). For this purpose a centrifuge Sorvall WX 80 ULTRA (Thermo Scientific, USA) was used (20 min at 18,000 rpm and 20 °C). Freeze-drying procedure was then carried out.

FT-IR

FT-IR spectra of Sclg sonicated and its derivatives with Penicillin-G were recorded in the range of 4000–400 cm^{-1} using KBr pellets and a Perkin-Elmer 1720 spectrophotometer. The resolution was 1 cm^{-1}. The number of scans was 64.

Size characterization of nanohydrogels

NHs size distributions were assessed by dynamic light scattering (DLS) by using a NICOMP 370 Autodilute Submicroscope (Specific Scientific Hiac/Roy Co., Santa Barbara, CA).

Experimental

Viscosity Measurements

Solutions of the sonicated polymer were prepared in 0.01 N NaOH in order to break the possible aggregates still present in solution [8, 9]. Viscosity measurements were carried out at 25 °C and the results are shown in Figure 1a.

The molecular weights of the various fractions were calculated from the intrinsic viscosities [η] of the samples (obtained from the intercepts in Figure 1a), according to the Mark-Houwink-Sakurada equations valid for Sclg [10],

$$[\eta] = KM_w^{1.7} \text{ for } M_w < 5 \times 10^5$$

$$[\eta] = KM_w^{1.2} \text{ for } M_w > 5 \times 10^5$$

where $K = 1.3 \times 10^{-7}$ cm^3 g^{-1}

It is possible to observe that, applying the sonication for only 10 min, the molecular weight of the polymer was reduced to one half.

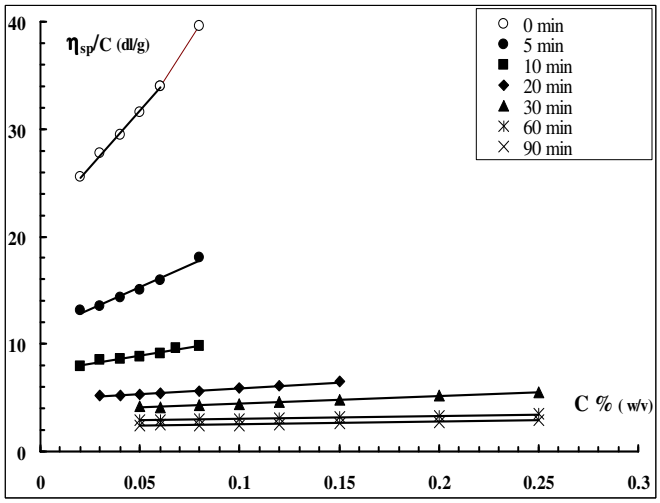

Figure 1. (a) Plot of $\eta_{specific}/c$ *vs.* polymer concentration for Sclg samples sonicated for different periods of time (NaOH = 0.01 N, T = 25 °C).

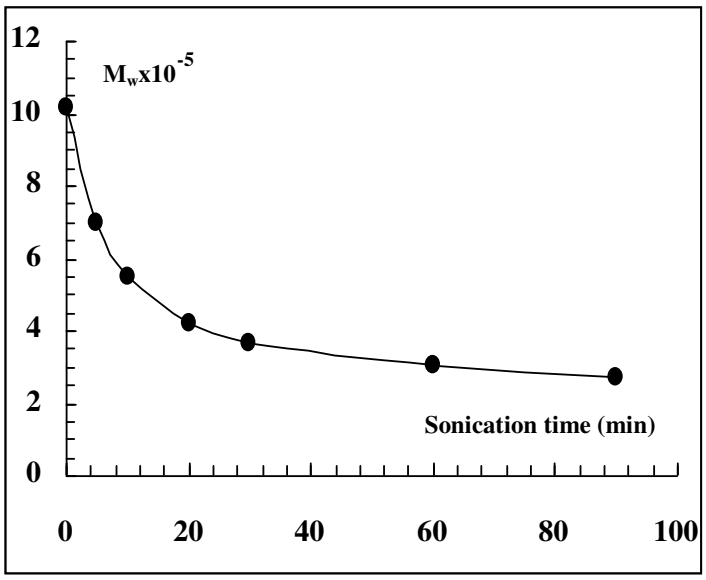

Figure 1. (b) Sclg molecular weight dependence on sonication time

The decrease of the molecular weight of native Sclg was strongly dependent on the ultrasound treatment time (Figure. 1b). The M_w decreased for sonication time up to 1 h and then remained at an almost stable value.

The M_w of Sclg, starting from about 10.2 x 10^5, was thus reduced to 3.07 x 10^5, by applying ultrasounds for 1 h.

Synthesis and characterization of Scleroglucan derivatives

Sclg was derivatized by applying different methods. Penicillin-G sodium salt or Levofloxacin, chosen as suitable drugs for the present work were not directly linked to the polymer backbone but a spacer was preliminary introduced in the two molecules. In order to find out the best system, different spacers were tested and the lists of the reactions carried out are listed below.

Method-1

Penicillin bromo-butyric acid derivative synthesis

In a typical synthesis, Penicillin-G sodium salt (200 mg, 0.56 mmol) was dissolved in dichloromethane (4 ml) and 4-bromobutyric acid (93.7 mg, 0.56 mmol) was separately dissolved in 2 ml of dichloromethane. Then 68.5 mg (0.56 mmol) of DMAP was added to Penicillin solution until complete solubilisation. The two solutions were then mixed and the reaction was kept under magnetic stirring for 48 hrs at room temperature (Scheme 1). The reaction was monitored by Thin Layer Chromatography (TLC) using cyclohexane: ethylacetate = 70: 30 as eluent.

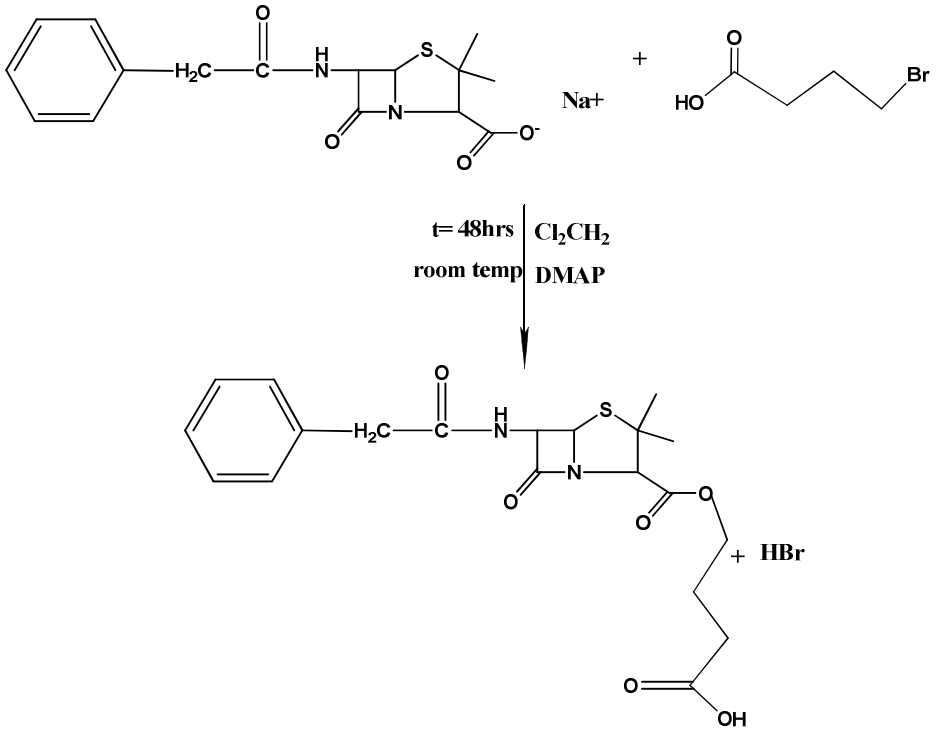

Scheme 1. Reaction scheme of the Br–Penicillin-G derivative.

Result: No product was obtained.

Method-2

Levofloxacin bromobutyric acid derivatives

In a typical synthesis, 50 mg Levofloxacin (0.135 mmol) was dissolved in dichloromethane (4 ml), then 19 µl (0.136 mmol) of triethylamine (Et_3N) was added; 23.0 mg of 4-bromobutyric acid (0.137 mmol) was separately dissolved in 0.5 ml of dichloromethane. The two solutions were then mixed and the reaction was kept under magnetic stirring for 24 hrs at room temperature (Scheme 2). The reaction was monitored by TLC using cyclohexane: ethylacetate = 70: 30 as eluent.

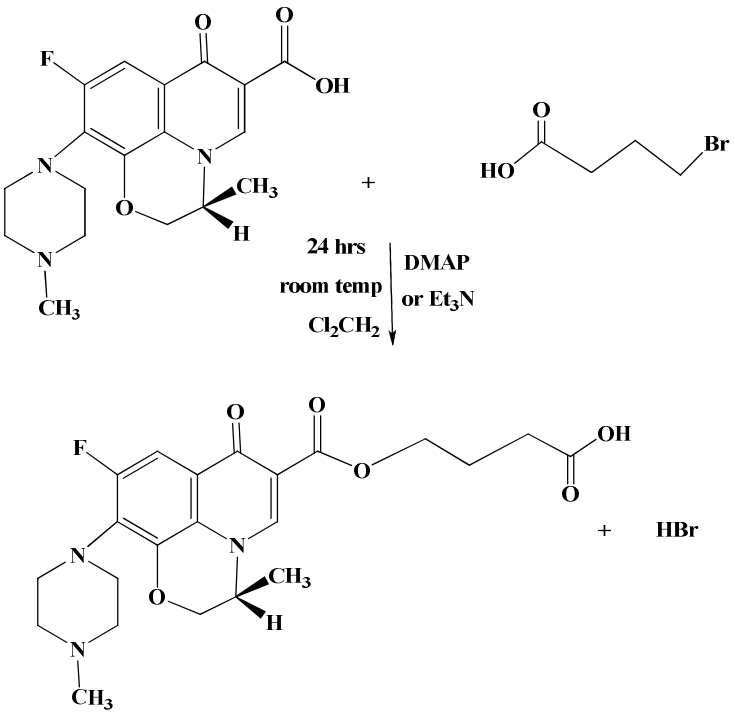

Scheme 2.Reaction scheme of the Br–Levofloxacin derivative.

Result: No product was obtained.

The reaction was carried out several times by changing the organic solvent and/or the type of organic base, using the experimental conditions reported in Table 1.

Table 1. List of the different conditions used for the reaction synthesis according to Method 2.

Reactions	Organic linker (mmol)	Levofloxacin (mmol)	Et_3N (mmol)	DMAP (mmol)	DMSO (ml)	CH_2Cl_2 (ml)
1	4-bromobutyric acid (0.137)	0.135	0.136	---	---	4.5
2	4-bromobutyric acid (0.137)	0.135	0.136	---	4.5	---
3	4-bromobutyric acid (0.137)	0.135	---	0.138	4.5	---
4	Ethyl-4-bromobutyrate (0.138)	0.135	0.136	---	4.5	---

Result: No products were obtained.

Method-3

Synthesis of Scleroglucan derivatives

In a typical synthesis 100 mg of Sclg sonicated for 60 min (Sclg60) was solubilised in 5 ml of DMSO (cp 2% w/v, 0.154 mmol). 18.8 mg (0.154 mmol) of DMAP was then added and the solution was stirred for 15 min. 55 mg of Levofloxacin (0.149 mmol) was dissolved in 1 ml of DMSO and then 88.7 mg of EDC.HCl (0.463 mmol) was added to the Levofloxacin solution.

The two solutions were then mixed and the reaction was kept for 48 hrs at room temperature under magnetic stirring (Scheme 3). 5 ml of water was then added and an exhaustive dialysis against distilled water (Visking tubing, cut-off: 12,000–14,000) was performed. The final reaction product was recovered by lyophilisation.

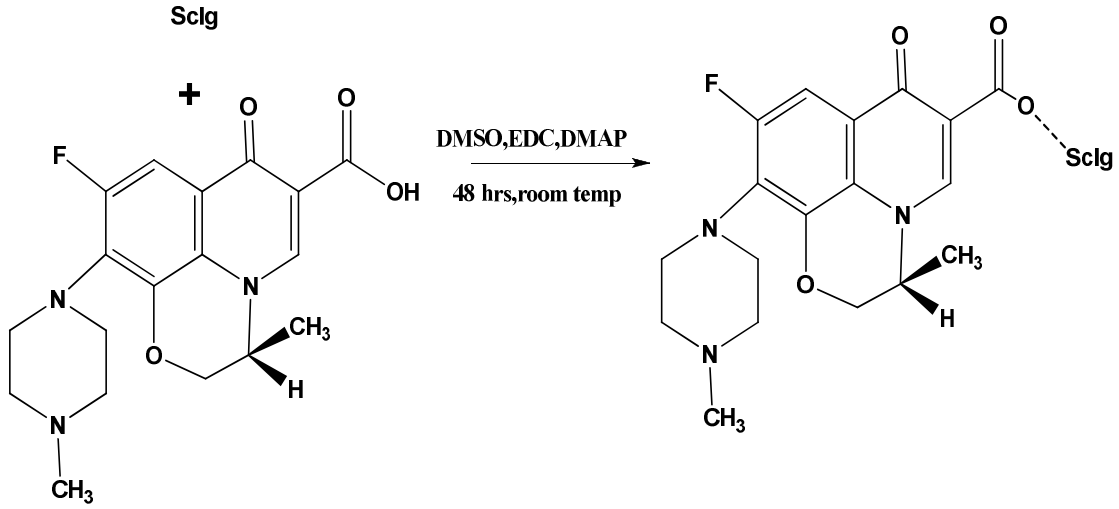

Scheme 3. Reaction scheme of the Sclg–Levofloxacin derivative.

Result: No product was obtained, as evidenced by FTIR analysis.

Method-4

Levofloxacin bromobutyric acid derivatives

In a typical synthesis 500 mg of Levofloxacin (1.35 mmol) was dissolved in THF (5 ml); then 385 µl (1.39 mmol) of Et_3N was added together with 84 mg (1.38 mmol) of DMAP. Ethyl-4-bromobutyrate (39.6 µl, 1.38 mmol) solution was added into solubilized Levofloxacin. The reaction was kept under magnetic stirring for 24 hours at room temperature. The reaction was monitored by TLC using cyclohexane : ethylacetate = 70 : 30 as eluent.

Extraction:

10 ml of CH_2Cl_2 was added to 2 ml of Levofloxacin reaction solution in THF. The first washing was done using 8 ml of water, the second washing was done using HCl 0.1 N and the third washing was done by using K_2CO_3 0.1 N (pH = 10-11).

The organic phase was then dried on $NaSO_4$ and evaporated, and the presence of the product was checked by Mass Spectroscopy (Figure 2).

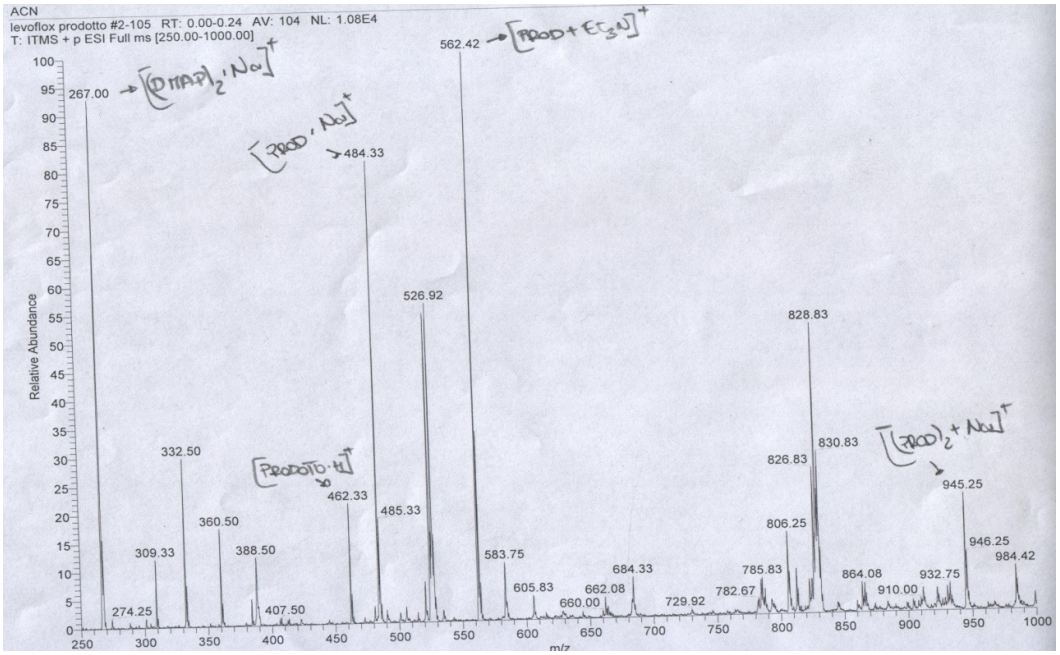

Figure 2. Mass spectra of the reaction product.

The following mass spectra (MS) peaks were obtained for the product: m/z 462, 484 and 562.

Result: a very small amount of product was obtained.

Method-5

Synthesis of Scleroglucan derivatives

Nanohydrogels of Scleroglucan Penicillin-G.

In a typical synthesis 100 mg of Sclg60 was solubilised in 5 ml of DMSO (cp 2% w/v, 0.154 mmol); 18.8 mg (0.154 mmol) of DMAP was then added and the solution was stirred for 15 min. 55 mg of Penicillin-G sodium salt (0.154 mmol) was dissolved in 1 ml of DMSO and then added, together with 29.5 mg of EDC.HCl (0.154 mmol), to the Penicillin solution.

The two solutions were then mixed and the reaction was kept for 48 hrs at room temperature under magnetic stirring (Scheme 4). 5 ml of water was then added and an exhaustive dialysis against distilled water (Visking tubing, cut-off: 12,000–14,000) was performed. The final product was recovered by lyophilisation. The Penicillin-G reaction was carried out by using different molar ratios, as reported in Table 2.

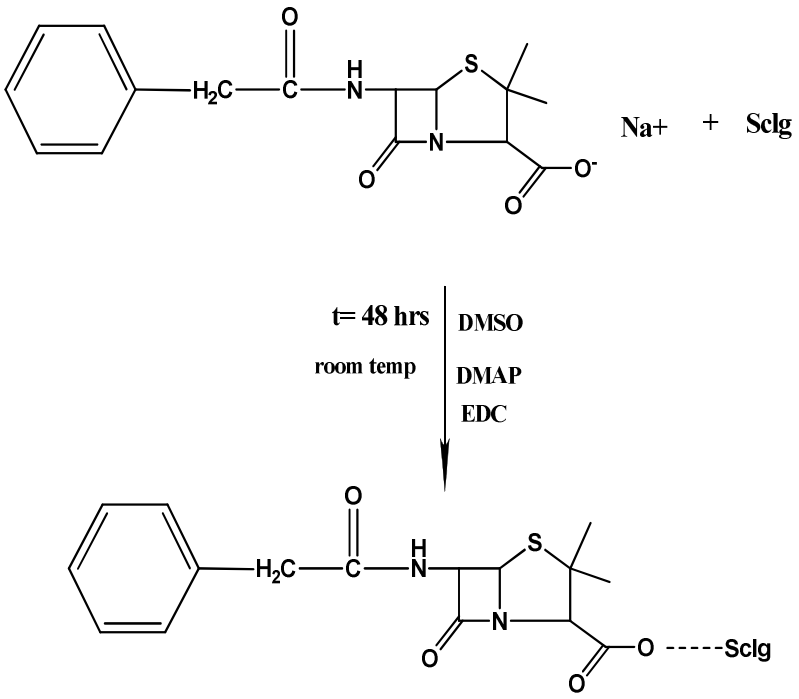

Scheme 4. Reaction scheme of the Sclg60–Penicillin-G derivative.

Table2. List of the different conditions used for the reaction synthesis according to Method 5.

Sample	Penicillin-G (mmol)	EDC (mmol)	DMAP (mmol)	Sclg60 (mmol)
Sclg60-Penicillin-G 30% molar ratio	0.046	0.046	0.0463	0.154
Sclg60-Penicillin-G 50% molar ratio	0.075	0.075	0.075	0.154
Sclg60-Penicillin-G 100 % molar ratio	0.154	0.154	0.154	0.154

FT-IR Analysis.

The following samples were analysed by FT-IR

1) Sclg60.
2) Sclg60-Penicillin-G 30% molar ratio
3) Sclg60-Penicillin-G 50% molar ratio
4) Sclg60-Penicillin-G 100% molar ratio

The Penicillin-G reaction was carried out using different percentage ratios: only the product obtained by using a molar ratio of 100% shows the band at 1700 cm^{-1} related to the asymmetric stretching of ester CO (Figure 3).

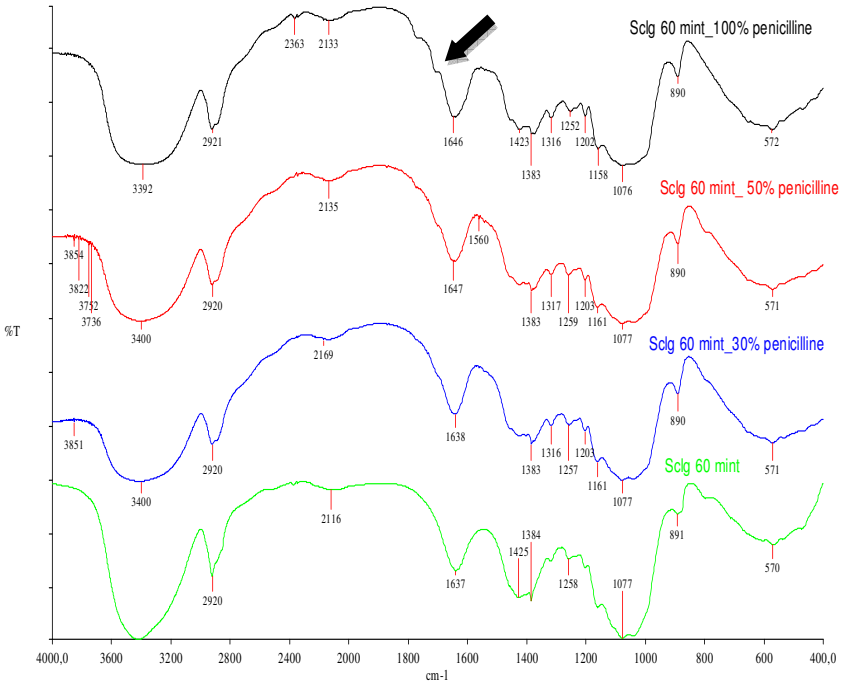

Figure 3. IR spectra of Sclg derivatives with different percentage ratios of Penicillin-G.

Preparation of Scleroglucan nanohydrogels and their size characterization.

We prepared Sclg NHs by self assembling of the polymer chains, after an appropriate chemical derivatization with Penicillin-G sodium salt. The Sclg was sonicated to reduce the molecular weight, thus obtaining a reliable and suitable polymer system for NHs formation. This approach allows us to combine the advantages of nanotechnology, such as high stability, high carrier capacity, and feasibility of different routes of administration.

3 mg of synthesized Sclg60-Penicillin-G 100% molar ratio was dissolved in 3 ml of water (cp= 0.1%). The suspension was then sonicated for 5 min by means of an ultrasonic bath sonicator at 25°C for the preparation of NHs. The sample was then filtered through 0.45 µm Millipore membranes before analysis.

Size distributions graph is presented in Figure 4. The Sclg60-Penicillin-G 100% molar ratio derivative instantly forms quite big aggregates of different size, as evidenced in the intensity weighting particle size analysis. When the same data were analysed in terms of volume occupied by the particles it was clear how the majority of the particles, more than 90%, had a

diameter in the range of 15-40 nm. This means that the polymer chains mostly give self-assembling structures of very small dimensions while a few chains form quite big aggregates. Consequently, the polydispersity index of the system was high and equal to 0.584.

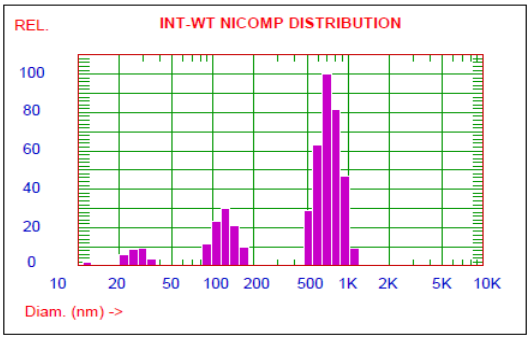

Intensity Weighting:

	Peak 1	Peak 2	Peak 3
Mean Diam.(nm)	11.6	27.6	124.2
Stnd Dev. (nm)	0.9	3.8	26.5
C. V.(%)	7.9	13.8	21.3
Percent (%)	4.6	22.1	73.3

Min. Diam. = 10 Plot Size = 45
Smoothing = 3 Plot Range = 1000

Volume Weighting:

	Peak 1	Peak 2	Peak 3
Mean Diam.(nm)	22.6	111.2	748.0
Stnd Dev. (nm)	5.3	22.3	140.3
C. V.(%)	23.4	20.1	18.8
Percent (%)	90.7	3.9	5.4

Figure 4. DLS measurements of Sclg60-Penicillin-G 1:1 molar ratio.

Method-6

Preparation and characterization of Scleroglucan nanohydrogels

Experimental

Sclg NHs was prepared using a nanoprecipitation/crosslinking method. For the reaction 50 mg of Sclg (cp=1%) sonicated for 20 min (Sclg20) was dissolved in 5 ml of DMSO to form the diffusing phase. 10 µl of Triton X-100 (0.1×10^{-3} mM), used as surfactant to stabilize the NHs, was then added. Nanoprecipitation was carried out by dropping the solution in water under moderate magnetic stirring. Finally, 500 µl of boric acid, used as crosslinker, was added to the solution (Figure 5). The system was poured inside a dialysis bag (Visking tubing, cut-off: 12,000–14,000) and dialysed for 24 hrs at room temperature to remove the excess of boric acid.

The solution was vortexed and sonicated in a water bath for 5 min at room temperature in order to get uniform NHs. The system was then filtered through 0.45 and 0.2 μm millipore membranes and characterized for the estimation of particle sizes.

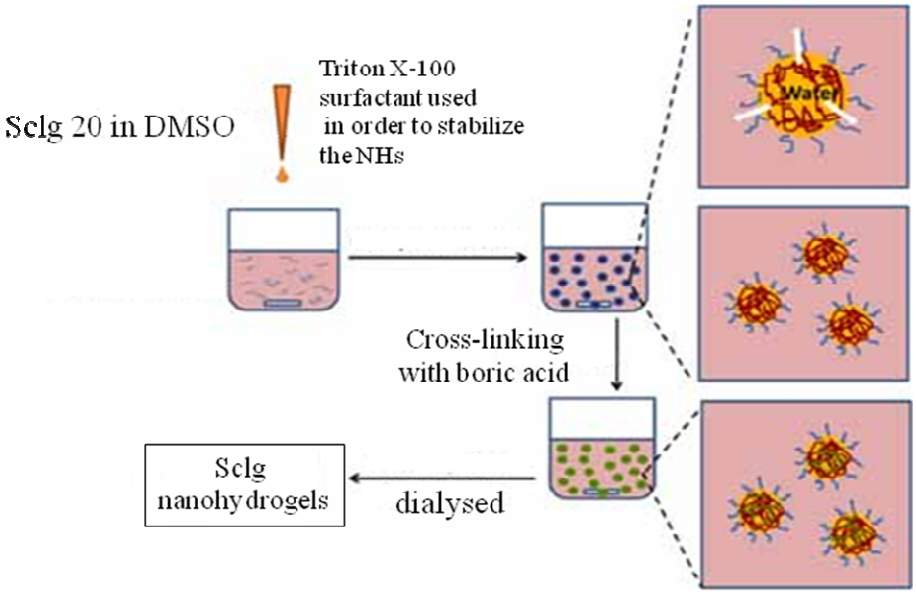

Figure 5. Schematic representation of Sclg20 NHs formation by nanoprecipitation/ crosslinking technique.

The size analysis of the sample, presented in Figure 6, indicates that more than 85% of particles show dimensions in the range of 15-40 nm.

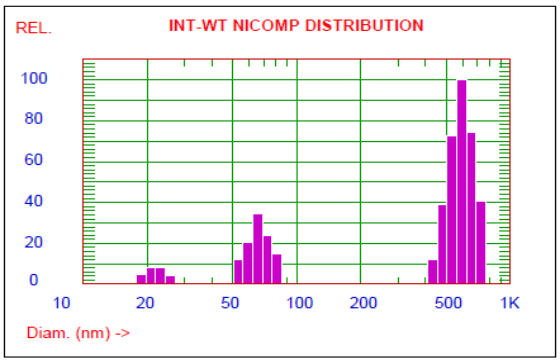

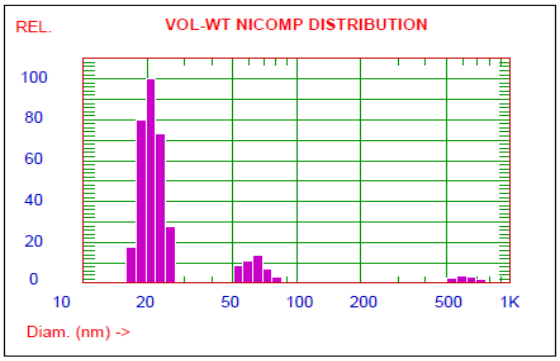

Figure 6. DLS measurements of Sclg20.

References

1. Yinsong W, Lingrong L, Jian W, Zhang Q. Carbohydr Polym. 2007;69:597.
2. Yuan X B, Yuan H L, Yuan Y B. Carbohydr Polym. 2006;65:337.
3. Akiyoshi K, Deguchi S, Moriguchi N, Yamaguchi S J. Macromolecules. 1993;26:3062.
4. Yamane S, Sugawara A, Watanabe A, Akiyoshi K. J Bioact Compat Polym. 2009;24:151.
5. Miyoshi E, Takaya T, Nishinari K. Carbohydr Polym. 1996;30:109.
6. Dreveton E, Monot F, Lecourtier J, Ballerini D, Choplin L. J Ferment Bioeng. 1996;82:272.
7. Matricardi P, Cencetti C, Ria R, Alhaique F, Coviello T. Molecules. 2009;14:3376.
8. Yanaki T, Kojima T, Norisuye T. Polym J. 1981;13:1135.
9. Yanaki T, Norisuye T. Polym J. 1983;15:389.
10. Yanaki T, Norisuye T, Fujita H. Macromolecules.1980;13:1462.

Preparation and characterization of Guar Gum (GG) nanohydrogels

Introduction

Nanohydrogels (NHs) act as potential carrier for several classes of drugs such as anticancer agents, antihypertensive agents, immunomodulators, hormones and macromolecules such as nucleic acids, proteins, peptides and antibodies [1,2]. The various methods used for the preparation of NHs include precipitation, sonochemistry, dialysis, coacervation, spray drying and a combination of these methods [3, 4]. Nanoprecipitation is a general route to prepare polymeric NHs under mild conditions, turning out to be suitable for biological applications [5].

GG and its derivatives are extensively used in many applications including food, drug-delivery and health care products because of natural abundance of GG and its low cost [6, 7].

GG is a water-soluble polysaccharide extracted from the seeds of *Cyamopsis tetragonoloba*. GG has been extensively studied in the pharmaceutical field for its possible uses in colon delivery [8, 9], due to its drug release retarding property and susceptibility to microbial degradation in the large intestine.

Herein, the preparation of GG nanohydrogels (NHs) by self-assembling of the polymer chains, after an appropriate chemical derivatization with Penicilin-G, is reported. GG was sonicated to reduce the molecular weight thus obtaining a reliable and suitable polymer system for NHs formation. Penicillin-G, a poorly water-soluble antimicrobial drug, was chemically conjugated to the GG sonicated for 30 min (GG30–Penicillin-G). Furthermore, also a nanoprecipitation/cross-linking method was applied for the preparation of GG NHs. Few information is available in the literature for the possibility to use GG based nanosized materials as a drug carrier.

Materials and Methods

Materials

The GG was provided by CarboMer (USA), N-(3-imethylaminopropyl)-N'-ethylcarbodiimide hydrochloride (EDC.HCl), 4-dimethylamino pyridine (DMAP), and

Penicillin-G sodium salt were Sigma products. All products and reagents were of analytical grade.

Guar Gum controlled depolymerisation

Methods

Probe Sonication

In order to reduce the GG molecular weight, a High Intensity Ultrasonic Processor (750 Watt model, probe type sonicator—Vibra Cell—VC 750, Cole- Parmer, USA) was used, working at 20 kHz, with a 6.5 mm microtip, applying an amplitude of 30% of the maximum power supplied by the instrument (corresponding to 20 watts), and applying pulser cycles of 30 s ON and 30 s OFF. Aqueous solutions (50 ml) of GG (0.5% (w/v)), prepared in glass beakers, were kept, during sonication, in an ice bath which allowed to keep an average temperature of the samples below 25°C.

Bath sonicator

A second source of ultrasound used was an ultrasonic bath "Starsonic 35 Basic-Liarre", with the following characteristics:

- Frequency: 28-34 kHz
- Voltage: 230 VAC / 50-60 Hz
- Power: 80-180 W
- Heating Power Supply: 100 W

The samples were sonicated in a water bath for 5 min at room temperature in order to get uniform NHs.

Ultracentrifugation used after probe sonication

GG samples were also prepared by centrifugation in order to separate the aggregates from the polymer solutions (cp = 0.5% w/v). For this purpose a centrifuge Sorvall WX 80 ULTRA (Thermo Scientific, USA) was used (20 min at 5000 rpm and 20 °C). Freeze-drying procedure was then carried out.

FT-IR

FT-IR spectra of GG sonicated and its derivatives with Penicillin-G were recorded in the range of 4000–400 cm^{-1} using KBr pellets and a Perkin-Elmer 1720 spectrophotometer. The resolution was 1 cm^{-1}. The number of scans was 64.

Size characterization of nanohydrogels

NHs size distributions were assessed by dynamic light scattering (DLS) by using a NICOMP 370 Autodilute Submicroscope (Specific Scientific Hiac/Roy Co., Santa Barbara, CA).

Experimental

Reduction of Guar Gum Solution Viscosity upon Sonication.

Aqueous solutions of sonicated samples were prepared for the viscosity measurements, carried out at 25°C and the results are shown in Figure 7a. From the intrinsic viscosities [η] of the samples (obtained from the intercepts in Figure 7a), the molecular weights of the various fractions were estimated according to the Mark-Houwink-Sakurada (MHS) equations valid for galactomannans [10].

$$[\eta] = K M_w^{a}$$

where $K = 5.13 \times 10^{-4}$ and $a = 0.72$.

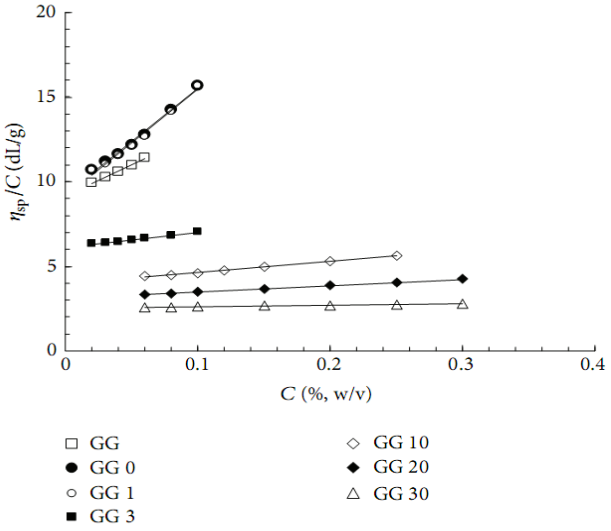

Figure 7. (a) η_{sp}/C *vs* polymer concentration for GG samples sonicated for different periods of time (T = 25°C).

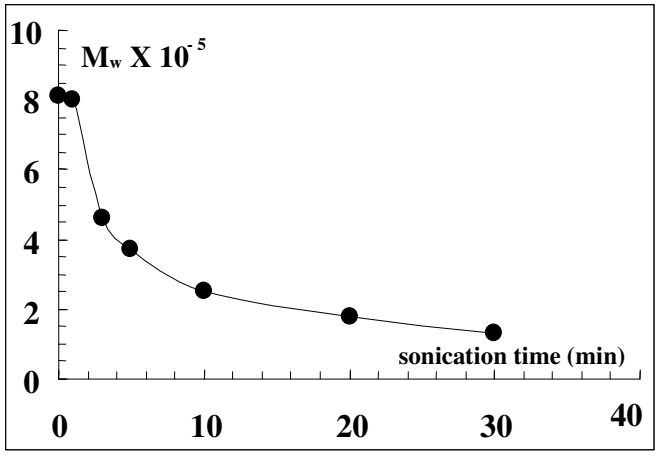

Figure 7. (b) GG molecular weight dependence on sonication time (T = 25 °C).

It is possible to observe that, applying the sonication for only 5 min, the GG molecular weight was reduced to more than one half (Figure 7b). The molecular weight reduction was further increased by increasing the sonication time. The M_w of GG, starting from about 8.0 x 10^5, was thus reduced to 1.32 x 10^5, by applying ultrasounds for 30 min.

Synthesis and characterization of the Guar Gum derivatives

GG was derivatized with Penicillin-G sodium salt, chosen as a suitable drug for the present work, by applying different methods. The lists of the reactions carried out are listed below.

Method-7

Nanohydrogels prepared with Guar gum Penicillin-G

In a typical synthesis 100 mg of GG30 was solubilised in 5 ml of water (cp = 2%w/v, 0.205 mmol). 25.1 mg (0.205 mmol) of DMAP was then added and the solution was stirred for 15 min. 73 mg of Penicillin-G sodium salt (0.204 mmol) was dissolved in 1 ml of DMSO and 39.4 mg of EDC.HCl (0.205 mmol) were added to the Penicillin solution.

The two solutions were then mixed and the reaction was kept for 48 hrs at room temperature under magnetic stirring (Scheme 5). 5 ml of water was then added and an exhaustive dialysis against distilled water (Visking tubing, cut-off: 12,000–14,000) was performed. The final product GG-Penicillin was recovered by lyophilisation. The Penicillin-G reaction was carried out by using different molar ratios, as reported in Table 3.

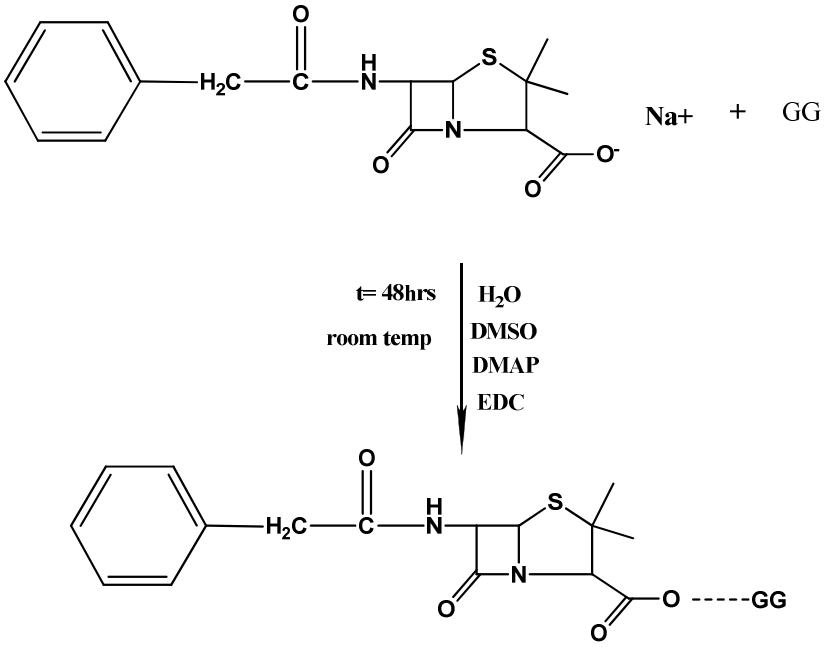

Scheme 5. Reaction scheme of the GG–Penicillin-G derivative.

Table 3. List of the different conditions used for the reaction synthesis according to Method 7.

Sample	Penicillin-G (mmol)	EDC (mmol)	DMAP (mmol)	GG30 (mmol)
GG30-Penicillin-G 30% molar ratio	0.061	0.061	0.061	0.205
GG30-Penicillin-G 50% molar ratio	0.102	0.102	0.102	0.205
GG30-Penicillin-G 100% molar ratio	0.204	0.204	0.204	0.205
GG30-Penicillin-G 300% molar ratio	0.614	0.614	0.614	0.205

FT-IR Analysis.

The following samples were analysed by FT-IR (by preparing tablets with KBr powder).

1) GG30
2) Penicillin-G drug
3) GG30-Penicillin-G 30% molar ratio
4) GG30-Penicillin-G 50% molar ratio
5) GG30-Penicillin-G 100% molar ratio
6) GG30-Penicillin-G 300% molar ratio

FT-IR spectra were recorded in the range of 4000–400 cm^{-1} using KBr pellets and a Perkin-Elmer 1720 spectrophotometer. The resolution was $1cm^{-1}$. The number of scans was 64.

The reaction with Penicillin-G was carried out using different percentage ratios. The occurrence of the reaction between GG30 and Penicillin-G has not been confirmed by FT-IR analysis (Figure 8).

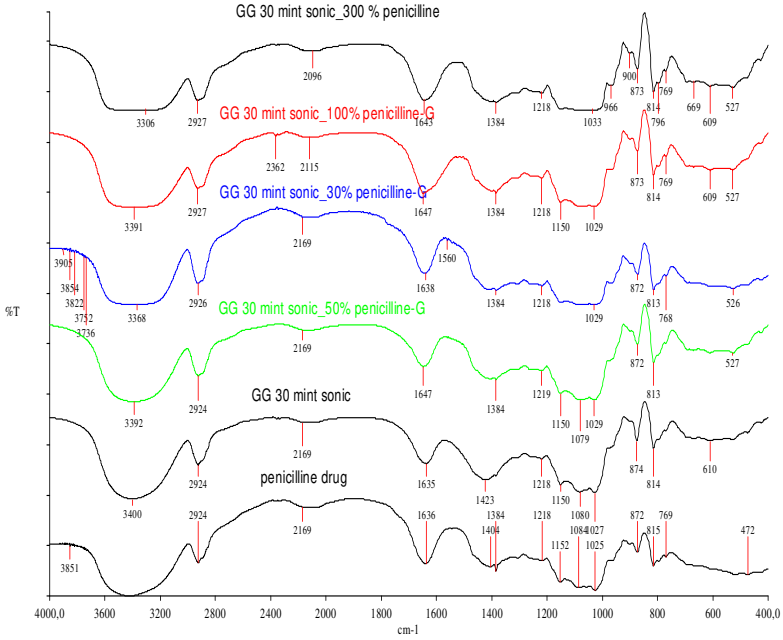

Figure 8. IR spectra of GG derivative with different concentration of penicillin-G.

Result: No product was obtained, as evidenced by FTIR analysis.

Method-8

Preparation and characterization of Guar gum nanoparticles

Experimental

GG NHs were prepared using a nanoprecipitation/crosslinking method .For the reaction 50 mg of GG (cp=1%) sonicated for 1 min (GG1) was dissolved in 5 ml of water to form the diffusing phase. 10 µl of Triton X-100 (0.1×10^{-3} mM), used as surfactant to stabilize the NHs, was then added. Nanoprecipitation was carried out by dropping the solution in IPA or DMSO, under moderate magnetic stirring. Finally, 500 µl of boric acid, used as crosslinker, was added to the solution (Figure 9). The system was poured inside a dialysis bag (Visking tubing, cut-off: 12,000–14,000) and dialysed for 24 hrs at room temperature to remove the excess of boric acid.

The solution was vortex and sonicated in a water bath for 5 min at room temperature in order to get uniform NHs. The system was then filtered through 0.45 and 0.2 µm Millipore membranes and characterized for the estimation of particle sizes.

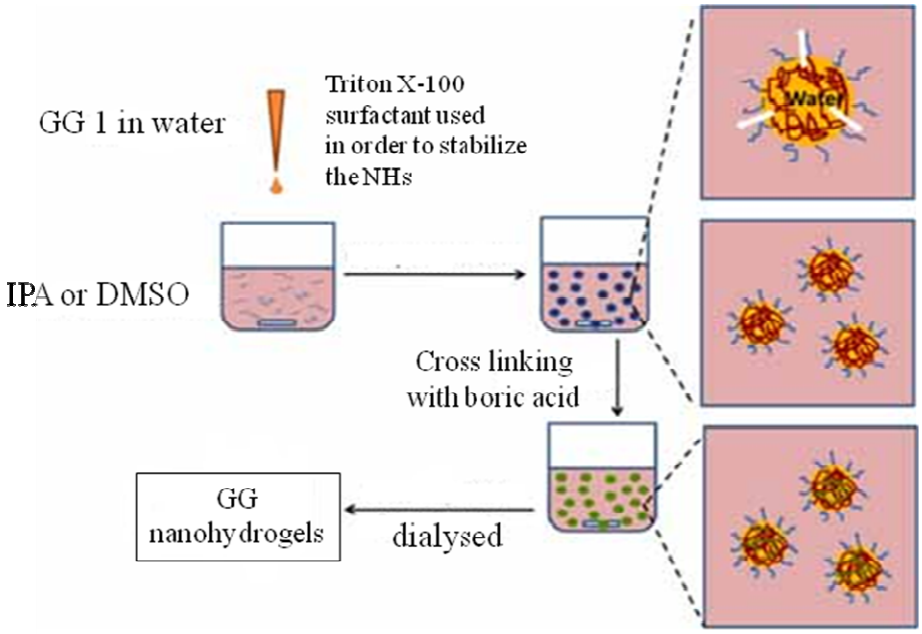

Figure 9: Schematic representation of GG NHs formation by nanoprecipitation/crosslinking technique.

Size distributions analysis of GG NHs prepared by a nanoprecipitation/ crosslinking method is presented in Figure 10. In this method the minimum size of NHs was obtained by using IPA as the non solvent. The GG NHs instantly forms quite big aggregates of different size, as evidenced in the intensity weighting particle size analysis. When the same data were analyzed in terms of volume occupied by the particles, it was clear how the majority of the particles, more than 90%, had a diameter in the range of 15-40 nm. This means that the polymer chains mostly give self-assembled structures of very small dimensions while a few chains form quite big aggregates.

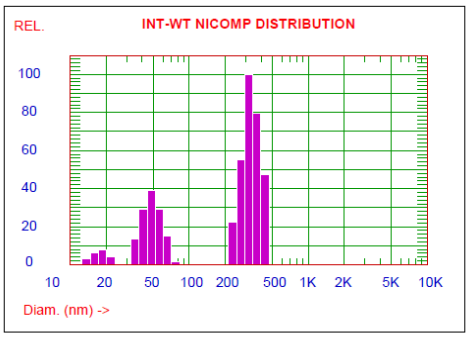

Figure 10. DLS measurements of GG1.

(a)

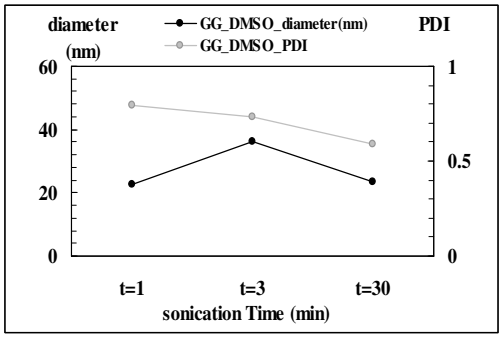

(b)

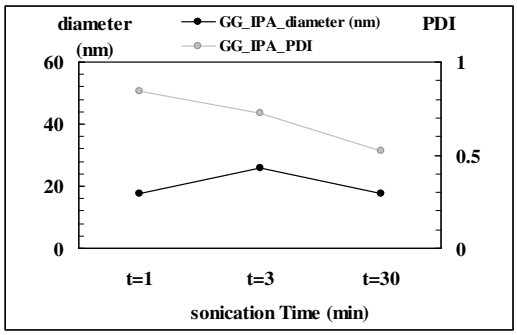

(c)

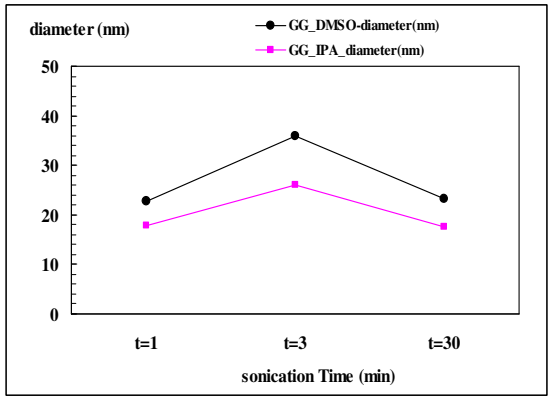

Figure 11. Effect of sonication time on the NHs dimensions and polydispersity index.
GG NHs prepared by a nanoprecipitation/crosslinking in DMSO (a) and in in IPA (b). Comparison of the dimensions of GG NHs prepared in different solvents(c).

The GG30 was used to prepare NHs by a nanoprecipitation/cross linking method in DMSO. The evaluation of the particle sizes of the NHs by DLS measurements shows that more than 90% of the particles have a diameter in the range of 15-40 nm with a PDI > 0.588 (Figure 11a). Similar results were obtained when the preparation of NHs was carried out in IPA: the nanoparticles show dimensions in the range of 15-40 nm with a PDI of 0.526, as reported in Figure 11b.
No significant differences in the dimensions of NHs were observed by changing the sonication time or the preparation solvent (Figure 11c).
Work is still in progress to optimize the effect of different solvents (IPA, DMSO), different crosslinkers and different surfactants, in order to obtain stable NHs of GG.

References

1. Akagi T, Higashi M, Kaneko T, Kida T, Akashi M. Biomacromolecules. 2006;7:297.
2. Torchilin V P. Pharm Res. 2007;24:1.
3. Gaucher G, Dufresne M H, Sant V P, Kang N, Maysinger D, Leroux J C. J Control Release. 2005;109:169.
4. Rema S S, Swapankumar G, Emilia T A. Int J Biological Macromolecules.2010;46:267.
5. Becer C R, Babiuch K, Pilz D, Hornig S, Heinze T, Gottschaldt M, Schubert U. Macromolecules. 2009;42:2387.
6. Tang Z X, Qian J Q, Shi L E. Material Letters. 2006;61:37.
7. Cheng Y, Brown K M, Prud'homme R K. Biomacromolecules. 2002;3:456.
8. Al Saidan S M, Krishnaiah Y S R, Satyanarayana V, Bhaskar P, Karthikeyan R S. Eur J Pharm Biopharm. 2004;58:697.
9. Sinha V R, Mittal B R, Kumria R. Int J Pharm. 2005;289:79.
10. Picout D R, Ross Murphy S B. Carbohydr Polym. 2007;70:145.

Chapter 5

DEVELOPMENT AND CHARACTERIZATION OF NEW SCLEROGLUCAN FILMS FOR TOPICAL ANTIFUNGAL THERAPY

Development and characterization of new Scleroglucan films for topical antifungal therapy

Abstract

A new formulation, a Sclg film loaded with tioconazole, a drug usually used for dermal therapies, was prepared. Dynamo-mechanical characterization and swelling studies of the novel delivery system were carried out. The films were prepared with Sclg and glycerol, used as plasticizer, and Labrasol, a surfactant used for increasing the solubility and bioavailability of the low-soluble drug. Preliminary "*in vitro*" studies showed the noticeable fungal activity of the new formulation against *Candida Albicans* infections.

Introduction

Fungal infections of the skin are one of the frequently facing dermatological diseases worldwide. It has been estimated that about 40 million people have suffered from fungal infections in developing and under developed nations. The progression of fungal infections can be rapid and serious due to the damage of immune functions [1, 2]. Topical therapy is an attractive choice for the treatment of the cutaneous infections due to its advantages such as targeting of drugs to the site of infection and reduction of the risk of systemic side effects. At this time, antifungal drugs are generally used as conventional cream and gel preparations in topical treatment. The effectiveness of that treatment depends on the penetration of drugs through the target layers of the skin at the effective concentrations. The physico-chemical characteristics of drug molecules and the type of the formulation are effective factors in topical drug delivery. Therefore, a number of formulation strategies have been investigated for delivering antifungal compounds through targeted sites of the skin.

*Dermatophytes*are one of the most frequent causes of tinea and o*nychomycosis*.Candidal infections are also among the most widespread superficial cutaneous fungal infections [3]. Even, *Candida* can infect deeper tissues as well as the blood that leads to life- threating systemic candidiasis, when the immune system is weakened [4].

Topical treatment of fungal infections has several advantages, including targeting of the infection site, reduction of the risk of systemic side effects, enhancement of the efficacy of treatment and, high patient compliance.

In this context, the formulation may play a major role for penetration of drugs into skin [5].

Development of alternative approaches for topical treatment of fungal infections of skin encompasses new carrier systems for approved and investigational compounds. Delivery of antifungal compounds into skin can be enhanced with the carriers including colloidal systems, vesicular carriers, and nanoparticles.

Furthermore, scientists have developed and proposed various formulation techniques to improve the solubility and bioavailability of poorly water-soluble compounds [6]. One of the most common approach involves the use of a solubilizing agent, such as Labrasol (saturated polyglycolyzed C_8 -C_{10} glyceride) [7], mixed with other pharmaceutical excipients, such as hydrophobic oils, lipids, and co solvents, to form micro emulsions or emulsion systems [8-11]. The drugs are held tightly in the more hydrophobic cores of the emulsion system, thus avoiding drug precipitation.

Topical Delivery of Antifungal via Skin

Human skin is a well-organized membrane and, it has three main layers, *epidermis*, *dermis* and *hypodermis*. *Stratum corneum*, the outermost layer of *epidermis*, is formed by dead and keratinized cells, and it is an excellent barrier to penetration of drugs through the skin [12]. Drugs should penetrate into skin layers to ensure effective drug concentrations following topical administration. In topical administration, the entering of drugs to systemic circulation is prevented or minimized. Thus, the systemic adverse effects of drugs are avoided [13]. Besides, topical preparations have better patient compliance due to their non- invasiveness and they can be self-administered [14, 15].

Materials

Sclg was provided by Cargill (Minneapolis, USA).Glycerol (analytical grade) and Labrasol was purchased by Gattefosse. Tioconazole, Levofloxacin and Theophylline were purchased by Sigma. For the sample preparations distilled water was used.

Methods

Preparation of Sclg Films

Sclg was purified by dialysis. An aqueous solution of Sclg (cp=1% w/v) and glycerol (2 % w/v) was prepared and kept at room temperature under magnetic stirring for 72 hrs.

Tioconazole, previously solubilised in Labrasol, was added to the polymer/glycerol solution. 4 ml of solution was poured in a plastic plate. The films were dried at 40°C for 1 hr and then

allowed to dry at room temperature (about 25°C) for a week. Translucent films were obtained.

Films were prepared with three different amounts of tioconazole, 5µg, 10µg and 20µg (Table 1). In Figure 1 the preparation of polymeric films by the casting solvent evaporation technique is reported. The original size of the films was 3x3cm^2. For the swelling studies and for the fungal activity tests 1x1 cm^2 samples were used.

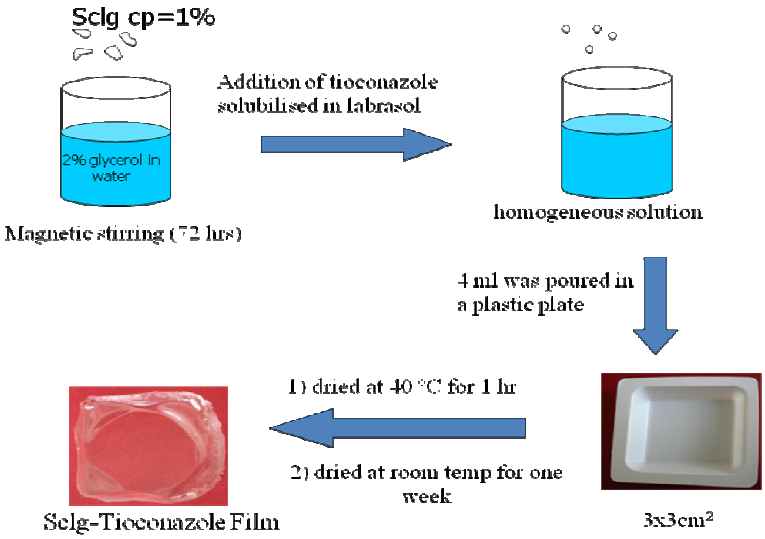

Figure 1. Schematic representation of Sclg film preparations.

Dynamo-mechanical analysis

The mechanical properties were investigated with a software-controlled dynamometer, TA-XT2*i* (Stable Micro Systems, UK), equipped with a 5-kg load cell. The accuracy of the force measurement was 0.0025 %, and the distance resolution was 0.0025 mm.

The film was placed in a holder with a cylindrical hole (*d*= 8.50 mm) and the diameter of the spherical probe was 6.35mm. The pre-test and post-test speeds were fixed at 2.00 mm/s, the test speed at 1.00 mm/s and the trigger force at 0.098 N.

The following parameters were calculated:

1) Puncture strength at break = F_{max} / ACS

Where F_{max} is the maximum applied force at film break, *A*CS is the cross-sectional area of the film above the hole of the film holder, *A*CS =2$r\delta$, where r is the radius of the hole and δ is the thickness of the film.

2) Elongation (%) at break $= \left[\frac{\left[\left(r^2 + D^2\right)\right]^{1/2} - r}{r} \right] \times 100$

Where r is the radius of the film exposed in the cylindrical hole of the film holder and D represents the displacement of the probe from the point of contact to point of puncture. The maximum load and the maximum displacement of films were measured, and then converted to puncture strength, and elongation at break.

Susceptibility testing method

The antimicrobial activity of the patches was evaluated against the test organisms *C. albicans* ATCC 24433, and the strain CO23 of *C. albicans*, which was isolated from a subject with vulvo-vaginal candidiasis, originally susceptible to micafungin (FK463, MIC 0.025 μg/ml) and fluconazole (FLC MIC 0.25 μg/ml). The strains CORFK and CO23 RFK were made resistant to FK463 or to FLC by ten growth passages in step wise-increasing concentrations in solidified agar, according to the National Committee of Clinical Laboratory Standards [16].

Evaluation of prepared films

Film thickness measurements

The thickness of the films was estimated by means of a posiTector 6000 digital thickness meter purchased by DeFelsko (USA). The thickness of the films was measured at five different positions and the obtained values always lay within 10% of the mean.

Water Uptake Studies

The Sclg films showed an extraordinary swelling. The water uptake behaviour was followed as a function of time. The experiments were carried out in distilled water at room temperature. At fixed time intervals the excess of water was removed from the films with soft filter paper for 5 sec, and then the corresponding weights were determined. All experiments were carried out in triplicate and the obtained values always lay within 10% of the mean.

Folding Endurance

The film folding endurances were manually measured. A strip of film was repeatedly folded at the same place till it broke. The number of times the film could be folded at the same place

without breaking gave the value of folding endurance. The folding endurance of prepared films was measured in triplicate and the obtained values always lay within 10% of the mean.

Results and discussion:

Water Uptake Studies

The water uptake results are reported as a function of time in Figure 2. The water uptake of the films significantly increased up to 24 hrs and after 30 hrs the films completely dissolved in the swelling medium.

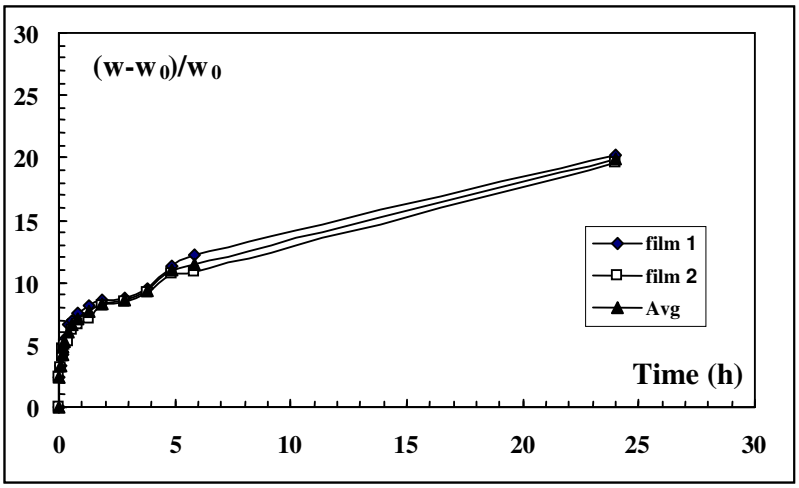

Figure 2. Water uptake $(w-w_0)/w_{0;}$ of Sclg films as a function of time.

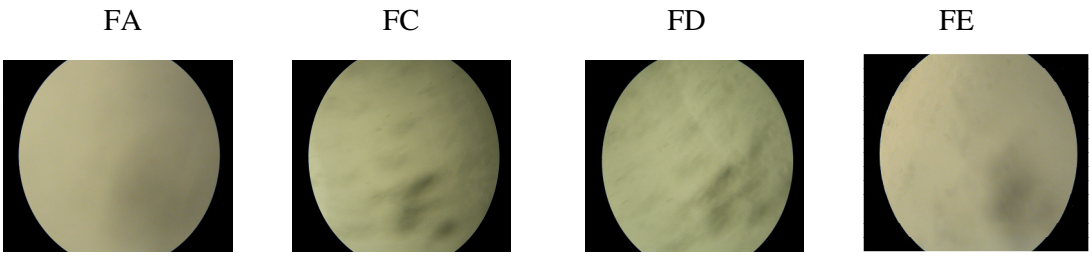

Figure 3. Optical microscope images of Sclg films prepared with different amount of the tioconazole drug. FA, FC, FD and FE (see Table 1).

In Figure 3 the films images recorded by means of an optical microscope show that the presence of the drug did not significantly influenced the appearance of the samples.

Physical and Dynamo-mechanical characterization of Sclg films

Different formulations of Sclg films were prepared, as listed in Table 1.

Table1: List of Sclg film formulations.

Formulations code	Sclg % (w/v)	Glycerol %(w/v)	Labrasol (µl)	Tioconazole (µg)	Distilled water (ml)	Surface area of Film (cm^2)
FA	**1**	**2**	**....**	**....**	**4**	**3x3**
FB	**1**	**2**	**5**	**....**	**4**	**3x3**
FC	**1**	**2**	**5**	**45**	**4**	**3x3**
FD	**1**	**2**	**5**	**90**	**4**	**3x3**
FE	**1**	**2**	**5**	**180**	**4**	**3x3**

In principle, an adequate film mechanical strength is required in order to withstand mechanical stress (e.g., filling and packaging processes, pushing through blister package, handling by patient).

Puncture strength is a measure of film toughness and is directly proportional to the resistance to break or fracture. Sclg films were capable to elongate the double of their initial size. In Table 2 the physical parameters evaluated for the Sclg films are reported.

Tablet 2. List of physical characteristics of Sclg films

Formulations code	Thickness (mm)	Film Weight (mg)	Folding Endurance (-)	Puncture strength (MPa)	Elongation (%)
FA	**0.110**	**153.6**	**87**	**10.73**	**95.71**
FB	**0.106**	**148.1**	**85**	**....**	**....**
FC	**0.102**	**147.3**	**83**	**....**	**....**
FD	**0.104**	**150.4**	**89**	**....**	**....**
FE	**0.102**	**150.7**	**95**	**6.48**	**72.23**

As an example, the mechanical properties of FA and FE formulations are shown in Figure 4.

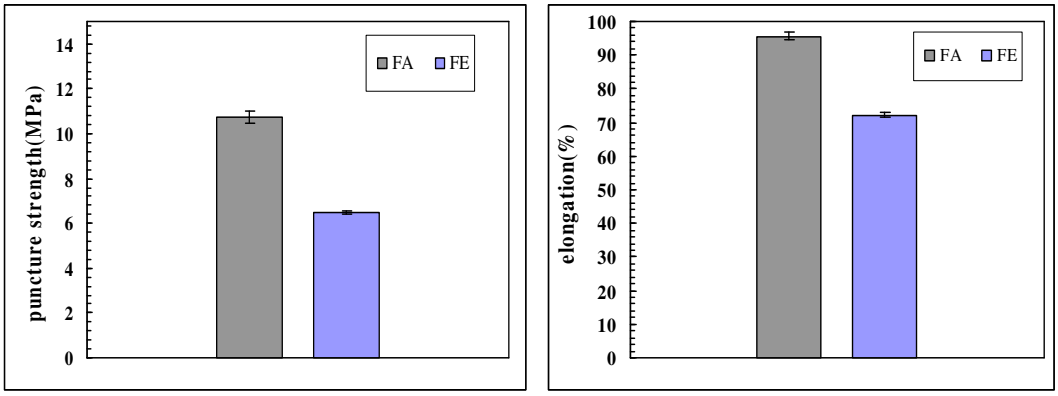

Figure 4. Mechanical properties (puncture strength, and elongation) of Sclg (FA) and Sclg-tioconazole (FE) films.

***C. albicans* activity tested on Sclg films loaded with tioconazole**

Petri plates were prepared by pouring 20 ml of Sabouraud medium that was allowed to solidify, and then dried for 30 min in a biological safety cabinet with vertical laminar flow. 10 µl of a standardized inoculum suspension of $2.5x10^3$ CFU/ml was poured and uniformly spread over the plates. Patches with different amounts of tioconazole (5, 10, 20 µg) were placed in the center of Petri plates. The Petri dishes were then incubated at 30 °C for 24 and 48 hrs. The antifungal activity was measured as the diameter of the inhibitory zone by a caliper and expressed in mm (disk diameter included) (Figure 5).

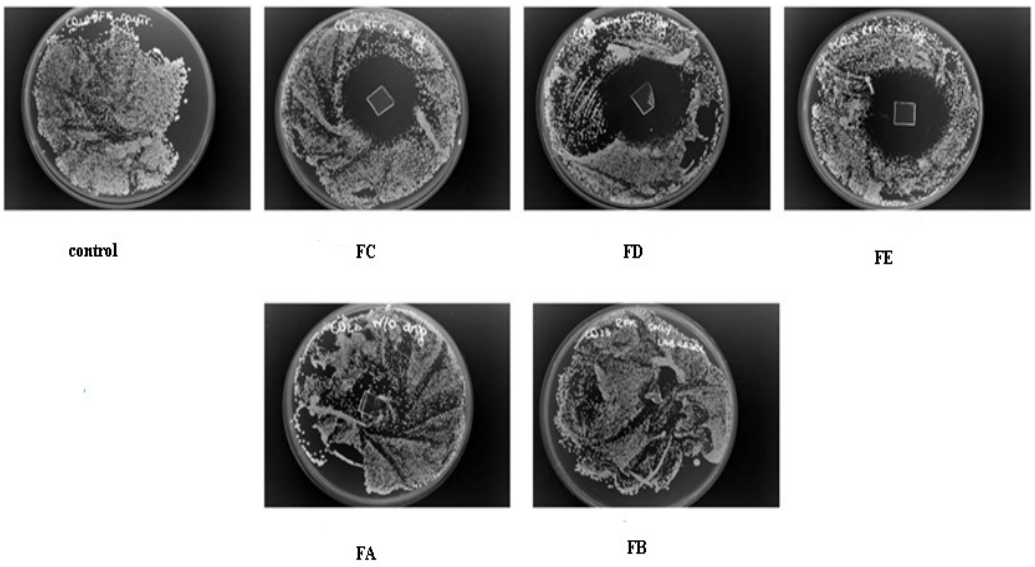

Figure 5. Pictures of different Sclg films loaded with tioconazole and incubated for 24 hrs.

The sensitivity to the different patches was classified by the diameter of the inhibition zone. An inhibitory zone with diameter less than 10 mm corresponds to lack of activity-

Table 3. Fungal activity of Sclg films loaded with tioconazole

C. albicans	**Sample**	**Inhibition zone (diameter expressed in mm after 24h)**	**Inhibition zone (diameter expressed in mm after 48h)**
Co23	control	+++	+++
Co23	FC	30 ±2.8	20±1.4
Co23	FD	38±1.4	26.5±3.18
Co23	FE	44±2.8	28.5±2.8
Co23	FA	+++	+++
Co23	FB	+++	+++
CO23 RFLC	control	+++	+++
CO23 RFLC	FC	18±0.70	+++
CO23 RFLC	FD	22±1.41	15.5±2.12
CO23 RFLC	FE	24±0.70	18±0.70
CO23 RFLC	FA	+++	+++
CO23 RFLC	FB	+++	+++
Co23RFK	control	+++	+++
Co23RFK	FC	40±1.41	33
Co23RFK	FD	40±0.70	34
Co23RFK	FE	42±2.8	35±2.12
Co23RFK	FA	+++	+++
Co23RFK	FB	+++	+++
ATCC 24433	control	+++	+++
ATCC 24433	FC	22±0.70	+++
ATCC 24433	FD	30±0.70	23±0.70
ATCC 24433	FE	30±2.8	24±0.70
ATCC 24433	FA	+++	+++
ATCC 24433	FB	+++	+++

CO23 sensitive to drugs
CO23 RFLC resistant to fluconazole
CO23 RFK resistant to micafungin
ATCC standard strain
+++ strain growth

Results

The inhibitory zones of samples containing 5, 10 and 20 µg of tioconazole were measured. As reported in Table 3, the patches showed an antimicrobial activity against all tested strains. An evident inhibition zone diameter, about 40 mm, for the strains sensitive to azoles (CO23 RFK and CO23) in comparison to strain resistant to fluconazole (CO23 RFLC) was observed. After 48 hours the inhibition zone diameters were reduced of about 6-7 mm in comparison to those observed after 24 hours of incubation. Patches without drug showed no activity; in

some cases no significant differences of inhibition zone between the patches with different concentrations of tioconazole (5 and 10 µg) were observed.

References

1. Ameen M. Clinical Dermatology. 2010;28:197.
2. Havlickova B, Friedrich M.Mycoses. 2008;51:2.
3. Zhang A Y, Camp W L, Elewski BE. Clinical. Dermatology. 2007; 25: 165.
4. Vermaand P, Pathak K. Nanomedicine. 2012;8:489.
5. Lee C M, Maibach H I. J Pharm Sci. 2006;95:1405.
6. Yalkowsky S H. Ed. Solubility and Solubilization in Aqueous Media, (Oxford University Press, (New York).2000.
7. Strickley R G.Pharm Res. 2004;21:201.
8. Barakat N S.J Pharm Pharmacol. 2010;62:173.
9. Kommuru T R. Int J Pharm.2001;212:233.
10. Kim H J .Drug Dev Ind Pharm.2000;26:523.
11. Venkatesh G. Drug Dev Ind Pharm.2010;36: 735.
12. Williams A C.Transdermal and Topical Drug Delivery. Pharmaceutical Press, London, 2003
13. Guy R H.Pharm Res. 1996;13:1765.
14. Guy R H. Drug Delivery Handbook of Experimental Pharmacology Volume. 2010;197:399.
15. Taner T, Mark R. Skin Res Tech. 2008;14:249.
16. National Committee of Clinical Laboratory Standards.CLSI.2007.

Short summary on polysaccharide films formulations for drug release studies.

Several kinds of film formulations, as reported in Tables 4-8, were prepared. Only formulation F24 and F29, which appeared to be the most stable, were tested for drug release. Unfortunately no good results were obtained, since the drug was immediately released from both films.

Table 4

Film composition	**Formulation code**					
	F1	F2	F3	F4	F5	F6
Sclg (0.7%)	90	10	50	100	100	....
PVA (0.7%)	10	90	50	....	....	100
Borax (µl)	486	54	270	540	....	....
Distilled water (ml)	10	10	10	10	10	10

Table 5

Film composition	**Formulation code**					
	F7	F8	F9	F10	F11	F12
Sclg (1%)	90	10	50	100	100	....
PVA (0.7%)	10	90	50	....	....	100
Borax (µl)	694	77	385	771	....	....
Distilled water (ml)	10	10	10	10	10	10

Table 6

Film composition	**Formulation code**					
	F13	F14	F15	F16	F17	F18
Sclg (0.7%)	50	10	50	50	33.3	47.5
PVA (0.7%)	50	90	....	....	33.3	5
GG (0.7%)	....	....	50	50	33.3	47.5
Borax (µl)	486	54	270	270	270	270
Theophylline (%)	10	10	....	10	....	....
Distilled water (ml)	10	10	10	10	10	10

Table 7				
Film composition	**Formulation code**			
	F19	F20	F21	F22
GG (0.7%)	50	10	90	100
PVA (0.7 %)	50	90	10	....
Borax (µl)	360	72	648	....
Distilled water (ml)	10	10	10	10

Table 8							
Film composition	**Formulation code**						
	F23	F24	F25	F26	F27	F28	F29
Sclg (1%)	100	100	....	....	100	50	100
GG (1%)	....	....	100	100	....	50	....
Glycerol (2%) in distilled water (ml)	10	10	10	10	10	10	10
Borax (µl)	....	....	....	....	771	....	....
Theophylline (%)	....	10	....	10	10	10	....
Levofloxacine (%)	....	....	....	....	....	....	10

In Table 9 the physical characteristics of the films (thickness and appearance) are shown, together with the time needed for the films to break or to dissolve. The most stable films were those of formulations F24 and F29.

Table 9. Characteristics of the polysaccharide film formulations.

Sample	Thickness (mm)	Breakage or film dissolution in water at 25 °C (min)	Film appearance
F1	0.018	>15	Not acceptable
F2	0.018	>15	Acceptable
F3	0.018	>15	Acceptable
F4	0.017	x	Not acceptable
F5	0.015	>15	Acceptable
F6	0.022	>15	Acceptable
F7	0.026	>20	Not acceptable

F8	---	>20	Acceptable
F9	---	>20	Not acceptable
F10	---	---	Acceptable
F11	---	---	Not acceptable
F12	0.022	---	Not acceptable
F13	---	< 60	Not acceptable
F14	---	< 60	Acceptable
F15	---	---	Acceptable
F16	---	---	Not acceptable
F17	---	< 150	Acceptable
F18	---	< 180	Acceptable
F19	---	>15	Acceptable
F20	---	>15	Acceptable
F21	---	>15	Acceptable
F22	---	---	Acceptable
F23	---	---	Acceptable
F24	0.102	< 24 hr	Acceptable
F25	---	---	Acceptable
F26	---	---	Acceptable
F27	---	---	Acceptable
F28	---	---	Acceptable
F29	0.104	< 24 hr	Acceptable

The release studies indicated that the tested films (F24 and F29) swelled very rapidly, with an almost immediate delivery of the entrapped drugs.

ACKNOWLEDGEMENT

"Completing a task is never one man's effort it is often the result invaluable contribution of number of individuals"

I thank almighty Allah for making me understand his creation scientifically and I seek peace & blessings on Prophet Muhammad and all messengers.

A sense of triumph is very much justified at this stage of completion of my dissertation even more so in the sense of gratitude to my reverend guide ***Prof. Tommasina Coviello*** *for her invaluable suggestions, especially during the difficult conceptual development stage. I really appreciate her willingness to meet me at short notice every time and going through several drafts of my thesis. I remain amazed that despite her busy schedule, she was able to go through the final draft of my thesis and meet me every day with comments and suggestions on almost every page. She is an inspiration and round the clock help and her keen interest that help me to put an extra bit into my thesis work. I also remain indebted for her understanding and support during the times when I was really down and depressed due to personal family problems.*

I am elated to express my deep sense of gratitude to ***Prof Franco Alhaique*** *and* ***Prof Pietro Matricardi,*** *for taking plans of making available the necessary facilities for the completion of this work. Their wide knowledge and logical way of thinking have great value for me.*

I am also thankful to ***Dr.Chiara Di Meo*** *and all my lab colleagues for their continuous encouragement and personal guidance have provided a good basis for my work.*

Very special thanks to the ***University of Rome "La Sapienza",*** *Italy for giving me the opportunity to carry out my doctoral research and for their financial support.*

Words cannot express the feelings I have for my parents; especially my father was motivation for me. Special thanks are also to my brother ***(Dr.Khalid Akhter Ansari)*** *and sister* ***(Dr.Shabana yasmeen Ansari)*** *and brother in-law for their amazing support.*

Finally, I would like to acknowledge the most important person in my life, my wife ***Sumaiya****. She has been a constant source of strength and inspiration. Without her encouragement and understanding, it was impossible for me to finish this work.*

From the core of my heart I thank to those person who have directly & indirectly helped me during PhD.

SIDDIQUE AKBER ANSARI